THERMAL STRESS PROBLEMS IN FGMS

A THESIS SUBMITTED TO
THE GRADUATE SCHOOL OF NATURAL AND APPLIED SCIENCES
OF
MIDDLE EAST TECHNICAL UNIVERSITY

BY

ESRA NUR AKDOĞAN

IN PARTIAL FULFILLMENT OF THE REQUIREMENTS
FOR
THE DEGREE OF MASTER OF SCIENCE
IN
MECHANICAL ENGINEERING

SEPTEMBER 2019

Approval of the thesis:

THERMAL STRESS PROBLEMS IN FGMS

submitted by **ESRA NUR AKDOĞAN** in partial fulfillment of the requirements for the degree of **Master of Science in Mechanical Engineering Department, Middle East Technical University** by,

Prof. Dr. Halil Kalıpçılar
Dean, Graduate School of **Natural and Applied Sciences** _____

Prof. Dr. Mehmet Ali Sahir Arıkan
Head of Department, **Mechanical Engineering** _____

Prof. Dr. Fevzi Suat Kadıoğlu
Supervisor, **Mechanical Engineering, METU** _____

Examining Committee Members:

Prof. Dr. Zafer Dursunkaya
Mechanical Engineering, METU _____

Prof. Dr. Fevzi Suat Kadıoğlu
Mechanical Engineering, METU _____

Prof. Dr. Hakan Işık Tarman
Mechanical Engineering, METU _____

Assoc. Prof. Dr. Merve Erdal Erdoğmuş
Mechanical Engineering, METU _____

Assoc. Prof. Dr. Barış Sabuncuoğlu
Mechanical Engineering, Hacettepe University _____

Date:

I hereby declare that all information in this document has been obtained and presented in accordance with academic rules and ethical conduct. I also declare that, as required by these rules and conduct, I have fully cited and referenced all material and results that are not original to this work.

Name, Surname: Esra Nur Akdoğan

Signature :

ABSTRACT

THERMAL STRESS PROBLEMS IN FGMS

Akdoğan, Esra Nur
M.S., Department of Mechanical Engineering
Supervisor: Prof. Dr. Fevzi Suat Kadıoğlu

September 2019, 141 pages

In this thesis transient temperature distribution, thermal stresses and thermal stress intensity factors (TSIFs) of an infinitely long functionally graded material (FGM) strip containing periodic cracks under thermal shock are studied. Thermal shock is applied by imposing a sudden change in the boundary temperatures. Solution of the present thermoelasticity problem is considered in three successive steps. First the thermal (conduction) problem is solved and the transient temperature distribution is determined. This is followed by the determination of thermal stresses by solving quasi-static elasticity problem. In the last step thermal stress intensity factors (TSIFs) are calculated.

In this work, the main focus is the calculation of the transient temperature distribution and the resulting thermal stresses. Since the thermomechanical properties are considered to be functions of a spatial variable, a perturbation technique developed in [1] and [2] is adopted to find an analytical solution of transient heat conduction equation in Laplace domain. Inverse Laplace transformation is achieved by using "residue theorem". After numerically calculating the transient temperature distribution, thermal

stresses are computed in the absence of any cracks for the FGM strip subjected to thermal shock. Then, by introducing the thermal stresses as the crack surface tractions in the singular integral equation which is derived in an earlier thesis [3], the TSIFs are determined.

Keywords: functionally graded material, FGM, transient temperature distribution, thermal stress, periodic cracks, thermal stress intensity factor

ÖZ

FONKSİYONEL DERECELENDİRİLMİŞ MALZEMELERDE ISIL GERİLME PROBLEMLERİ

Akdoğan, Esra Nur
Yüksek Lisans, Makina Mühendisliği Bölümü
Tez Yöneticisi: Prof. Dr. Fevzi Suat Kadıoğlu

Eylül 2019 , 141 sayfa

Bu tezde, periyodik çatlaklar içeren sonsuz uzunluktaki fonksiyonel derecelendirilmiş malzemeden (FDM) bir levhanın kararsız sıcaklık dağılımı, ısıl gerilmeleri ve ısıl gerilme şiddeti faktörleri incelenmiştir. Isıl şok, sınır sıcaklıklarına ani bir değişiklik empoze edilerek uygulanmıştır. Mevcut termoelastisite probleminin çözümü birbirini takip eden üç adımda ele alınmıştır. İlk olarak ısıl problem (ısıl iletim problemi) çözülmüş ve kararsız sıcaklık dağılımı belirlenmiştir. Bunu yarı-statik elastisite problemi çözülerek ısıl gerilmelerin belirlenmesi takip etmiştir. Son adımda ise ısıl gerilme şiddeti faktörleri hesaplanmıştır.

Bu çalışmada asıl odak, kararsız sıcaklık dağılımının ve buna bağlı ortaya çıkan ısıl gerilmelerin hesaplanmasıdır. Termomekanik özellikler konum değişkeninin bir fonksiyonu olarak düşünüldüğünden, Laplace dönüşüm uzayında kararsız ısı iletimi denkleminin analitik bir çözümünü bulmak için [1] ve [2] çalışmalarında geliştirilen bir pertürbasyon tekniği benimsenmiştir. Ters Laplace dönüşümü "artık teoremi" kullanılarak bulunur. Kararsız sıcaklık dağılımının sayısal olarak hesaplanmasından sonra, ısıl şoka maruz kalan ve herhangi bir çatlak bulundurmayan FDM şeridi için ısıl ge-

rilmeler hesaplanmıştır. Daha sonra ise bulunmuş ısıl gerilmelerini daha önceki dönemlerde yazılan bir tezdeki [3] tekil integral denklemine çatlak yüzeyi yükleri olarak tanıtmak suretiyle, TSIF'ler belirlenmiştir.

Anahtar Kelimeler: fonksiyonel derecelendirilmiş malzeme, FDM, karasız sıcaklık dağılımı, ısıl gerilme, periyodik çatlak, ısıl gerilme şiddeti faktörü

This page is left blank intentionally

ACKNOWLEDGMENTS

First and foremost I express my sincere appreciations to professor Fevzi Suat Kadıoğlu for allowing me to conduct this study under his supervision. From the very beginning of this study he always guided me excellently, provided encouragement and patience continuously. As a supervisor he always allocated time, made constructive observations, gave helpful comments and suggestions to shape and improve this study. It will always be an honor for me to be his graduate student.

I extend my sincere appreciations to all professors of the Department of Mechanical Engineering at Hacettepe University. During my undergraduate education I learned so much from each of them and they prepared the ground for this study to be completed. It would be unfair to ignore their contributions even if not directly.

I am also very grateful to all professors that I had opportunity to attend their classes at METU. Among them I wish to single out professors Merve Erdal, Serkan Dağ and Zafer Dursunkaya especially. This study required many advanced theoretical knowledge of their area of expertise and I had greatly benefited from what they taught me in the classes.

Special thanks go to my dear friend, colleague and mentor İlke for his unwavering support and trust. I am also very indebted to my housemate, Ayşegül, for her friendship and care during this period. Also to my old friends Ahmet and Mali, I owe a debt of gratitude to each for helping me to be a more successful student than I could on my own.

Lastly, for their unconditional love I would thank to my family. They all mean so much to me.

TABLE OF CONTENTS

LIST OF TABLES

TABLES

LIST OF FIGURES

FIGURES

LIST OF ABBREVIATIONS

FG	functionally graded
FGM	functionally graded material
FGPM	functionally graded piezo-electric material
FEM	finite element methods
SIF	stress intensity factor
TSIF	thermal stress intensity factor
1D	one dimension(-al)
2D	two dimension(-al)
3D	three dimension(-al)
ODE	ordinary differential equation

LIST OF SYMBOLS

$\lambda(x)$	thermal conductivity $[W/mK]$
$C(x)$	specific heat $[kJ/kgK]$
$\rho(x)$	density $[kg/m^3]$
$\alpha(x)$	linear expansion coefficient $[1/K]$
$E(x)$	Young's modulus $[GPa]$
$\kappa(x)$	thermal diffusivity $[m^2/s]$
$\mu(x)$	shear modulus $[GPa]$
ν	Poisson's ratio
γ	Kolosov's constant
h	thickness $[m]$
w	width $[m]$
b	crack length $[m]$
c	periodic cracks spacing $[m]$
$T(x,t)$	transient temperature distribution $[K]$
T_0	initial temperature $[K]$
T_{01}	temperature imposed at $x = 0$ $[K]$
T_{02}	temperature imposed at $x = h$ $[K]$
$\tilde{T}(x,t)$	transient temperature change $[K]$

CHAPTER 1

INTRODUCTION

1.1 Introduction to the FGMs

Functionally graded material (FGM) is an advanced composite material with the sharp interface that exists in the traditional composite materials being replaced with the gradually changing interface that helps the material to be able to survive in extreme working environments [5]. Owing to continuous (or stepwise [6]) gradient in composition, FGMs have continuously changing properties. Gradation in the material properties results in reduction of thermal and residual stresses, stress concentration factors and improvement of bonding strength, toughness, corrosion and fatigue crack growth resistance [7]. FGMs usually consist of ceramics and metals. The concept of FGM was proposed in 1984 in Japan, as a means of preparing thermal barrier coatings capable of withstanding a surface temperature of 2000K and a temperature drop of 1000K in a cross-section of less than 10 mm for aerospace structures and fusion reactors [8, 9]. The ceramic in the FGM offers thermal barrier effect and protects the metal from corrosion and oxidation and it is toughened and strengtened by the metalic constituent [10]. FGMs are currently being applied in a number of industries. The practical application examples include space shuttles, turbine wheels, thermal barrier/anti oxidant coatings, racing car brakes, pressure vessels, cutting tools, thermoelectric and piezoelectric materials, optical films [9, 11].

1.2 Literature Survey

Experiments showed that; even though the absence of sharp interfaces does alleviate problems with interface fracture, cracks still occur in FGMs [12]. As the literature is reviewed it is seen that; fracture behavior of the cracked FGMs under different loading conditions is studied by many researchers. In this literature survey, it is fundamentally focused on FGMs fracture (cracking) behavior under thermal loading or more specifically thermal shock.

Some of early reviews and investigations on FGMs performed in last decade of the 20^{th} century are included in [13–18]. In [13], some typical problem areas relating to the fracture mechanics of FGMs are considered. It is shown that the FGMs offer certain advantages over the traditional composite materials. Bao and Wang [14] come to the following conclusion that FGM coatings have high hardness and oxidation resistance and experience much lower thermal residual stress. To characterize the material, fracture toughness data is required. In order to obtain the fracture toughness data, stress intensity factors (SIFs) are needed [12]. Jin and Noda [15] studied the singular stress and heat flux at the tip of the crack. In this study it is noticed that the crack-tip field singularities and angular distributions are the same in FGMs as those in the homogeneous materials. Therefore, calculating SIFs in the FGMs is a way to examine the fracture behavior of FGMs. Tanigawa [16] described the theoretical treatment of thermoelasticity problems for nonhomogeneous and isotropic materials regarding the linearization of the nonlinear equation systems. It is noted that; as the nonhomogeneous material properties change, the thermal stress distribution and SIF change remarkably. Investigation of thermal stresses and TSIFs in the FGMs subjected to a cycle of heating and cooling [17] and to steady temperature fields or thermal shock [18] are made in order to find the optimal composition profile for decreasing thermal stress intensity factor. The results show that thermal stresses in the FGMs can be decreased when the volumetric ratio of the composition is appropriately selected.

Various researchers addressed the thermal stress problems in FGMs differently to find analytical solutions. From the literature it is seen that; there are three main types of analytical methods. The first group of researchers assumed the thermomechanical

properties to be constant or in the form of particular functions such as exponential, power law etc. In the series of articles [19–22] material properties are assumed to be exponentially dependent on the position variable. Ueda [19] studied a functionally graded piezo-electric material (FGPM) contains a finite crack perpendicular to its boundaries, subjected to pure thermal shock. The integral transform methods are used to formulate the problem in terms of a singular integral equation. In [20] Ueda studied an FGPM containing an embedded crack or an edge crack subjected to thermal shock under mode-I mechanical loading. The articles [19, 20] show that increasing the nonhomogeneity parameter results in decreasing TSIFs for the lower crack tip of the embedded crack and for the crack tip of the edge crack, whereas decreasing the nonhomogeneity parameter reduces the TSIFs of the embedded crack due to the heating and of the edge crack due to cooling. Ueda and Ashida [21] analyzed an FGPM with an infinite row of parallel cracks under static mechanical and transient thermal loading. By using the Laplace and Fourier transforms, the thermoelectromechanical problem is reduced to a singular integral equation. TSIFs for both the embedded and edge cracks are computed. Very recently Ueda and Nakano [22] considered FG thermal barrier coating and calculated SIF for the various values of the nonhomogeneous and geometric parameters. In [21, 22] numerical results show that; SIFs are lowered by the interaction among cracks and they depend on geometric and material properties. Besides, increasing the nonhomogeneity parameter reduces SIFs in FGMs under pure mechanical loading whereas decreasing the nonhomogeneity parameter also reduces the TSIFs under pure thermal load. Dag et al. [23] examined orthotropic FGM under mechanical and thermal loading conditions with the assumption of mechanical properties to be exponential functions and the thermal properties to be constant. It is shown that the influence of material nonhomogeneity parameter is dependent on the relative location of the crack and the type of the external boundary conditions. In, [3] the influences of grading, crack length and cracks spacing are investigated in an FG layer containing periodic cracks under thermal shock. Young's modulus and thermal conductivity are considered to be exponentially varying whereas the thermal diffusivity is considered to be constant. Ding and Li [24] investigated a functionally graded (FG) layered structure with an interface crack under thermal loading. The effect of the material nonhomogeneity parameters and dimensionless thermal resistance on TSIFs are investigated. B.Yıldırım et al. [25] considered periodically

cracked FGM half plane under various loading conditions including thermal shock under the assumption of constant thermal diffusivity. It is observed that for a stiffening half plane with increasing coefficient of thermal expansion, TSIFs are greater than those of a homogeneous half plane, as for a softening half plane with decreasing coefficient of thermal expansion, TSIFs are lower than those of a homogeneous half plane. Recently A.Yıldırım et al. [26] solved the thermal stresses in axisymmetric thin FG annular fin analytically assuming the material properties to be graded along the fin radius as a power-law function. A steady state thermal distribution is considered. Thermal conductivity parameter has an inversely proportional effect on both temperature gradient and thermal stresses, whereas modulus of elasticity parameter has a directly proportional effect only on the thermal stresses. Increase in thermal expansion coefficient parameter causes an increase in radial stress as a tensile stress and decrease in linear thermal expansion coefficient causes an increase in radial stress as a compressive stress.

Second group of researchers used the analytical methods with general thermomechanical properties to obtain the transient thermal distribution. Here by "general thermomechanical properties" it is meant that, without using some particular functions such as exponential, power law etc. (which facilitate the closed form solutions of governing differential equations) for the variation of thermomechanical properties, an analytical solution is found. Since transient heat conduction equation requires the thermal conductivity, specific heat and density to be substituted in, these properties are defined as functions of a spatial variable. However there are very few analytical methods that can be used to solve thermal shock problem of an FGM with general thermomechanical properties [1]. When general thermomechanical properties are considered, a perturbation technique is developed by artificially introducing a small parameter for the sake of the solution. In a series of articles [1, 2, 27, 28], Noda and his coworkers introduced and applied the perturbation technique that they developed to the thermal shock problems of FGM plates and cylinders which are modeled as plates on an elastic foundation. They provided the details of the developed analytical method and presented extensive numerical results for transient temperature distributions and TSIFs for edge cracks by assuming different thermomechanical property variations. It is found that perturbation solutions with two terms (zeroth and first order) can ap-

proximate the exact result (when it is available for some special thermomechanical property variations) very well. The numerical results show that the thermal shock is much more potent to result in failure than the steady thermal loading, the TSIF gets to a large peak value at early times following the thermal shock and then tends to the steady state value. This phenomenon implies that the thermal shock can introduce a dangerous state which may result in fracture failure. In [1], different from the [2, 28], a piecewise model is also developed to deal with the general mechanical properties. Jun et al. [29] derived unsteady temperature field and thermal stress field for an uncracked FGM plate with symmetrical structure by using same perturbation method as in [1, 2, 27, 28]. Under surface cooling at the steady state, the residual compressive stress is generated in the surface region of the strip, while the residual tensile stress is generated in the middle region since the thermal expansion coefficient of the surface region is lower than that of the middle region. In the case of surface cooling and heating, the absolute values of the thermal stresses of FGM strip are always lower than those of the conventional ceramic strips.

Third group of researchers studied FGM by using layer-wise theories. Wang and Mai [30] analyzed multiple surface cracking to study thermal shock resistance behavior of temperature dependent FGM by using finite element method (FEM). It is found that thermal stresses and TSIFs can be reduced considerably by reducing crack spacing. The thermal shock strength of the FGMs can be improved considerably by increasing metal contents in the FGMs and as the cracks become longer, thermal shock resistance behavior prevails. Jin and Paulino [31] employed homogeneous multi-layered material model assuming that the Young's modulus and Poisson's ratio to be constant for each layer of the FGM strip. In this study, the effects of the various volume fraction profiles on TSIFs are investigated. Considering the general thermomechanical properties, Pan et al. [32] recently reduced the thermal stress problem in a cracked FGM strip to a perturbation problem by using nonhomogeneous multilayered method. In this work, the temperature distribution is assumed to be steady, and material properties are varying along the thickness direction as the cracks in the strip are located colinear in the same direction. The results show that the variation characteristics of the TSIFs corresponding to different types of material properties may be different, namely one should not assume the variation of thermomechanical

properties to be only as exponential functions to analyze the crack problems of FGMs. Zhang et al. [33] studied an FGP by developing a domain-independent interaction energy integral method to solve the crack problem. Here the transient thermal distribution is calculated by using the same perturbation method in [1, 2, 27, 28] as well. The TSIFs at the early stages of thermal shock is dominant factor in fracture failure; the distribution patterns of material properties may have different effects on the peak values and steady values of the TSIFs and hence, the structural design of FGPMs under thermal loadings should consider the property distribution patterns. Nikolarakis and Theotokoglou [34] considered three-layered FG strip under uniform thermal loading. It is observed that the variation of the relaxation times of the materials has significant influence on the thermomechanical response of the layer.

Some researchers studied the FGMs in higher dimensions. Liu et al. [35] analyzed a three-dimensional FG piezoelectric spherical shell subjected to various thermal boundary conditions. Thermal field is resolved by using the state space method. It is seen that inhomogeneity parameter has a significant effect on the distributions of stresses and electric displacements in the sphere. Alibeigloo [36] investigated an FG solid and annular circular plate subjected to thermomechanical loading. Steady thermal field is derived by differential qudrature in radial direction and state-space method along the thickness direction. The plate is assumed to be transversely isotropic and the thermoelastic properties to be exponentially dependent on the position. The results reveal that the variations of material properties in the thickness direction affect the thermoelastic behavior of plate. Ohmici et al. [37] considered plane heat conduction problems for two-dimensional FG orthotropic materials assuming the material properties to be exponentially varying. Guo et al. [38] analyzed the nonhomogeneous piezoelectric materials under thermal loading by interaction energy integral method. The 2D steady temperature field is determined by using FEM. It is found that mechanical, electrical, and thermal property mismatch at the interface, crack angle and the temperature boundary condition can significantly influence the TSIFs and electric displacement intensity factor. Tokovyy and Ma [39] proposed a new technique to analyze the three dimensional heat conduction and thermoelasticity problems for an inhomogeneous layer. Temperature field is assumed to be steady and it is calculated by solving Fourier double-integral transformation. Pawar et al. [40] analyzed an FG

solid sphere under the assumption of exponentially varying properties. In that work the transient thermal distribution is considered. It is observed that the nonuniform heat source influences the temperature distribution and the stresses.

Feng and Jin [41] considered an Al_2O_3/Si_3N_4 FGM plate with parallel surface cracks of alternating lengths subjected to thermal shocks. It is shown that; smaller crack spacing and larger initial crack length leads to higher residual strength, which means the higher load carrying capacity [42], thermal shock residual strength of the FGM plate undergoes a small sudden increase at a thermal shock and the FGM with smaller density gradation enhances both critical thermal shock and the residual strength for the shocked FGM.

As seen in the literature, TSIFs in FGMs are calculated mostly under the assumption that the material gradation is varying as a particular known function (e.g., exponential or power law). Since Gu and Asaro [12] and Tanigawa [16] showed that material gradients have strong effects on the stress intensity factors and the phase angle, which measures mode mixity, i.e., the proportion of the shear traction to the normal traction ahead of the crack tip; certain assumed property distributions must be used with care as they are not physically realizable for certain material combination [43].

1.3 Scope of this Study

In [21, 25] an FGM (or FGPM) strip containing periodic cracks subjected to thermal shock is studied under the assumption of both thermal and mechanical properties to be exponentially graded. However with general thermal properties, the periodic cracking of an FGM layer under thermal shock has not been studied yet to the best of author's knowledge. The scope of this study is to find analytical solution for transient temperature distribution and resulting thermal stresses of an infinitely long functionally graded material (FGM) strip containing periodic cracks under thermal shock with general thermomechanical properties. As in previous studies dealing with the general thermal properties, a perturbation technique which is developed in [27] and applied in [1,2,28] will be used to solve the conduction problem. Thermal stress intensity factors (TSIFs) are then calculated by using exponential Young's modulus variation.

CHAPTER 2

TRANSIENT TEMPERATURE DISTRIBUTION

2.1 Problem Description and Mathematical Formulation

An infinitely long FGM strip with periodic surface cracks is shown in Figure 2.1. Its thermomechanical properties are position dependent and varying along only the thickness direction, i.e., the x-axis. The thermal conductivity, specific heat, density, linear expansion coefficient, shear modulus, Young's modulus, and Poisson's ratio are defined as $\lambda(x)$, $C(x)$, $\rho(x)$, $\alpha(x)$, $\mu(x)$, $E(x)$ and v, respectively. In many papers in literature Poisson's ratio is usually considered to be constant [28]. Periodic cracks are perpendicular to both surfaces. The initial temperature of the strip is T_0. As it is subjected to a thermal shock; the boundary surfaces of the strip are abruptly subjected to the constant temperature changes T_{01} and T_{02}.

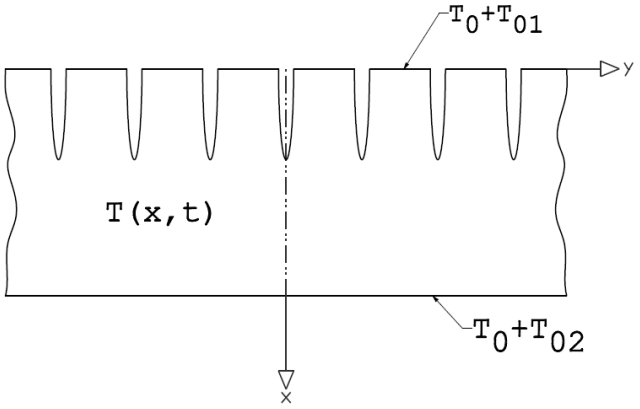

Figure 2.1: Periodically cracked FGM strip at an initial temperature T_0 subjected to thermal shock

The thermoelasticity problem stated above and shown in Figure 2.1 can be addressed by successively solving a thermal and an elasticity problem. These two subproblems with geometric dimensions are depicted in Figure 2.2a and 2.2b, respectively.

In the following; the thermal and the elasticity problem will be solved in order. To give some more details; first the transient temperature distribution for the uncracked FGM strip with thickness h, will be obtained. Then the resulting thermal stresses for the uncracked strip are determined. Finally TSIFs for the cracked strip are calculated by applying the opposite of the transient thermal stresses as crack surface tractions.

Let the transient temperature distribution be $T(x,t)$, the transient temperature change may then be defined as

$$\tilde{T}(x,t) = T(x,t) - T_0 \tag{2.1.1}$$

So the transient temperature distribution in terms of transient temperature change is determined by solving the heat conduction equation

$$\frac{\partial}{\partial x}\left\{\lambda(x)\frac{\partial \tilde{T}(x,t)}{\partial x}\right\} = C(x)\rho(x)\frac{\partial \tilde{T}(x,t)}{\partial t} \tag{2.1.2}$$

The boundary conditions are (for $t > 0$)

$$\tilde{T}(x,t)\Big|_{x=0} = T_{01} \tag{2.1.3a}$$

$$\tilde{T}(x,t)\Big|_{x=h} = T_{02} \tag{2.1.3b}$$

where T_{01} and T_{02} are constant imposed boundary temperature changes from the initial temperature T_0. Initial condition is (for $0 < x < h$)

$$\tilde{T}(x,t)\Big|_{t=0} = 0 \tag{2.1.4}$$

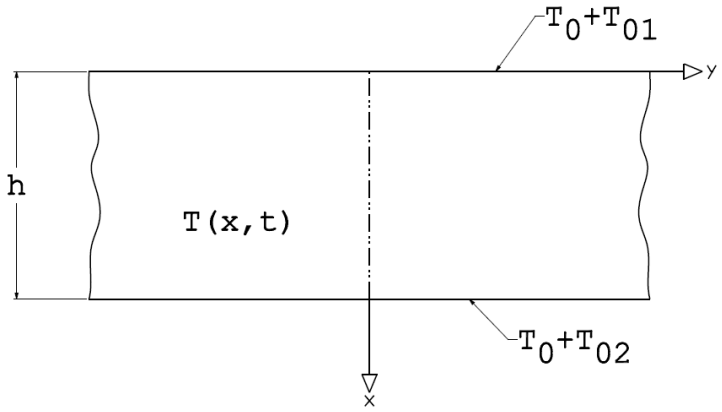

(a)

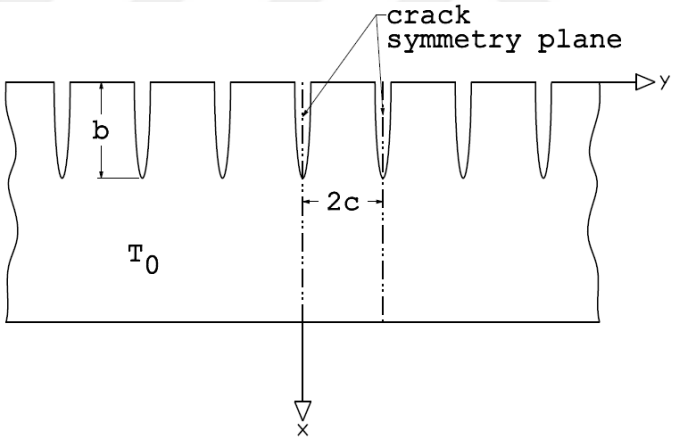

(b)

Figure 2.2: Depictions of the thermal problem of crack-free FGM strip under thermal shock (a) and the elasticity problem with geometry of periodic cracks (b)

Equation (2.1.2) may be expanded as follows

$$\frac{d\lambda(x)}{dx}\frac{\partial\tilde{T}(x,t)}{\partial x}+\lambda(x)\frac{\partial^2\tilde{T}(x,t)}{\partial x^2}=C(x)\rho(x)\frac{\partial\tilde{T}(x,t)}{\partial t}$$

Dividing both sides by $C(x)\rho(x)$ gives

$$\frac{1}{C(x)\rho(x)}\frac{d\lambda(x)}{dx}\frac{\partial\tilde{T}(x,t)}{\partial x}+\frac{\lambda(x)}{C(x)\rho(x)}\frac{\partial^2\tilde{T}(x,t)}{\partial x^2}=\frac{\partial\tilde{T}(x,t)}{\partial t} \tag{2.1.5}$$

To solve the transient heat conduction equation (2.1.5), following the studies [1,2,28] an auxiliary variable is introduced

$$\xi(x)=\int_0^x\frac{1}{\sqrt{\kappa(r)}}dr \tag{2.1.6}$$

where

$$\kappa(r)=\frac{\lambda(r)}{C(r)\rho(r)},\qquad 0\leq r\leq x \tag{2.1.7}$$

κ is known as thermal diffusivity. Recalling the first and second order chain rule

$$\frac{\partial}{\partial x}=\frac{d\xi}{dx}\frac{\partial}{\partial\xi}\quad\text{and}\quad\frac{\partial^2}{\partial x^2}=\frac{\partial}{\partial x}\frac{\partial}{\partial x}=\frac{d\xi}{dx}\frac{\partial}{\partial\xi}\left\{\frac{d\xi}{dx}\frac{\partial}{\partial\xi}\right\}$$

and applying them to (2.1.5) gives

$$\frac{1}{C(\xi)\rho(\xi)}\frac{d\xi}{dx}\frac{d\lambda(\xi)}{d\xi}\frac{d\xi}{dx}\frac{\partial\tilde{T}(\xi,t)}{\partial\xi}+\frac{\lambda(\xi)}{C(\xi)\rho(\xi)}\frac{d\xi}{dx}\frac{\partial}{\partial\xi}\left\{\frac{d\xi}{dx}\frac{\partial\tilde{T}(\xi,t)}{\partial\xi}\right\}=\frac{\partial\tilde{T}(\xi,t)}{\partial t} \tag{2.1.8}$$

According to the fundamental theorem of differential calculus [44], the following equation may be written

$$\frac{d\xi}{dx}=\frac{1}{\sqrt{\kappa(x)}}=\sqrt{\frac{C(x)\rho(x)}{\lambda(x)}}$$

(2.1.8) then becomes

$$\frac{1}{C(\xi)\rho(\xi)}\sqrt{\frac{C(\xi)\rho(\xi)}{\lambda(\xi)}}\frac{d\lambda(\xi)}{d\xi}\sqrt{\frac{C(\xi)\rho(\xi)}{\lambda(\xi)}}\frac{\partial\tilde{T}}{\partial\xi} + \frac{\lambda(\xi)}{C(\xi)\rho(\xi)}\sqrt{\frac{C(\xi)\rho(\xi)}{\lambda(\xi)}}\frac{\partial}{\partial\xi}\left\{\sqrt{\frac{C(\xi)\rho(\xi)}{\lambda(\xi)}}\frac{\partial\tilde{T}(\xi,t)}{\partial\xi}\right\} = \frac{\partial\tilde{T}(\xi,t)}{\partial t}$$

Doing mathematical calculations and simplifications give

$$\frac{1}{\lambda(\xi)}\frac{d\lambda(\xi)}{d\xi}\frac{\partial\tilde{T}(\xi,t)}{\partial\xi}+\sqrt{\frac{\lambda(\xi)}{C(\xi)\rho(\xi)}}\left\{\frac{\partial}{\partial\xi}\sqrt{\frac{C(\xi)\rho(\xi)}{\lambda(\xi)}}\frac{\partial\tilde{T}(\xi,t)}{\partial\xi}+\sqrt{\frac{C(\xi)\rho(\xi)}{\lambda(\xi)}}\frac{\partial^2\tilde{T}}{\partial\xi^2}\right\} = \frac{\partial\tilde{T}(\xi,t)}{\partial t}$$

and it reduces to

$$\frac{\partial^2\tilde{T}(\xi),t}{\partial\xi^2}+\left\{\frac{1}{\lambda(\xi)}\frac{d\lambda(\xi)}{d\xi}+\sqrt{\frac{\lambda(\xi)}{C(\xi)\rho(\xi)}}\frac{d}{d\xi}\sqrt{\frac{C(\xi)\rho(\xi)}{\lambda(\xi)}}\right\}\frac{\partial\tilde{T}(\xi,t)}{\partial\xi} = \frac{\partial\tilde{T}(\xi,t)}{\partial t} \tag{2.1.9}$$

where

$$\frac{1}{\lambda(\xi)}\frac{d\lambda(\xi)}{d\xi} = \frac{d}{d\xi}\ln\lambda(\xi)$$

and

$$\sqrt{\frac{\lambda(\xi)}{C(\xi)\rho(\xi)}}\frac{d}{d\xi}\sqrt{\frac{C(\xi)\rho(\xi)}{\lambda(\xi)}} = \frac{d}{d\xi}\ln\sqrt{\frac{C(\xi)\rho(\xi)}{\lambda(\xi)}}$$

(2.1.9) may then be written as

$$\frac{\partial^2\tilde{T}(\xi,t)}{\partial\xi^2}+\left\{\frac{d}{d\xi}\ln\lambda(\xi)+\frac{d}{d\xi}\ln\sqrt{\frac{C(\xi)\rho(\xi)}{\lambda(\xi)}}\right\}\frac{\partial\tilde{T}(\xi,t)}{\partial\xi} = \frac{\partial\tilde{T}(\xi,t)}{\partial t}$$

Using (A.1) from Appendix section gives

$$\frac{\partial^2 \tilde{T}(\xi,t)}{\partial \xi^2} + \left\{ \frac{d}{d\xi} \ln \left(\lambda(\xi) \sqrt{\frac{C(\xi)\rho(\xi)}{\lambda(\xi)}} \right) \right\} \frac{\partial \tilde{T}(\xi,t)}{\partial \xi} = \frac{\partial \tilde{T}(\xi,t)}{\partial t}$$

After simplification, the following equation is obtained

$$\frac{\partial^2 \tilde{T}(\xi,t)}{\partial \xi^2} + \left\{ \frac{d}{d\xi} \ln \left(\sqrt{\lambda(\xi) C(\xi) \rho(\xi)} \right) \right\} \frac{\partial \tilde{T}(\xi,t)}{\partial \xi} = \frac{\partial \tilde{T}(\xi,t)}{\partial t}$$

Defining

$$\eta(\xi) = \sqrt{\lambda(\xi) C(\xi) \rho(\xi)} \tag{2.1.10}$$

yields the final form of transient heat conduction equation in terms of $\xi(x)$ as follows

$$\frac{\partial^2 \tilde{T}(\xi,t)}{\partial \xi^2} + \frac{d}{d\xi} \ln \left[\eta(\xi) \right] \frac{\partial \tilde{T}(\xi,t)}{\partial \xi} = \frac{\partial \tilde{T}(\xi,t)}{\partial t} \tag{2.1.11}$$

Boundary conditions (2.1.3a), (2.1.3b) and the initial condition (2.1.4) may then be redefined below in terms of $\xi(x)$

$$\tilde{T}(\xi,t)\Big|_{\xi=\xi_0} = T_{01} \tag{2.1.12a}$$

$$\tilde{T}(\xi,t)\Big|_{\xi=\xi_h} = T_{02} \tag{2.1.12b}$$

$$\tilde{T}(\xi,t)\Big|_{t=0} = 0 \tag{2.1.13}$$

where

$$\xi_0 = \xi(0) = 0$$

and

$$\xi_h = \xi(h) = \int_0^h \frac{1}{\sqrt{\kappa(r)}} dr$$

Considering the homogeneous initial condition (2.1.13), Laplace transform is applied to (2.1.11) and the transient heat conduction equation in Laplace domain becomes

$$\frac{\partial^2}{\partial \xi^2}\tilde{T}^*(\xi,p) + \frac{\partial}{\partial \xi}\ln\left[\eta(\xi)\right]\frac{\partial}{\partial \xi}\tilde{T}^*(\xi,p) - p\tilde{T}^*(\xi,p) + \tilde{T}(\xi,0) = 0 \qquad (2.1.14)$$

where p is the Laplace transform variable and

$$\tilde{T}^*(\xi,p) = \mathcal{L}\left\{\tilde{T}(\xi,t)\right\} = \int_0^\infty \tilde{T}(\xi,t)e^{-pt}dt$$

2.2 Perturbation Method

Since the FGM strip has general properties varying along its thickness, it may not be possible to solve equation (2.1.14) directly. Therefore, the *perturbation method* developled in [27] is applied by introducing a small, non-zero and arbitrary parameter δ and a function of position $w(\xi)$, where

$$\delta w(\xi) = \frac{d}{d\xi}\ln\left[\eta(\xi)\right] \qquad (2.2.1)$$

Note that δ is not an actual parameter of the problem under consideration. It is introduced for the sake of the solution. By substituting (2.2.1) into (2.1.14), the perturbed equation which is used to construct an approximate solution is obtained as follows

$$\frac{\partial^2}{\partial \xi^2}\tilde{T}^*(\xi,p) + \delta w(\xi)\frac{\partial}{\partial \xi}\tilde{T}^*(\xi,p) - p\tilde{T}^*(\xi,p) + \tilde{T}(\xi,0) = 0 \qquad (2.2.2)$$

Assuming a solution of the following form

$$\tilde{T}^*(\xi,p)=\sum_{m=0}^{\infty}\delta^m\tilde{T}_m^*(\xi,p)=\delta^0\tilde{T}_0^*(\xi,p)+\delta^1\tilde{T}_1^*(\xi,p)+\delta^2\tilde{T}_2^*(\xi,p)+O(\delta^3)\cdots \tag{2.2.3}$$

Unknowns $\tilde{T}_0^*(\xi,p)$, $\tilde{T}_1^*(\xi,p)\cdots$ are to be solved recursively. Substituting (2.1.13) and the assumed series solution (2.2.3) which contains the δ parameter, into the perturbed equation (2.2.2) and grouping the terms which contain the identical powers of δ, the following expression is obtained, where, for clarity, only a three terms expansion is considered

$$\frac{\partial^2}{\partial\xi^2}\left\{\delta^0\tilde{T}_0^*+\delta^1\tilde{T}_1^*+\delta^2\tilde{T}_2^*\right\}+\delta w(\xi)\frac{\partial}{\partial\xi}\left\{\delta^0\tilde{T}_0^*+\delta^1\tilde{T}_1^*+\delta^2\tilde{T}_2^*\right\}$$
$$-p\left\{\delta^0\tilde{T}_0^*+\delta^1\tilde{T}_1^*+\delta^2\tilde{T}_2^*\right\}=0$$

Expanding all the terms

$$\delta^0\frac{\partial^2\tilde{T}_0^*}{\partial\xi^2}+\delta^1\frac{\partial^2\tilde{T}_1^*}{\partial\xi^2}+\delta^2\frac{\partial^2\tilde{T}_2^*}{\partial\xi^2}+\delta^1 w\frac{\partial\tilde{T}_0^*}{\partial\xi}+\delta^2 w\frac{\partial\tilde{T}_1^*}{\partial\xi}+\delta^3 w\frac{\partial\tilde{T}_2^*}{\partial\xi}$$
$$-p\delta^0\tilde{T}_0^*-p\delta^1\tilde{T}_1^*-p\delta^2\tilde{T}_2^*=0$$

and then collecting the terms with identical powers of δ

$$\delta^0\left\{\frac{\partial^2\tilde{T}_0^*}{\partial\xi^2}-p\tilde{T}_0^*\right\}+\delta^1\left\{\frac{\partial^2\tilde{T}_1^*}{\partial\xi^2}+w\frac{\partial\tilde{T}_0^*}{\partial\xi}-p\tilde{T}_1^*\right\}+\delta^2\left\{\frac{\partial^2\tilde{T}_2^*}{\partial\xi^2}+w\frac{\partial\tilde{T}_1^*}{\partial\xi}-p\tilde{T}_2^*\right\}$$
$$+\delta^3 w\cancel{\left\{\frac{\partial\tilde{T}_2^*}{\partial\xi}+\cdots\right\}}^{neglected}=0 \tag{2.2.4}$$

Since δ is assumed to be small, δ^3 is negligibly small. If δ^3 term was introduced, there would be more terms in (2.2.4). Since δ is a small but a non-zero and arbitrary parameter, the only way (2.2.4) could be satisfied, is if each coefficient of δ^m is equal to zero, such that

$$\delta^0 \left\{ \frac{\partial^2 \tilde{T}_0^*}{\partial \xi^2} - p\tilde{T}_0^* \right\} = 0 \qquad \rightarrow \qquad \frac{\partial^2 \tilde{T}_0^*}{\partial \xi^2} - p\tilde{T}_0^* = 0$$

$$\delta^1 \left\{ \frac{\partial^2 \tilde{T}_1^*}{\partial \xi^2} + w\frac{\partial \tilde{T}_0^*}{\partial \xi} - p\tilde{T}_1^* \right\} = 0 \qquad \rightarrow \qquad \frac{\partial^2 \tilde{T}_1^*}{\partial \xi^2} - p\tilde{T}_1^* = -w\frac{\partial \tilde{T}_0^*}{\partial \xi}$$

$$\delta^2 \left\{ \frac{\partial^2 \tilde{T}_2^*}{\partial \xi^2} + w\frac{\partial \tilde{T}_1^*}{\partial \xi} - p\tilde{T}_2^* \right\} = 0 \qquad \rightarrow \qquad \frac{\partial^2 \tilde{T}_2^*}{\partial \xi^2} - p\tilde{T}_2^* = -w\frac{\partial \tilde{T}_1^*}{\partial \xi}$$

At this point, one homogeneous linear ordinary differential equation (ODE) which is *unperturbed* and two nonhomogeneous linear ODEs which are *perturbed* are obtained. As attentive readers may notice; each nonhomogeneous linear ODE shows the same trend of homogeneous part. For the perturbed equations, the right hand sides may be solved recursively. Now by induction, considering the last two equations, for a general power of δ, namely δ^m

$$\frac{\partial^2 \tilde{T}_m^*}{\partial \xi^2} - p\tilde{T}_m^* = -w\frac{\partial \tilde{T}_{m-1}^*}{\partial \xi} \qquad m \geq 1$$

This equation is to be solved recursively. For instance, since $\tilde{T}_2^*$ depends on $\tilde{T}_1^*$ one can not find the solution of $\tilde{T}_2^*$ before finding $\tilde{T}_1^*$. This applies for every $\tilde{T}_m^*$ as $m \geq 1$. Multiplying both sides of the equation above with δ^m which is a constant gives

$$\delta^m \frac{\partial^2 \tilde{T}_m^*}{\partial \xi^2} - p\delta^m \tilde{T}_m^* = -w\delta^m \frac{\partial \tilde{T}_{m-1}^*}{\partial \xi}$$

or more conveniently [17]

$$\delta^m \frac{\partial^2 \tilde{T}_m^*}{\partial \xi^2} - p\delta^m \tilde{T}_m^* = -\delta w \frac{\partial \delta^{m-1} \tilde{T}_{m-1}^*}{\partial \xi}$$

Finally the equations are generalized in the Laplace domain as follows

$$\frac{\partial^2 \tilde{T}_0^*(\xi, p)}{\partial \xi^2} - p\tilde{T}_0^*(\xi, p) = 0 \qquad m = 0 \qquad \text{(2.2.5a)}$$

$$\frac{\partial^2 \delta^m \tilde{T}_m^*(\xi,p)}{\partial \xi^2} - p\delta^m \tilde{T}_m^*(\xi,p) = -\delta w(\xi)\frac{\partial \delta^{m-1}\tilde{T}_{m-1}^*(\xi,p)}{\partial \xi} \qquad m \geq 1 \qquad (2.2.5b)$$

That is the *perturbation method* that is adopted to find the analytical solution of the transient heat conduction equation. Now by solving the terms $\delta^m \tilde{T}_m^*(\xi,p)$ and substituting them into (2.2.3) the solution can be constructed. By applying Laplace transform to the boundary conditions (2.1.12a), (2.1.12b)

$$\tilde{T}^*(\xi,p)\Big|_{\xi=\xi_0} = \mathcal{L}\left\{\tilde{T}(\xi,t)\Big|_{\xi=\xi_0}\right\} = \mathcal{L}\left\{T_{01}\right\} = \int_0^\infty T_{01}e^{-pt}dt$$
$$= -T_{01}\frac{e^{-pt}}{p}\Big|_0^\infty = 0 - \frac{-T_{01}}{p} = \frac{T_{01}}{p}$$

$$\tilde{T}^*(\xi,p)\Big|_{\xi=\xi_h} = \mathcal{L}\left\{\tilde{T}(\xi,t)\Big|_{\xi=\xi_h}\right\} = \mathcal{L}\left\{T_{02}\right\} = \int_0^\infty T_{02}e^{-pt}dt$$
$$= -T_{02}\frac{e^{-pt}}{p}\Big|_0^\infty = 0 - \frac{-T_{02}}{p} = \frac{T_{02}}{p}$$

boundary conditions in Laplace domain are obtained. The nonhomogeneous boundary conditions are to be satisfied by the unperturbed solution. So, for $m = 0$

$$\tilde{T}_0^*(\xi_0,p) = \frac{T_{01}}{p} \qquad (2.2.6a)$$

$$\tilde{T}_0^*(\xi_h,p) = \frac{T_{02}}{p} \qquad (2.2.6b)$$

On the other hand, perturbed solutions will be obtained by applying the homogeneous boundary conditions. So for $m \geq 1$

$$\delta^m \tilde{T}_m^*(\xi_0,p) = 0 \qquad (2.2.7a)$$

$$\delta^m \tilde{T}_m^*(\xi_h, p) = 0 \tag{2.2.7b}$$

Thus the overall solution of (2.2.3) satisfies the boundary conditions. By applying the respective boundary conditions in Laplace domain, (2.2.5a) and (2.2.5b) are to be solved respectively.

2.3 Solutions of ODEs in Laplace Transform Domain

2.3.1 Solution of $\tilde{T}_0^*(\xi, p)$

Since (2.2.5a) is a homogeneous linear ODE, a solution is sought in the form of

$$\tilde{T}_0^* = e^{k\xi} \tag{2.3.1}$$

Substituting (2.3.1) into (2.2.5a) gives

$$k^2 e^{k\xi} - p e^{k\xi} = 0$$

The characteristic equation is then obtained as

$$k^2 - p = 0$$

Solving the characteristic equation gives

$$k_1 = \sqrt{p} \quad \text{and} \quad k_2 = -\sqrt{p}$$

The solution of (2.2.5a) is then obtained as follows

$$\tilde{T}_0^*(\xi, p) = A e^{\sqrt{p}\xi} + B e^{-\sqrt{p}\xi}$$

where A and B are arbitrary coefficients to be obtained by applying (2.2.6a) and (2.2.6b). Considering (A.2) and (A.3) $\tilde{T}_0^*(\xi, p)$ may also be written as

$$\tilde{T}_0^*(\xi, p) = C_1 \sinh(\sqrt{p}\xi) + C_2 \cosh(\sqrt{p}\xi) \tag{2.3.2}$$

To find a solution, any of these forms may be used, however considering (2.2.6a) and (2.2.6b), it may be seen that calculating C_1 and C_2 is easier than calculating A and B. Therefore applying (2.2.6a) to (2.3.2) gives

$$\tilde{T}_0^*(0, p) = C_1 \cancelto{0}{\sinh(0)} + C_2 \cancelto{1}{\cosh(0)} = \frac{T_{01}}{p}$$

which leads to

$$C_2 = \frac{T_{01}}{p}$$

By substituting C_2, updated version of (2.3.2) may then be written as

$$\tilde{T}_0^*(\xi, p) = C_1 \sinh(\sqrt{p}\xi) + \frac{T_{01}}{p} \cosh(\sqrt{p}\xi) \tag{2.3.3}$$

Applying (2.2.6b) to (2.3.3) then gives

$$\tilde{T}_0^*(\xi_h, p) = C_1 \sinh(\sqrt{p}\xi_h) + \frac{T_{01}}{p} \cosh(\sqrt{p}\xi_h) = \frac{T_{02}}{p} \tag{2.3.4}$$

which yields the following result

$$C_1 = \frac{T_{02} - T_{01} \cosh(\sqrt{p}\xi_h)}{p \sinh(\sqrt{p}\xi_h)}$$

By substituting C_1 into (2.3.3), $\tilde{T}_0^*(\xi, p)$ is obtained as follows

$$\tilde{T}_0^*(\xi, p) = \frac{T_{02} - T_{01} \cosh(\sqrt{p}\xi_h)}{p \sinh(\sqrt{p}\xi_h)} \sinh(\sqrt{p}\xi) + \frac{T_{01}}{p} \cosh(\sqrt{p}\xi)$$

which may be expanded as

$$\tilde{T}_0^*(\xi,p)=\frac{T_{02}\sinh(\sqrt{p}\xi)-T_{01}\left\{\sinh(\sqrt{p}\xi)\cosh(\sqrt{p}\xi_h)-\sinh(\sqrt{p}\xi_h)\cosh(\sqrt{p}\xi)\right\}}{p\sinh(\sqrt{p}\xi_h)} \tag{2.3.5}$$

Using (A.4) the following equation holds

$$\sinh(\sqrt{p}\xi)\cosh(\sqrt{p}\xi_h)-\sinh(\sqrt{p}\xi_h)\cosh(\sqrt{p}\xi)=\sinh\left[\sqrt{p}(\xi-\xi_h)\right]$$

$\tilde{T}_0^*(\xi,p)$ is then obtained as follows

$$\tilde{T}_0^*(\xi,p)=\frac{T_{02}\sinh(\sqrt{p}\xi)-T_{01}\sinh\left[\sqrt{p}(\xi-\xi_h)\right]}{p\sinh(\sqrt{p}\xi_h)} \tag{2.3.6}$$

2.3.2 Solution of $\delta^m\tilde{T}_m^*(\xi,p)$ for $m\geq 1$

Before finding a solution for (2.2.5b), it is duplicated below

$$\frac{\partial^2\delta^m\tilde{T}_m^*(\xi,p)}{\partial\xi^2}-p\delta^m\tilde{T}_m^*(\xi,p)=-\delta w(\xi)\frac{\partial\delta^{m-1}\tilde{T}_{m-1}^*(\xi,p)}{\partial\xi}\qquad m\geq 1$$

Since (2.2.5b) is a nonhomogeneous linear ODE, one should find its homogeneous and particular solutions separately. Let the homogeneous solution be y_h and particular solution be y_p. So $\delta^m\tilde{T}_m^*(\xi,p)=y_h+y_p$. Starting with y_h; one may seek the solution in the form of $\delta^m\tilde{T}_m^*=e^{k\xi}$. Substituting it into (2.2.5b) gives

$$k^2e^{k\xi}-pe^{k\xi}=0$$

Thus the characteristic equation is

$$k^2-p=0$$

Solving the characteristic equation gives

$$k_1 = \sqrt{p} \quad \text{and} \quad k_2 = -\sqrt{p}$$

The solution of this ODE is then obtained in the form of

$$y_h(\xi, p) = De^{\sqrt{p}\xi} + Ee^{-\sqrt{p}\xi}$$

where D and E are arbitrary coefficients to be obtained by applying the boundary conditions. Proceeding similar to the solution of $\tilde{T}_0^*(\xi, p)$, $y_h(\xi, p)$ is as follows

$$y_h(\xi, p) = C_3 \sinh(\sqrt{p}\xi) + C_4 \cosh(\sqrt{p}\xi) \tag{2.3.7}$$

For the particular solution, *variation of parameters* technique is employed. A solution in the following form is sought

$$y_p(\xi, p) = C_3(\xi) \sinh(\sqrt{p}\xi) + C_4(\xi) \cosh(\sqrt{p}\xi) \tag{2.3.8}$$

Let the first linearly independent homogeneous solution, $\sinh(\sqrt{p}\xi)$, be $y_1(\xi)$; the second linearly independent homogeneous solution, $\cosh(\sqrt{p}\xi)$ be $y_2(\xi)$ and the right hand side of (2.2.5b), $-\delta w(\xi)\partial\delta^{m-1}\tilde{T}^*_{m-1}(\xi, p)/\partial\xi$ be $f(\xi)$. According to *variation of parameters* technique, $C_3(\xi)$ and $C_4(\xi)$ can be obtained by solving the following equations simultaneously [45]

$$\begin{aligned} y_1(\xi)C_3'(\xi) + y_2(\xi)C_4'(\xi) &= 0 \\ y_1'(\xi)C_3'(\xi) + y_2'(\xi)C_4'(\xi) &= f(\xi) \end{aligned} \tag{2.3.9}$$

Solving (2.3.9) by Cramer's rule gives

$$C_3'(\xi) = \frac{\begin{vmatrix} 0 & y_2(\xi) \\ f & y_2'(\xi) \end{vmatrix}}{\begin{vmatrix} y_1(\xi) & y_2(\xi) \\ y_1'(\xi) & y_2'(\xi) \end{vmatrix}} = \frac{W_1(\xi)}{W(\xi)}, \qquad C_4'(\xi) = \frac{\begin{vmatrix} y_1(\xi) & 0 \\ y_1'(\xi) & f \end{vmatrix}}{\begin{vmatrix} y_1(\xi) & y_2(\xi) \\ y_1'(\xi) & y_2'(\xi) \end{vmatrix}} = \frac{W_2(\xi)}{W(\xi)}$$

Integrating these equations and substituting the results in (2.3.8) gives

$$y_p(\xi) = \left[\int^{\xi} \frac{W_1(\xi_1)}{W(\xi_1)} d\xi_1\right] y_1(\xi) + \left[\int^{\xi} \frac{W_2(\xi_1)}{W(\xi_1)} d\xi_1\right] y_2(\xi) \tag{2.3.10}$$

where

$$W(\xi) = \begin{vmatrix} \sinh(\sqrt{p}\xi) & \cosh(\sqrt{p}\xi) \\ \sqrt{p}\cosh(\sqrt{p}\xi) & \sqrt{p}\sinh(\sqrt{p}\xi) \end{vmatrix} = \sqrt{p}\left[\sinh^2(\sqrt{p}\xi) - \cosh^2(\sqrt{p}\xi)\right]$$

By using (A.5), following equation may be written

$$\sinh^2(\sqrt{p}\xi) - \cosh^2(\sqrt{p}\xi) = -\cosh(\sqrt{p}\xi - \sqrt{p}\xi) = -\cosh(0) = -1$$

which yields

$$W(\xi) = -\sqrt{p}$$

$W_1(\xi)$ and $W_2(\xi)$ may be calculated as follows

$$W_1(\xi) = \begin{vmatrix} 0 & \cosh(\sqrt{p}\xi) \\ f & \sqrt{p}\sinh(\sqrt{p}\xi) \end{vmatrix} = \delta w(\xi) \frac{\partial \delta^{m-1} \tilde{T}^*_{m-1}(\xi, p)}{\partial \xi} \cosh(\sqrt{p}\xi) \tag{2.3.11}$$

$$W_2(\xi) = \begin{vmatrix} \sinh(\sqrt{p}\xi) & 0 \\ \sqrt{p}\cosh(\sqrt{p}\xi) & f \end{vmatrix} = -\delta w(\xi) \frac{\partial \delta^{m-1} \tilde{T}^*_{m-1}(\xi, p)}{\partial \xi} \sinh(\sqrt{p}\xi) \tag{2.3.12}$$

Substituting (2.3.11) and (2.3.12) into (2.3.10) gives

$$y_p(\xi) = -\int_0^{\xi} \frac{1}{\sqrt{p}}\delta w(\xi_1)\frac{\partial \delta^{m-1}\tilde{T}^*_{m-1}(\xi_1,p)}{\partial \xi_1}\sinh(\sqrt{p}\xi)\cosh(\sqrt{p}\xi_1)d\xi_1 + \int_0^{\xi} \frac{1}{\sqrt{p}}\delta w(\xi_1)\frac{\partial \delta^{m-1}\tilde{T}^*_{m-1}(\xi_1,p)}{\partial \xi_1}\cosh(\sqrt{p}\xi)\sinh(\sqrt{p}\xi_1)d\xi_1$$

$y_p(\xi)$ may then be reduced in factored form, such that

$$y_p(\xi) = -\int_0^{\xi} \frac{1}{\sqrt{p}}\delta w(\xi_1)\frac{\partial \delta^{m-1}\tilde{T}^*_{m-1}(\xi_1,p)}{\partial \xi_1}.. .. \left\{\sinh(\sqrt{p}\xi)\cosh(\sqrt{p}\xi_1) - \cosh(\sqrt{p}\xi)\sinh(\sqrt{p}\xi_1)\right\} d\xi_1$$

Using (A.4) gives the following equation

$$\sinh(\sqrt{p}\xi)\cosh(\sqrt{p}\xi_1) - \cosh(\sqrt{p}\xi)\sinh(\sqrt{p}\xi_1) = \sinh(\sqrt{p}[\xi - \xi_1])$$

Final form of $y_p(\xi)$ is then obtained as follows

$$y_p(\xi) = -\int_0^{\xi} \frac{1}{\sqrt{p}}\delta w(\xi_1)\frac{\partial \delta^{m-1}\tilde{T}^*_{m-1}(\xi_1,p)}{\partial \xi_1}\sinh(\sqrt{p}[\xi - \xi_1])d\xi_1 \tag{2.3.13}$$

At this point, particular solution for $\delta^m\tilde{T}^*_m(\xi,p)$ is calculated. To find the overall solution for $\delta^m\tilde{T}^*_m(\xi,p)$, coefficients C_3 and C_4 in (2.3.7) must be determined. Summing (2.3.7) and (2.3.13) gives

$$\delta^m\tilde{T}^*_m(\xi,p) = C_3\sinh(\sqrt{p}\xi) + C_4\cosh(\sqrt{p}\xi) - \int_0^{\xi} \frac{1}{\sqrt{p}}\delta w(\xi_1)\frac{\partial \delta^{m-1}\tilde{T}^*_{m-1}(\xi_1,p)}{\partial \xi_1}\sinh(\sqrt{p}[\xi - \xi_1])d\xi_1 \tag{2.3.14}$$

The conditions (2.2.7a) and (2.2.7b) are applied to (2.3.14) respectively, such that

$$\delta^m \tilde{T}^*_m(0,p) = C_3 \cancelto{0}{\sinh(0)} + C_4 \cancelto{1}{\cosh(0)}$$

$$- \int_0^{\xi} \frac{1}{\sqrt{p}} \delta w(\xi_1) \frac{\partial \delta^{m-1} \tilde{T}^*_{m-1}(\xi_1,p)}{\partial \xi_1} \sinh(\sqrt{p}[\xi - \xi_1]) d\xi_1 \Big|_{\xi=0} = \cancelto{0}{0}$$

giving

$$C_4 = 0$$

By substituting C_4, (2.3.14) may be updated as follows

$$\delta^m \tilde{T}^*_m(\xi,p) = C_3 \sinh(\sqrt{p}\xi) - \int_0^{\xi} \frac{1}{\sqrt{p}} \delta w(\xi_1) \frac{\partial \delta^{m-1} \tilde{T}^*_{m-1}(\xi_1,p)}{\partial \xi_1} \sinh(\sqrt{p}[\xi - \xi_1]) d\xi_1 \tag{2.3.15}$$

By applying (2.2.7b) to (2.3.15)

$$\delta^m \tilde{T}^*_m(\xi_h,p) = C_3 \sinh(\sqrt{p}\xi_h)$$

$$- \int_0^{\xi_h} \frac{1}{\sqrt{p}} \delta w(\xi_1) \frac{\partial \delta^{m-1} \tilde{T}^*_{m-1}(\xi_1,p)}{\partial \xi_1} \sinh(\sqrt{p}[\xi_h - \xi_1]) d\xi_1 = 0$$

which gives

$$C_3 = \frac{1}{\sqrt{p}\sinh(\sqrt{p}\xi_h)} \int_0^{\xi_h} \delta w(\xi_1) \frac{\partial \delta^{m-1} \tilde{T}^*_{m-1}(\xi_1,p)}{\partial \xi_1} \sinh\left[\sqrt{p}(\xi_h - \xi_1)\right] d\xi_1$$

$\delta^m \tilde{T}^*_m(\xi,p)$ is then obtained as follows

$$\delta^m \tilde{T}^*_m(\xi,p) = \frac{\sinh(\sqrt{p}\xi)}{\sqrt{p}\sinh(\sqrt{p}\xi_h)} \int_0^{\xi_h} \delta w(\xi_1) \frac{\partial \delta^{m-1} \tilde{T}^*_{m-1}(\xi_1,p)}{\partial \xi_1} \sinh\left[(\sqrt{p}(\xi_h - \xi_1))\right] d\xi_1$$
$$- \int_0^{\xi} \frac{1}{\sqrt{p}} \delta w(\xi_1) \frac{\partial \delta^{m-1} \tilde{T}^*_{m-1}(\xi_1,p)}{\partial \xi_1} \sinh\left[\sqrt{p}(\xi - \xi_1)\right] d\xi_1 \quad (2.3.16)$$

Since (2.3.6) and (2.3.16) are now obtained; summing them gives the transient temperature distribution in Laplace domain, such that

$$\tilde{T}^*(\xi,p) = \tilde{T}^*_0(\xi,p) + \sum_{m=1}^{\infty} \delta^m \tilde{T}^*_m(\xi,p)$$
$$= \frac{T_{02}\sinh(\sqrt{p}\xi) - T_{01}\sinh\left[\sqrt{p}(\xi - \xi_h)\right]}{p\sinh(\sqrt{p}\xi_h)}$$
$$+ \sum_{m=1}^{\infty} \left\{ \frac{\sinh(\sqrt{p}\xi)}{\sqrt{p}\sinh(\sqrt{p}\xi_h)} \int_0^{\xi_h} \delta w(\xi_1) \frac{\partial \delta^{m-1} \tilde{T}^*_{m-1}(\xi_1,p)}{\partial \xi_1} \sinh\left[\sqrt{p}(\xi_h - \xi_1)\right] d\xi_1 \right.$$
$$\left. - \int_0^{\xi} \frac{1}{\sqrt{p}} \delta w(\xi_1) \frac{\partial \delta^{m-1} \tilde{T}^*_{m-1}(\xi_1,p)}{\partial \xi_1} \sinh\left[\sqrt{p}(\xi - \xi_1)\right] d\xi_1 \right\}$$

Even though the upper limit of the series is going to the infinity, usually a finite number of the series terms is enough to obtain a convergent solution [2]. In this study only the first two terms of the series will be kept. The analytical form of the transient temperature distribution in the transformed domain is then taken to be as follows

$$\tilde{T}^*(\xi,p) = \tilde{T}^*_0(\xi,p) + \delta \tilde{T}^*_1(\xi,p)$$
$$= \frac{T_{02}\sinh(\sqrt{p}\xi) - T_{01}\sinh\left[\sqrt{p}(\xi - \xi_h)\right]}{p\sinh(\sqrt{p}\xi_h)}$$
$$+ \frac{\sinh(\sqrt{p}\xi)}{\sqrt{p}\sinh(\sqrt{p}\xi_h)} \int_0^{\xi_h} \delta w(\xi_1) \frac{\partial \tilde{T}^*_0(\xi_1,p)}{\partial \xi_1} \sinh\left[\sqrt{p}(\xi_h - \xi_1)\right] d\xi_1$$
$$- \int_0^{\xi} \frac{1}{\sqrt{p}} \delta w(\xi_1) \frac{\partial \tilde{T}^*_0(\xi_1,p)}{\partial \xi_1} \sinh\left[\sqrt{p}(\xi - \xi_1)\right] d\xi_1 \quad (2.3.17)$$

Here one should recall from (2.2.1) that $\delta w(\xi_1) = d\ln\left[\eta(\xi_1)\right]/d\xi$. In the next section,

(2.3.17) is to be transformed back into time domain.

2.4 Inverse Laplace Transform of the Solution for $\tilde{T}^*(\xi, p)$

2.4.1 Quick Review on Residue Theorem

The Laplace transform of a function $f(t)$ is given by [45]

$$F(p) = \mathcal{L}\{f(t)\} = \int_0^\infty e^{-pt} f(t) dt$$

The inverse Laplace transform of $F(p)$ by the contour integral is given by [46]

$$\mathcal{L}^{-1}\{F(p)\} = \frac{1}{2\pi i} \lim_{R\to\infty} \int_{\gamma-iR}^{\gamma+iR} e^{pt} F(p) dp = f(t) \tag{2.4.1}$$

This integration is along the line $x = \gamma$ (Bromwich line) in the complex plane as shown in the Figure 2.3.

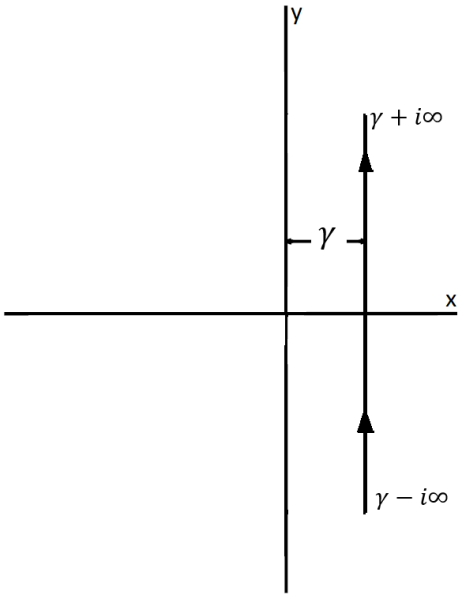

Figure 2.3: Integration performed along the Bromwich line

The conditions which γ should satisfy is given in [46]. Bromwich integral is generally evaluated by using residue theorem. To do this, a contour as depicted in Figure 2.4 is formed.

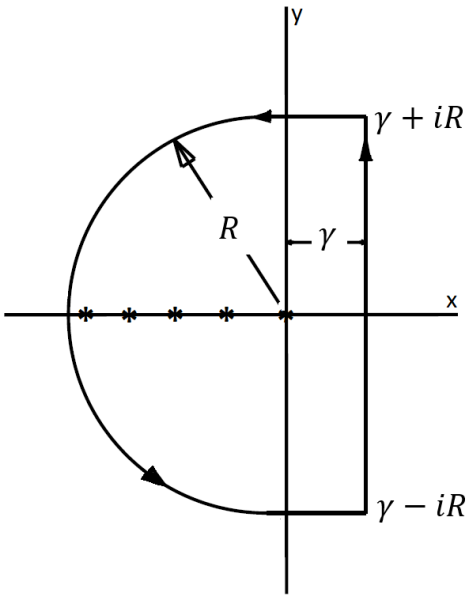

Figure 2.4: Bromwich contour

Here one should note that all the poles of $F(p)$ are to the left of Bromwich line and they are encircled by the defined closed contour as $R \to \infty$. This closed loop includes Bromwich line as well as a circular arc portion and horizontal straight line paths. Under certain conditions [46], the contributions of the integrals along the circular arc portion as well as the upper and lower horizontal straight line paths vanish and the contour integral becomes equal to Bromwich integral.

In this case the inverse Laplace transform can be written as

$$f(t) = \sum Res\left\{e^{pt}F(p), poles\right\} \tag{2.4.2}$$

by virtue of residue theorem. The following rules may be stated regarding residues of complex functions.

Rule 1: Let $f(z)$ be a function of a complex variable z. If $f(z)$ has a pole order of 1

(simple pole) at $z = z_0$, then

$$Res\left[f(z), z_0\right] = \lim_{z \to z_0} \left(z - z_0\right) f(z). \tag{2.4.3}$$

Let us assume that $f(z)$ is in the form of $f(z) = g(z)/h(z)$ and it has a simple pole at z_0 and $g(z_0) \neq 0$. Thus $h(z)$ has a zero of first order at z_0. Applying Rule 1 gives

$$Res\left[f(z), z_0\right] = \lim_{z \to z_0} \left(z - z_0\right) \frac{g(z)}{h(z)}$$

which results in an indeterminate form of $0/0$. Using L'Hôpital's Rule, residue is obtained as

$$\lim_{z \to z_0} \left(z - z_0\right) \frac{g(z)}{h(z)} = \lim_{z \to z_0} \frac{(z - z_0)g'(z) + g(z)}{h'(z)} = \frac{g(z_0)}{h'(z_0)} \tag{2.4.4}$$

Rule 2: If $f(z)$ has a pole of order 2 (double pole) at $z = z_0$, then

$$Res\left[f(z), z_0\right] = \lim_{z \to z_0} \frac{d}{dz}[(z - z_0)^2 f(z)] \tag{2.4.5}$$

Consider the analytic function $f(z) = g(z)/h(z)$, having a pole at z_0. Let $g(z_0) \neq 0$, $h(z_0) = h'(z_0) = 0$, $h''(z_0) \neq 0$. Thus $f(z)$ has a double pole at $z = z_0$, and from [47]

$$Res[f(z), z_0] = \frac{2g'(z_0)}{h''(z_0)} - \frac{2}{3}\frac{g(z_0)h'''(z_0)}{[h''(z_0)]^2} \tag{2.4.6}$$

To find the inverse Laplace transform of $\delta^m \tilde{T}_m^*(\xi, p)$, residue theorem and regarding rules will be employed.

2.4.2 Solution of $\tilde{T}_0(\xi, t)$

The multiplication of (2.3.1) by e^{pt}

$$e^{pt}\tilde{T}_0^*(\xi, p) = \frac{e^{pt}\left\{T_{02}\sinh(\sqrt{p}\xi) - T_{01}\sinh\left[\sqrt{p}(\xi - \xi_h)\right]\right\}}{p\sinh(\sqrt{p}\xi_h)} \tag{2.4.7}$$

Due to the $\sqrt{p}$ in the denominator, (2.4.7) appears to have a branch point at $p = 0$. However by expanding

$$\frac{T_{02}\sinh(\sqrt{p}\xi) - T_{01}\sinh\left[\sqrt{p}(\xi - \xi_h)\right]}{\sinh(\sqrt{p}\xi_h)} \tag{2.4.8}$$

into series by using Wolfram Mathematica 11.2, it could be observed that $\sqrt{p}$ terms in the numerator and denominator cancel out. Therefore based on this series expansion and the derivation in [1, 2, 28], it is concluded that (2.4.7) has a simple pole at 0. Related script and the output of the program is given in (B).

So (2.4.7) has a simple pole at $p_1 = 0$ and infinitely many simples poles at $p_n = -n^2\pi^2/\xi_h^2$, where $n = 1, 2, 3, \cdots$. Thus inverse Laplace transform of (2.3.6) may be obtained such that

$$\tilde{T}_0(\xi, t) = Res\left\{e^{pt}\tilde{T}_0^*(\xi, p), p_1\right\} + \sum_{n=1}^{\infty} Res\left\{e^{p_n t}\tilde{T}_0^*(\xi, p_n), p_n\right\} \tag{2.4.9}$$

Since $p_1 = 0$ is a simple pole, $Res\left\{e^{pt}\tilde{T}_0^*(\xi, p), 0\right\}$ may be calculated by Rule 1. By using (2.4.3)

$$Res\left\{e^{pt}\tilde{T}_0^*(\xi, p), 0\right\} = \lim_{p\to 0}\frac{e^{pt}\left\{T_{02}\sinh(\sqrt{p}\xi) - T_{01}\sinh\left[\sqrt{p}(\xi - \xi_h)\right]\right\}}{\sinh(\sqrt{p}\xi_h)}$$

which results in an indeterminate form of $0/0$. Applying L'Hôpital's Rule once gives

$$Res\left\{e^{pt}\tilde{T}_0^*(\xi, p), 0\right\} = \lim_{p\to 0}\frac{e^{pt}\left\{\xi T_{02}\cosh(\sqrt{p}\xi) - (\xi - \xi_h)T_{01}\cosh\left[\sqrt{p}(\xi - \xi_h)\right]\right\}}{\xi_h\cosh(\sqrt{p}\xi_h)}$$

$$+\lim_{p\to 0}\frac{te^{pt}\left\{T_{02}\sinh(\sqrt{p}\xi)-T_{01}\sinh\left[\sqrt{p}(\xi-\xi_h)\right]\right\}}{\xi_h\cosh(\sqrt{p}\xi_h)}$$

As p goes to 0

$$Res\left\{e^{pt}\tilde{T}_0^*(\xi,p),0\right\}=\frac{\cancel{e^{0t}}^{1}\left\{\xi T_{02}\cancel{\cosh(0)}^{1}-(\xi-\xi_h)T_{01}\cancel{\cosh(0)}^{1}\right\}}{\xi_h\cancel{\cosh(0)}^{1}}$$
$$+\frac{t\cancel{e^{0t}}^{1}\left\{T_{02}\cancel{\sinh(0)}^{0}-T_{01}\cancel{\sinh(0)}^{0}\right\}}{\xi_h\cancel{\cosh(0)}^{1}}$$

with mathematical simplifications, it then reduces to

$$Res\left\{e^{pt}\tilde{T}_0^*(\xi,p),0\right\}=T_{01}+(T_{02}-T_{01})\frac{\xi}{\xi_h} \tag{2.4.10}$$

Since $p_n=-n^2\pi^2/\xi_h^2$ are simple poles, $\sum_{n=1}^{\infty}Res\left\{e^{p_nt}\tilde{T}_0^*(\xi,p_n),-n^2\pi^2/\xi_h^2\right\}$ may also be determined by Rule 1. By using (2.4.4)

$$\sum_{n=1}^{\infty}Res\left\{e^{p_nt}\tilde{T}_0^*(\xi,p_n),-\frac{n^2\pi^2}{\xi_h^2}\right\}$$
$$=\sum_{n=1}^{\infty}\lim_{p_n\to-\frac{n^2\pi^2}{\xi_h^2}}\left(p_n+\frac{n^2\pi^2}{\xi_h^2}\right)\frac{e^{p_nt}\left\{T_{02}\sinh(\sqrt{p_n}\xi)-T_{01}\sinh\left[\sqrt{p_n}(\xi-\xi_h)\right]\right\}}{p_n\sinh(\sqrt{p_n}\xi_h)}$$
$$=\sum_{n=1}^{\infty}\left.\frac{e^{p_nt}\left\{T_{02}\sinh(\sqrt{p_n}\xi)-T_{01}\sinh\left[\sqrt{p_n}(\xi-\xi_h)\right]\right\}}{\cancel{\sinh(\sqrt{p_n}\xi_h)}^{0}+p_n\frac{\xi_h}{2\sqrt{p_n}}\cosh(\sqrt{p_n}\xi_h)}\right|_{p_n=-\frac{n^2\pi^2}{\xi_h^2}}$$

which leads to

$$\sum_{n=1}^{\infty}Res\left\{e^{p_nt}\tilde{T}_0^*(\xi,p_n),-\frac{n^2\pi^2}{\xi_h^2}\right\}$$
$$=\sum_{n=1}^{\infty}\left.\frac{2e^{p_nt}\left\{T_{02}\sinh(\sqrt{p_n}\xi)-T_{01}\sinh\left[\sqrt{p_n}(\xi-\xi_h)\right]\right\}}{n\pi i\cosh(n\pi i)}\right|_{p_n=-\frac{n^2\pi^2}{\xi_h^2}} \tag{2.4.11}$$

By using (A.8)

$$T_{02}\sinh(\sqrt{p_n}\xi) - T_{01}\sinh\left[\sqrt{p_n}(\xi-\xi_h)\right] = iT_{02}\sin(n\pi\frac{\xi}{\xi_h}) - iT_{01}\sin(n\pi\frac{\xi}{\xi_h} - n\pi)$$

(2.4.11) then becomes

$$\sum_{n=1}^{\infty} Res\left\{e^{p_n t}\tilde{T}_0^*(\xi,p_n), -\frac{n^2\pi^2}{\xi_h^2}\right\} = \sum_{n=1}^{\infty}\frac{2e^{p_n t}\left\{iT_{02}\sin(n\pi\frac{\xi}{\xi_h}) - iT_{01}\sin(n\pi\frac{\xi}{\xi_h} - n\pi)\right\}}{n\pi i\cos(n\pi)} \quad (2.4.12)$$

Using (A.4) gives

$$\sin(n\pi\frac{\xi}{\xi_h} - n\pi) = \sin(n\pi\frac{\xi}{\xi_h})\cancel{\cos(n\pi)}^{(-1)^n} - \cancel{\sin(n\pi)\cos(n\pi\frac{\xi}{\xi_h})}^{0} = (-1)^n\sin(n\pi\frac{\xi}{\xi_h})$$

Doing mathematical manipulations and simplifications give

$$\sum_{n=1}^{\infty} Res\left\{e^{p_n t}\tilde{T}_0^*(\xi,p_n), -\frac{n^2\pi^2}{\xi_h^2}\right\} = \sum_{n=1}^{\infty} 2e^{-\frac{n^2\pi^2}{\xi_h^2}t}\frac{(-1)^n T_{02} - T_{01}}{n\pi}\sin(n\pi\frac{\xi}{\xi_h}) \quad (2.4.13)$$

Substituting (2.4.10) and (2.4.13) into (2.4.9) gives $\tilde{T}_0(\xi,t)$ as follows

$$\tilde{T}_0(\xi,t) = T_{01} + (T_{02}-T_{01})\frac{\xi}{\xi_h} + \sum_{n=1}^{\infty} 2e^{-\frac{n^2\pi^2}{\xi_h^2}t}\frac{(-1)^n T_{02} - T_{01}}{n\pi}\sin(n\pi\frac{\xi}{\xi_h}) \quad (2.4.14)$$

First term of the series of transient temperature distribution is now calculated.

2.4.3 Solution of $\delta\tilde{T}_1(\xi,t)$

Before beginning the solution of second term of transient temperature distribution series, $\delta\tilde{T}_1^*(\xi,p)$, it is duplicated below

$$\delta\tilde{T}_1^*(\xi,p)=\frac{\sinh(\sqrt{p}\xi)}{\sqrt{p}\sinh(\sqrt{p}\xi_h)}\int_0^{\xi_h}\delta w(\xi_1)\frac{\partial\tilde{T}_0^*(\xi_1,p)}{\partial\xi_1}\sinh[\sqrt{p}(\xi_h-\xi_1)]d\xi_1$$
$$-\frac{1}{\sqrt{p}}\int_0^{\xi}\delta w(\xi_1)\frac{\partial\tilde{T}_0^*(\xi_1,p)}{\partial\xi_1}\sinh[\sqrt{p}(\xi-\xi_1)]d\xi_1 \tag{2.4.15}$$

This equation is actually the solution of the *perturbed equation* for $m=1$ in Laplace domain. Substituting (2.2.1) and (2.3.6) into (2.4.15) gives

$$\delta\tilde{T}_1^*(\xi,p)=\frac{1}{p\sinh^2(\sqrt{p}\xi_h)}\int_0^{\xi_h}\{T_{02}\cosh(\sqrt{p}\xi_1)-T_{01}\cosh[\sqrt{p}(\xi_1-\xi_h)]\}\,..$$
$$..\sinh[\sqrt{p}(\xi_h-\xi_1)]\sinh(\sqrt{p}\xi)\frac{d\ln[\eta(\xi_1)]}{d\xi_1}d\xi_1$$
$$-\frac{1}{p\sinh(\sqrt{p}\xi_h)}\int_0^{\xi}\{T_{02}\cosh(\sqrt{p}\xi_1)-T_{01}\cosh[\sqrt{p}(\xi_1-\xi_h)]\}\sinh[\sqrt{p}(\xi-\xi_1)]..$$
$$..\frac{d\ln[\eta(\xi_1)]}{d\xi_1}d\xi_1 \tag{2.4.16}$$

Let the first term of (2.4.16) be $I_1^*(\xi,p)$ and the second term be $I_2^*(\xi,p)$, such that

$$I_1^*(\xi,p)=\frac{1}{p\sinh^2(\sqrt{p}\xi_h)}\int_0^{\xi_h}\{T_{02}\cosh(\sqrt{p}\xi_1)-T_{01}\cosh[\sqrt{p}(\xi_1-\xi_h)]\}\,..$$
$$..\sinh[\sqrt{p}(\xi_h-\xi_1)]\sinh(\sqrt{p}\xi)\frac{d\ln[\eta(\xi_1)]}{d\xi_1}d\xi_1$$

and

$$I_2^*(\xi,p)=-\frac{1}{p\sinh(\sqrt{p}\xi_h)}\int_0^{\xi}\{T_{02}\cosh(\sqrt{p}\xi_1)-T_{01}\cosh[\sqrt{p}(\xi_1-\xi_h)]\}\,..$$

$$.. \sinh[\sqrt{p}(\xi - \xi_1)] \frac{d \ln[\eta(\xi_1)]}{d\xi_1} d\xi_1$$

2.4.3.1 Solution for I_1

Defining

$$\mathcal{L}^{-1}\{I_1^*(\xi, p)\} = I_1(\xi, t) \tag{2.4.17}$$

The multiplication of I_1^* by e^{pt} is as follows

$$e^{pt} I_1^*(\xi, p) = \frac{e^{pt}}{p \sinh^2(\sqrt{p}\xi_h)} \int_0^{\xi_h} \{T_{02} \cosh(\sqrt{p}\xi_1) - T_{01} \cosh[\sqrt{p}(\xi_1 - \xi_h)]\} .. \\ .. \sinh[\sqrt{p}(\xi_h - \xi_1)] \sinh(\sqrt{p}\xi) \frac{d \ln[\eta(\xi_1)]}{d\xi_1} d\xi_1 \tag{2.4.18}$$

where (2.4.18) has a simple pole at $p_1 = 0$ and infinitely many double simple poles at $p_n = -n^2\pi^2/\xi_h^2$ where $n = 1, 2, 3, \cdots$. Thus inverse Laplace transform of $I_1^*(\xi, p)$ may be obtained by

$$I_1(\xi, t) = Res\left\{e^{pt} I_1^*(\xi, p), p_1\right\} + \sum_{n=1}^{\infty} Res\left\{e^{p_n t} I_1(\xi, p_n), p_n\right\} \tag{2.4.19}$$

Since $p_1 = 0$ is a simple pole, $Res\left\{e^{pt} I_1^*(\xi, p), 0\right\}$ may be calculated by Rule 1. By (2.4.3)

$$Res\left\{e^{pt} I_1^*(\xi, p), 0\right\} = \lim_{p \to 0} \frac{e^{pt}}{\sinh^2(\sqrt{p}\xi_h)} .. \\ .. \int_0^{\xi_h} \{T_{02} \cosh(\sqrt{p}\xi_1) - T_{01} \cosh[\sqrt{p}(\xi_1 - \xi_h)]\} ..$$

$$.. \sinh[\sqrt{p}(\xi_h - \xi_1)] \sinh(\sqrt{p}\xi) \frac{d \ln[\eta(\xi_1)]}{d\xi_1} d\xi_1$$

Assuming the integrand is well behaved, i.e., it is a continuous function, by Liebniz integral rule [48]

$$Res\left\{e^{pt} I_1^*(\xi, p), 0\right\} = \lim_{p\to 0} \frac{e^{pt}}{\sinh^2(\sqrt{p}\xi_h)} ..$$
$$.. \int_0^{\xi_h} \lim_{p\to 0} \{T_{02} \cosh(\sqrt{p}\xi_1) - T_{01} \cosh[\sqrt{p}(\xi_1 - \xi_h)]\} ..$$
$$.. \sinh[\sqrt{p}(\xi_h - \xi_1)] \sinh(\sqrt{p}\xi) \frac{d \ln[\eta(\xi_1)]}{d\xi_1} d\xi_1$$

which results in an indeterminate form of $0/0$. Applying L'Hôpital's Rule once gives

$$Res\left\{e^{pt} I_1^*(\xi, p), 0\right\} = \lim_{p\to 0} \frac{\sqrt{p} t e^{pt}}{\xi_h \sinh(\sqrt{p}\xi_h) \cosh(\sqrt{p}\xi_h)} ..$$
$$.. \int_0^{\xi_h} \lim_{p\to 0} \{T_{02} \cosh(\sqrt{p}\xi_1) - T_{01} \cosh[\sqrt{p}(\xi_1 - \xi_h)]\} ..$$
$$.. \sinh[\sqrt{p}(\xi_h - \xi_1)] \sinh(\sqrt{p}\xi) \frac{d \ln[\eta(\xi_1)]}{d\xi_1} d\xi_1$$
$$+ \lim_{p\to 0} \frac{e^{pt}}{2\xi_h \sinh(\sqrt{p}\xi_h) \cosh(\sqrt{p}\xi_h)} ..$$
$$.. \int_0^{\xi_h} \lim_{p\to 0} \{\xi_1 T_{02} \sinh(\sqrt{p}\xi_1) - (\xi_1 - \xi_h) T_{01} \sinh[\sqrt{p}(\xi_1 - \xi_h)]\} ..$$
$$.. \sinh(\sqrt{p}[\xi_h - \xi_1]) \sinh(\sqrt{p}\xi) \frac{d \ln[\eta(\xi_1)]}{d\xi_1} d\xi_1$$
$$+ \lim_{p\to 0} \frac{e^{pt}}{2\xi_h \sinh(\sqrt{p}\xi_h) \cosh(\sqrt{p}\xi_h)} ..$$
$$.. \int_0^{\xi_h} \lim_{p\to 0} \{T_{02} \cosh(\sqrt{p}\xi_1) - T_{01} \cosh[\sqrt{p}(\xi_1 - \xi_h)]\} ..$$
$$..(\xi_h - \xi_1) \cosh[\sqrt{p}(\xi_h - \xi_1)] \sinh(\sqrt{p}\xi) \frac{d \ln[\eta(\xi_1)]}{d\xi_1} d\xi_1$$
$$+ \lim_{p\to 0} \frac{e^{pt}}{2\xi_h \sinh(\sqrt{p}\xi_h) \cosh(\sqrt{p}\xi_h)} ..$$

$$.. \int_0^{\xi_h} \lim_{p\to 0} \{T_{02}\cosh(\sqrt{p}\xi_1) - T_{01}\cosh[\sqrt{p}(\xi_1-\xi_h)]\} ..$$

$$.. \sinh[\sqrt{p}(\xi_h-\xi_1)]\xi\cosh(\sqrt{p}\xi)\frac{d\ln[\eta(\xi_1)]}{d\xi_1}d\xi_1$$

Indeterminate form of $0/0$ still continues. Therefore L'Hôpital's Rule is applied one more time, such that

$$Res\left\{e^{pt}I_1^*(\xi,p),0\right\} = \lim_{p\to 0}\frac{te^{pt}+2pt^2e^{pt}}{\xi_h^2\left[\cosh^2(\sqrt{p}\xi_h)+\sinh^2(\sqrt{p}\xi_h)\right]}..$$

$$.. \int_0^{\xi_h} \lim_{p\to 0} \{T_{02}\cosh(\sqrt{p}\xi_1) - T_{01}\cosh[\sqrt{p}(\xi_1-\xi_h)]\} ..$$

$$.. \sinh[\sqrt{p}(\xi_h-\xi_1)]\sinh(\sqrt{p}\xi)\frac{d\ln[\eta(\xi_1)]}{d\xi_1}d\xi_1$$

$$+\lim_{p\to 0}\frac{\sqrt{p}te^{pt}}{\xi_h^2\left[\cosh^2(\sqrt{p}\xi_h)+\sinh^2(\sqrt{p}\xi_h)\right]}..$$

$$.. \int_0^{\xi_h} \lim_{p\to 0} \{\xi_1 T_{02}\sinh(\sqrt{p}\xi_1) - (\xi_1-\xi_h)T_{01}\sinh[\sqrt{p}(\xi_1-\xi_h)]\} ..$$

$$.. \sinh[\sqrt{p}(\xi_h-\xi_1)]\sinh(\sqrt{p}\xi)\frac{d\ln[\eta(\xi_1)]}{d\xi_1}d\xi_1$$

$$+\lim_{p\to 0}\frac{\sqrt{p}te^{pt}}{\xi_h^2\left[\cosh^2(\sqrt{p}\xi_h)+\sinh^2(\sqrt{p}\xi_h)\right]}..$$

$$.. \int_0^{\xi_h} \lim_{p\to 0} \{T_{02}\cosh(\sqrt{p}\xi_1) - T_{01}\cosh[\sqrt{p}(\xi_1-\xi_h)]\} ..$$

$$..(\xi_h-\xi_1)\cosh[\sqrt{p}(\xi_h-\xi_1)]\sinh(\sqrt{p}\xi)\frac{d\ln[\eta(\xi_1)]}{d\xi_1}d\xi_1$$

$$+\lim_{p\to 0}\frac{\sqrt{p}te^{pt}}{\xi_h^2\left[\cosh^2(\sqrt{p}\xi_h)+\sinh^2(\sqrt{p}\xi_h)\right]}..$$

$$.. \int_0^{\xi_h} \lim_{p\to 0} \{T_{02}\cosh(\sqrt{p}\xi_1) - T_{01}\cosh[\sqrt{p}(\xi_1-\xi_h)]\} ..$$

$$.. \sinh[\sqrt{p}(\xi_h-\xi_1)]\xi\cosh(\sqrt{p}\xi)\frac{d\ln[\eta(\xi_1)]}{d\xi_1}d\xi_1$$

$$+\lim_{p\to 0}\frac{te^{pt}}{2\xi_h^2\left[\cosh^2(\sqrt{p}\xi_h)+\sinh^2(\sqrt{p}\xi_h)\right]}..$$

$$.. \int_0^{\xi_h} \lim_{p\to 0} \{\xi_1 T_{02} \sinh(\sqrt{p}\xi_1) - (\xi_1 - \xi_h) T_{01} \sinh[\sqrt{p}(\xi_1 - \xi_h)]\} ..$$

$$.. \sinh(\sqrt{p}[\xi_h - \xi_1]) \sinh(\sqrt{p}\xi) \frac{d \ln[\eta(\xi_1)]}{d\xi_1} d\xi_1$$

$$+ \lim_{p\to 0} \frac{e^{pt}}{2\xi_h^2 \left[\cosh^2(\sqrt{p}\xi_h) + \sinh^2(\sqrt{p}\xi_h)\right]} ..$$

$$.. \int_0^{\xi_h} \lim_{p\to 0} \left\{\xi_1^2 T_{02} \cosh(\sqrt{p}\xi_1) - (\xi_1 - \xi_h)^2 T_{01} \cosh[\sqrt{p}(\xi_1 - \xi_h)]\right\} ..$$

$$.. \sinh(\sqrt{p}[\xi_h - \xi_1]) \sinh(\sqrt{p}\xi) \frac{d \ln[\eta(\xi_1)]}{d\xi_1} d\xi_1$$

$$+ \lim_{p\to 0} \frac{e^{pt}}{2\xi_h^2 \left[\cosh^2(\sqrt{p}\xi_h) + \sinh^2(\sqrt{p}\xi_h)\right]} ..$$

$$.. \int_0^{\xi_h} \lim_{p\to 0} \{\xi_1 T_{02} \sinh(\sqrt{p}\xi_1) - (\xi_1 - \xi_h) T_{01} \sinh[\sqrt{p}(\xi_1 - \xi_h)]\} ..$$

$$..(\xi_h - \xi_1) \cosh\left[\sqrt{p}(\xi_h - \xi_1)\right] \sinh(\sqrt{p}\xi) \frac{d \ln[\eta(\xi_1)]}{d\xi_1} d\xi_1$$

$$+ \lim_{p\to 0} \frac{e^{pt}}{2\xi_h^2 \left[\cosh^2(\sqrt{p}\xi_h) + \sinh^2(\sqrt{p}\xi_h)\right]} ..$$

$$.. \int_0^{\xi_h} \lim_{p\to 0} \{\xi_1 T_{02} \sinh(\sqrt{p}\xi_1) - (\xi_1 - \xi_h) T_{01} \sinh[\sqrt{p}(\xi_1 - \xi_h)]\} ..$$

$$.. \sinh(\sqrt{p}[\xi_h - \xi_1]) \xi \cosh(\sqrt{p}\xi) \frac{d \ln[\eta(\xi_1)]}{d\xi_1} d\xi_1$$

$$+ \lim_{p\to 0} \frac{te^{pt}}{2\xi_h^2 \left[\cosh^2(\sqrt{p}\xi_h) + \sinh^2(\sqrt{p}\xi_h)\right]} ..$$

$$.. \int_0^{\xi_h} \lim_{p\to 0} \{T_{02} \cosh(\sqrt{p}\xi_1) - T_{01} \cosh[\sqrt{p}(\xi_1 - \xi_h)]\} ..$$

$$..(\xi_h - \xi_1) \cosh[\sqrt{p}(\xi_h - \xi_1)] \sinh(\sqrt{p}\xi) \frac{d \ln[\eta(\xi_1)]}{d\xi_1} d\xi_1$$

$$+ \lim_{p\to 0} \frac{e^{pt}}{2\xi_h^2 \left[\cosh^2(\sqrt{p}\xi_h) + \sinh^2(\sqrt{p}\xi_h)\right]} ..$$

$$.. \int_0^{\xi_h} \lim_{p\to 0} \{\xi_1 T_{02} \sinh(\sqrt{p}\xi_1) - (\xi_1 - \xi_h) T_{01} \sinh[\sqrt{p}(\xi_1 - \xi_h)]\} ..$$

$$..(\xi_h - \xi_1) \cosh[\sqrt{p}(\xi_h - \xi_1)] \sinh(\sqrt{p}\xi) \frac{d \ln[\eta(\xi_1)]}{d\xi_1} d\xi_1$$

$$+\lim_{p\to 0}\frac{e^{pt}}{2\xi_h^2\left[\cosh^2(\sqrt{p}\xi_h)+\sinh^2(\sqrt{p}\xi_h)\right]}..$$

$$..\int_0^{\xi_h}\lim_{p\to 0}\{T_{02}\cosh(\sqrt{p}\xi_1)-T_{01}\cosh[\sqrt{p}(\xi_1-\xi_h)]\}..$$

$$..(\xi_h-\xi_1)^2\sinh[\sqrt{p}(\xi_h-\xi_1)]\sinh(\sqrt{p}\xi)\frac{d\ln[\eta(\xi_1)]}{d\xi_1}d\xi_1$$

$$+\lim_{p\to 0}\frac{e^{pt}}{2\xi_h^2\left[\cosh^2(\sqrt{p}\xi_h)+\sinh^2(\sqrt{p}\xi_h)\right]}..$$

$$..\int_0^{\xi_h}\lim_{p\to 0}\{T_{02}\cosh(\sqrt{p}\xi_1)-T_{01}\cosh[\sqrt{p}(\xi_1-\xi_h)]\}..$$

$$..(\xi_h-\xi_1)\cosh[\sqrt{p}(\xi_h-\xi_1)]\xi\cosh(\sqrt{p}\xi)\frac{d\ln[\eta(\xi_1)]}{d\xi_1}d\xi_1$$

$$+\lim_{p\to 0}\frac{te^{pt}}{2\xi_h^2\left[\cosh^2(\sqrt{p}\xi_h)+\sinh^2(\sqrt{p}\xi_h)\right]}..$$

$$..\int_0^{\xi_h}\lim_{p\to 0}\{T_{02}\cosh(\sqrt{p}\xi_1)-T_{01}\cosh[\sqrt{p}(\xi_1-\xi_h)]\}..$$

$$..\sinh[\sqrt{p}(\xi_h-\xi_1)]\xi\cosh(\sqrt{p}\xi)\frac{d\ln[\eta(\xi_1)]}{d\xi_1}d\xi_1$$

$$+\lim_{p\to 0}\frac{e^{pt}}{2\xi_h^2\left[\cosh^2(\sqrt{p}\xi_h)+\sinh^2(\sqrt{p}\xi_h)\right]}..$$

$$..\int_0^{\xi_h}\lim_{p\to 0}\{\xi_1 T_{02}\sinh(\sqrt{p}\xi_1)-(\xi_1-\xi_h)T_{01}\sinh[\sqrt{p}(\xi_1-\xi_h)]\}..$$

$$..\sinh[\sqrt{p}(\xi_h-\xi_1)]\xi\cosh(\sqrt{p}\xi)\frac{d\ln[\eta(\xi_1)]}{d\xi_1}d\xi_1$$

$$+\lim_{p\to 0}\frac{e^{pt}}{2\xi_h^2\left[\cosh^2(\sqrt{p}\xi_h)+\sinh^2(\sqrt{p}\xi_h)\right]}..$$

$$..\int_0^{\xi_h}\lim_{p\to 0}\{T_{02}\cosh(\sqrt{p}\xi_1)-T_{01}\cosh[\sqrt{p}(\xi_1-\xi_h)]\}..$$

$$..(\xi_h-\xi_1)\cosh[\sqrt{p}(\xi_h-\xi_1)]\xi\cosh(\sqrt{p}\xi)\frac{d\ln[\eta(\xi_1)]}{d\xi_1}d\xi_1$$

$$+\lim_{p\to 0}\frac{e^{pt}}{2\xi_h^2\left[\cosh^2(\sqrt{p}\xi_h)+\sinh^2(\sqrt{p}\xi_h)\right]}..$$

$$..\int_0^{\xi_h}\lim_{p\to 0}\{T_{02}\cosh(\sqrt{p}\xi_1)-T_{01}\cosh[\sqrt{p}(\xi_1-\xi_h)]\}..$$

$$.. \sinh[\sqrt{p}(\xi_h - \xi_1)]\xi^2 \sinh(\sqrt{p}\xi)\frac{d\ln[\eta(\xi_1)]}{d\xi_1}d\xi_1$$

It may be seen that; none of the denominators will be zero any more. Each converges either to ξ_h^2 or $2\xi_h^2$ as p goes to 0. So there will be no more indeterminate form of $0/0$. The limits that contain at least one of the multipliers either $\sinh[\sqrt{p}(\xi_h - \xi_1)]$ or $\sinh(\sqrt{p}\xi)$ in their numerators result in zero, since as p goes to 0, these multipliers go to 0. In the following one only finds non-zero results of the limits, namely the contributing terms only, such that

$$\begin{aligned}
Res\left\{e^{pt}I_1^*(\xi,p),0\right\} &= \lim_{p\to 0}\frac{e^{pt}}{2\xi_h^2\cosh^2(\sqrt{p}\xi_h)}.. \\
&.. \int_0^{\xi_h} \lim_{p\to 0}\left\{T_{02}\cosh(\sqrt{p}\xi_1) - T_{01}\cosh[\sqrt{p}(\xi_1-\xi_h)]\right\}.. \\
&..(\xi_h-\xi_1)\cosh[\sqrt{p}(\xi_h-\xi_1)]\xi\cosh(\sqrt{p}\xi)\frac{d\ln[\eta(\xi_1)]}{d\xi_1}d\xi_1 \\
+\lim_{p\to 0}\frac{e^{pt}}{2\xi_h^2\cosh^2(\sqrt{p}\xi_h)} &\int_0^{\xi_h} \lim_{p\to 0}\left\{T_{02}\cosh(\sqrt{p}\xi_1) - T_{01}\cosh[\sqrt{p}(\xi_1-\xi_h)]\right\}.. \\
&..(\xi_h-\xi_1)\cosh[\sqrt{p}(\xi_h-\xi_1)]\xi\cosh(\sqrt{p}\xi)\frac{d\ln[\eta(\xi_1)]}{d\xi_1}d\xi_1
\end{aligned}$$

Since these two limits are equal to each other, summation is straightforward such that

$$\begin{aligned}
Res\left\{e^{pt}I_1^*(\xi,p),0\right\} &= \lim_{p\to 0}\frac{e^{pt}}{\xi_h^2\cosh^2(\sqrt{p}\xi_h)}.. \\
&.. \int_0^{\xi_h} \left\{T_{02}\cosh(\sqrt{p}\xi_1) - T_{01}\cosh[\sqrt{p}(\xi_1-\xi_h)]\right\}.. \\
&..(\xi_h-\xi_1)\cosh[\sqrt{p}(\xi_h-\xi_1)]\xi\cosh(\sqrt{p}\xi)\frac{d\ln[\eta(\xi_1)]}{d\xi_1}d\xi_1
\end{aligned}$$

which gives the final form of $Res\left\{e^{pt}I_1^*(\xi,p),0\right\}$ as follows

$$Res\left\{e^{pt}I_1^*(\xi,p),0\right\} = \frac{\xi\left\{T_{01}-T_{02}\right\}}{\xi_h^2}\int_0^{\xi_h}(\xi_1-\xi_h)\frac{d\ln[\eta(\xi_1)]}{d\xi_1}d\xi_1 \qquad (2.4.20)$$

Since $p_n = -n^2\pi^2/\xi_h^2$ $(n = 1, 2, 3, \cdots)$ are double poles,
$\sum_{n=1}^{\infty} Res\left\{e^{p_n t} I_1(\xi, p_n), -n^2\pi^2/\xi_h^2\right\}$ may be calculated by the Rule 2, such that

$$\sum_{n=1}^{\infty} Res\left\{e^{p_n t} I_1(\xi, p_n), -\frac{n^2\pi^2}{\xi_h^2}\right\} = \sum_{n=1}^{\infty} \lim_{p_n \to -\frac{n^2\pi^2}{\xi_h^2}} \frac{d}{dp} \frac{(p_n + \frac{n^2\pi^2}{\xi_h^2})^2 e^{p_n t}}{\sinh^2(\sqrt{p_n}\xi_h)} ..$$
$$.. \int_0^{\xi_h} \frac{\left\{T_{02}\cosh(\sqrt{p_n}\xi_1) - T_{01}\cosh[\sqrt{p_n}(\xi_1 - \xi_h)]\right\}}{p_n} ..$$
$$.. \sinh[\sqrt{p_n}(\xi_h - \xi_1)]\sinh(\sqrt{p_n}\xi)\frac{d\ln[\eta(\xi_1)]}{d\xi_1} d\xi_1$$

It may be seen that (2.4.18) is in the form of $g(p_n)/h(p_n)$ and $g(p_n) \neq 0$, $h(p_n) = h'(p_n) = 0$ and $h''(p_n) \neq 0$ as p_n goes to $-n^2\pi^2/\xi_h^2$ where $n = 1, 2, 3, \cdots$. Therefore (2.4.6) can be employed here. Defining

$$k(p_n) = \int_0^{\xi_h} \frac{\left\{T_{02}\cosh(\sqrt{p_n}\xi_1) - T_{01}\cosh[\sqrt{p_n}(\xi_1 - \xi_h)]\right\}}{p_n} ..$$
$$.. \sinh[\sqrt{p_n}(\xi_h - \xi_1)]\sinh(\sqrt{p_n}\xi)\frac{d\ln[\eta(\xi_1)]}{d\xi_1} d\xi_1 \quad (2.4.21)$$

Substituting (2.4.21) into (2.4.6) gives

$$\sum_{n=1}^{\infty} Res\left\{e^{p_n t} I_1(\xi, p_n), -\frac{n^2\pi^2}{\xi_h^2}\right\} = \sum_{n=1}^{\infty} \frac{2\left[e^{p_n t} k(p_n)\right]'}{\left[\sinh^2(\sqrt{p_n}\xi_h)\right]''}$$
$$- \frac{2}{3}\frac{e^{p_n t} k(p_n)\left[\sinh^2(\sqrt{p_n}\xi_h)\right]'''}{\left\{\left[\sinh^2(\sqrt{p_n}\xi_h)\right]''\right\}^2}$$

Here the derivatives are taken by using MATLAB® symbolic toolbox. Related script is given in (C). Using the output of program and substituting $p_n = -n^2\pi^2/\xi_h^2$ gives

$$\sum_{n=1}^{\infty} Res\left\{e^{pt} I_1^*(\xi, p), -\frac{n^2\pi^2}{\xi_h^2}\right\} = \sum_{n=1}^{\infty} \left\{-\frac{4n^2\pi^2}{\xi_h^4} t + \frac{2}{\xi_h^2}\right\} ..$$

$$..e^{p_n t}k(p_n) - \frac{4n^2\pi^2}{\xi_h^4}e^{p_n t}k'(p_n)\Big|_{p_n=-\frac{n^2\pi^2}{\xi_h^2}} \tag{2.4.22}$$

Summing (2.4.20) and (2.4.22) gives the expression of $I_1(\xi,t)$ as written below

$$\begin{aligned} I_1(\xi,t) = {} & \frac{\xi\left\{T_{01}-T_{02}\right\}}{\xi_h^2}\int_0^{\xi_h}(\xi_1-\xi_h)\frac{d\ln[\eta(\xi_1)]}{d\xi_1}d\xi_1 \\ & + \sum_{n=1}^{\infty}\left\{-\frac{4n^2\pi^2}{\xi_h^4}t+\frac{2}{\xi_h^2}\right\}e^{p_n t}k(p_n) - \sum_{n=1}^{\infty}\frac{4n^2\pi^2}{\xi_h^4}e^{p_n t}k'(p_n)\Big|_{p_n=-\frac{n^2\pi^2}{\xi_h^2}} \end{aligned} \tag{2.4.23}$$

where $k'(p_n)$ is derivative of $k(p_n)$ with respect to p. Clear form of $I_1(\xi,t)$ is also expressed as follows

$$\begin{aligned} I_1(\xi,t) = {} & \xi\frac{\{T_{01}-T_{02}\}}{\xi_h^2}\int_0^{\xi_h}(\xi_1-\xi_h)\frac{d\ln[\eta(\xi_1)]}{d\xi_1}d\xi_1 \\ & + \sum_{n=1}^{\infty}\left\{-\frac{4n^2\pi^2}{\xi_h^4}t+\frac{2}{\xi_h^2}\right\}e^{p_n t}.. \\ & ..\int_0^{\xi_h}\frac{\left\{T_{02}\cosh(\sqrt{p_n}\xi_1)-T_{01}\cosh[\sqrt{p_n}(\xi_1-\xi_h)]\right\}}{p_n}.. \\ & ..\sinh[\sqrt{p_n}(\xi_h-\xi_1)]\sinh(\sqrt{p_n}\xi)\frac{d\ln[\eta(\xi_1)]}{d\xi_1}d\xi_1\Big|_{p_n=-\frac{n^2\pi^2}{\xi_h^2}} \\ & - \sum_{n=1}^{\infty}\frac{4n^2\pi^2}{\xi_h^4}e^{p_n t}.. \\ & ..\frac{\partial}{\partial p}\int_0^{\xi_h}\frac{\left\{T_{02}\cosh(\sqrt{p_n}\xi_1)-T_{01}\cosh[\sqrt{p_n}(\xi_1-\xi_h)]\right\}}{p_n}.. \\ & ..\sinh[\sqrt{p_n}(\xi_h-\xi_1)]\sinh(\sqrt{p_n}\xi)\frac{d\ln[\eta(\xi_1)]}{d\xi_1}d\xi_1\Big|_{p_n=-\frac{n^2\pi^2}{\xi_h^2}} \end{aligned}$$

Here in the last summation sign, it may be seen that there is an integration under a differentiation sign. Assumming that the integrand is well behaved, using the Liebniz integral rule [48] gives p-derivative of the ξ_1-integral of this function equals to the ξ_1-integral of the p-derivative of itself, namely

$$\frac{\partial}{\partial p}\int_0^{\xi_h}\frac{T_{02}\cosh(\sqrt{p_n}\xi_1)-T_{01}\cosh[\sqrt{p_n}(\xi_1-\xi_h)]}{p_n}..$$
$$..\sinh[\sqrt{p_n}(\xi_h-\xi_1)]\sinh(\sqrt{p_n}\xi)\frac{d\ln[\eta(\xi_1)]}{d\xi_1}d\xi_1\Big|_{p_n=-\frac{n^2\pi^2}{\xi_h^2}}$$
$$=\int_0^{\xi_h}\frac{\partial}{\partial p}\left[\frac{T_{02}\cosh(\sqrt{p_n}\xi_1)-T_{01}\cosh[\sqrt{p_n}(\xi_1-\xi_h)]}{p_n}..\right.$$
$$\left..\sinh[\sqrt{p_n}(\xi_h-\xi_1)]\sinh(\sqrt{p_n}\xi)\frac{d\ln[\eta(\xi_1)]}{d\xi_1}d\xi_1\right]\Big|_{p_n=-\frac{n^2\pi^2}{\xi_h^2}} \quad (2.4.24)$$

In this manner, the derivation may be calculated by using MATLAB® symbolic toolbox first, and then the integration may be calculated numerically. Note that variables p and ξ_1 are independent of each other. The final form of $I_1(\xi,t)$ then equals to

$$I_1(\xi,t)=\xi\frac{\{T_{01}-T_{02}\}}{\xi_h^2}\int_0^{\xi_h}(\xi_1-\xi_h)\frac{d\ln[\eta(\xi_1)]}{d\xi_1}d\xi_1$$
$$+\sum_{n=1}^{\infty}\left\{-\frac{4n^2\pi^2}{\xi_h^4}t+\frac{2}{\xi_h^2}\right\}e^{p_nt}..$$
$$..\int_0^{\xi_h}\frac{\left\{T_{02}\cosh(\sqrt{p_n}\xi_1)-T_{01}\cosh[\sqrt{p_n}(\xi_1-\xi_h)]\right\}}{p_n}..$$
$$..\sinh[\sqrt{p_n}(\xi_h-\xi_1)]\sinh(\sqrt{p_n}\xi)\frac{d\ln[\eta(\xi_1)]}{d\xi_1}d\xi_1\Big|_{p_n=-\frac{n^2\pi^2}{\xi_h^2}}$$
$$-\sum_{n=1}^{\infty}\frac{4n^2\pi^2}{\xi_h^4}e^{p_nt}..$$
$$..\int_0^{\xi_h}\frac{\partial}{\partial p}\left[\frac{T_{02}\cosh(\sqrt{p_n}\xi_1)-T_{01}\cosh[\sqrt{p_n}(\xi_1-\xi_h)]}{p_n}..\right.$$
$$\left..\sinh[\sqrt{p_n}(\xi_h-\xi_1)]\sinh(\sqrt{p_n}\xi)\frac{d\ln[\eta(\xi_1)]}{d\xi_1}d\xi_1\right]\Big|_{p_n=-\frac{n^2\pi^2}{\xi_h^2}} \quad (2.4.25)$$

2.4.3.2 Solution for I_2

Defining

$$\mathcal{L}^{-1}\{I_2^*(\xi,p)\} = I_2(\xi,t) \tag{2.4.26}$$

The multiplication of I_2^* by e^{pt} is as follows

$$e^{pt}I_2^*(\xi,p) = -\frac{e^{pt}}{p\sinh(\sqrt{p}\xi_h)}\int_0^{\xi}\{T_{02}\cosh(\sqrt{p}\xi_1) - T_{01}\cosh[\sqrt{p}(\xi_1-\xi_h)]\}\,..$$
$$..\,\sinh[\sqrt{p}(\xi-\xi_1)]\frac{d\ln[\eta(\xi_1)]}{d\xi_1}d\xi_1 \tag{2.4.27}$$

where (2.4.27) has a simple pole at $p_1 = 0$ and infinitely many simple poles at $p_n = -n^2\pi^2/\xi_h^2$ where $n = 1, 2, 3, \cdots$. Inverse Laplace transform of $I_2^*(\xi,p)$ may be obtained by

$$I_2(\xi,t) = Res\left\{e^{pt}I_2^*(\xi,p), p_1\right\} + \sum_{n=1}^{\infty} Res\left\{e^{p_n t}I_2^*(\xi,p_n), p_n\right\} \tag{2.4.28}$$

Since $p_1 = 0$ is a simple pole, $Res\{e^{pt}I_2^*(\xi,p), 0\}$ may be calculated by Rule 1. By (2.4.3)

$$Res\left\{e^{pt}I_2^*(\xi,p), 0\right\} = -\lim_{p\to 0}\frac{e^{pt}}{\sinh(\sqrt{p}\xi_h)}..$$
$$..\int_0^{\xi}\{T_{02}\cosh(\sqrt{p}\xi_1) - T_{01}\cosh[\sqrt{p}(\xi_1-\xi_h)]\}\sinh[\sqrt{p}(\xi-\xi_1)]\frac{d\ln[\eta(\xi_1)]}{d\xi_1}d\xi_1$$

Assuming the integrand is well behaved, by Liebniz integral rule [48]

$$Res\left\{e^{pt}I_2^*(\xi,p), 0\right\} = -\lim_{p\to 0}\frac{e^{pt}}{\sinh(\sqrt{p}\xi_h)}..$$
$$..\int_0^{\xi}\lim_{p\to 0}\{T_{02}\cosh(\sqrt{p}\xi_1) - T_{01}\cosh[\sqrt{p}(\xi_1-\xi_h)]\}\sinh[\sqrt{p}(\xi-\xi_1)]\frac{d\ln[\eta(\xi_1)]}{d\xi_1}d\xi_1$$

which results in an indeterminate form of $0/0$ as p goes to 0. Using L'Hôpital's Rule

$$
\begin{aligned}
Res\left\{e^{pt}I_2^*(\xi,p),0\right\} = &-\lim_{p\to 0}\frac{e^{pt}}{\xi_h\cosh(\sqrt{p}\xi_h)}..\\
&..\int_0^{\xi}\lim_{p\to 0}\left\{\xi_1 T_{02}\sinh(\sqrt{p}\xi_1)-T_{01}(\xi_1-\xi_h)\sinh[\sqrt{p}(\xi_1-\xi_h)]\right\}..\\
&..\sinh[\sqrt{p}(\xi-\xi_1)]\frac{d\ln[\eta(\xi_1)]}{d\xi_1}d\xi_1\\
&-\lim_{p\to 0}\frac{e^{pt}}{\xi_h\cosh(\sqrt{p}\xi_h)}..\\
&..\int_0^{\xi}\lim_{p\to 0}\left\{T_{02}\cosh(\sqrt{p}\xi_1)-T_{01}\cosh[\sqrt{p}(\xi_1-\xi_h)]\right\}..\\
&..(\xi-\xi_1)\cosh[\sqrt{p}(\xi-\xi_1)]\frac{d\ln[\eta(\xi_1)]}{d\xi_1}d\xi_1\\
&-\lim_{p\to 0}\frac{te^{pt}}{\xi_h\cosh(\sqrt{p}\xi_h)}..\\
&..\int_0^{\xi}\lim_{p\to 0}\left\{T_{02}\cosh(\sqrt{p}\xi_1)-T_{01}\cosh[\sqrt{p}(\xi_1-\xi_h)]\right\}..\\
&..\sinh[\sqrt{p}(\xi-\xi_1)]\frac{d\ln[\eta(\xi_1)]}{d\xi_1}d\xi_1
\end{aligned}
$$

The terms containing $\sinh(\sqrt{p}\xi_1)$, $\sinh[\sqrt{p}(\xi_1-\xi_h)]$ and $\sinh[\sqrt{p}(\xi-\xi_1)]$ multipliers, will have no contribution since $\sinh(0)=0$. In the following only contributing terms are stated

$$
\begin{aligned}
Res\left\{e^{pt}I_2^*(\xi,p),0\right\} = &-\lim_{p\to 0}\frac{e^{pt}}{\xi_h\cosh(\sqrt{p}\xi_h)}..\\
&..\int_0^{\xi}\left\{T_{02}\cosh(\sqrt{p}\xi_1)-T_{01}\cosh[\sqrt{p}(\xi_1-\xi_h)]\right\}..\\
&..(\xi-\xi_1)\cosh[\sqrt{p}(\xi-\xi_1)]\frac{d\ln[\eta(\xi_1)]}{d\xi_1}d\xi_1
\end{aligned}
$$

Since $\cosh(0)=1$, the solution of $Res\left\{e^{pt}I_2^*(\xi,p),0\right\}$ then equals to

$$Res\left\{e^{pt}I_2^*(\xi,p),0\right\}=\frac{T_{02}-T_{01}}{\xi_h}\int_0^{\xi}(\xi_1-\xi)\frac{d\ln[\eta(\xi_1)]}{d\xi_1}d\xi_1 \tag{2.4.29}$$

Since $p_n=-n^2\pi^2/\xi_h^2$ $(n=1,2,3,\cdots)$ are simple poles,
$\sum_{n=1}^{\infty} Res\left\{e^{p_nt}I_2(\xi,p_n),-n^2\pi^2/\xi_h^2\right\}$ may be calculated by Rule 1. By using (2.4.4)

$$\sum_{n=1}^{\infty}Res\left\{e^{p_nt}I_2(\xi,p_n),-\frac{n^2\pi^2}{\xi_h^2}\right\}=-\sum_{n=1}^{\infty}\frac{2\sqrt{p_n}e^{p_nt}}{\xi_h\cosh(\sqrt{p_n}\xi_h)}..$$
$$..\int_0^{\xi}\frac{\left\{T_{02}\cosh(\sqrt{p_n}\xi_1)-T_{01}\cosh[\sqrt{p_n}(\xi_1-\xi_h)]\right\}\sinh[\sqrt{p_n}(\xi-\xi_1)]}{p_n}..$$
$$..\frac{d\ln[\eta(\xi_1)]}{d\xi_1}d\xi_1\Big|_{p_n=-\frac{n^2\pi^2}{\xi_h^2}}$$

which is equal to

$$\sum_{n=1}^{\infty}Res\left\{e^{pt}I_2^*(\xi,p),-\frac{n^2\pi^2}{\xi_h^2}\right\}=-\sum_{n=1}^{\infty}\frac{2(-1)^n n\pi i e^{-\frac{n^2\pi^2}{\xi_h^2}t}}{\xi_h^2}..$$
$$..\int_0^{\xi}\frac{\left\{T_{02}\cosh(\sqrt{p_n}\xi_1)-T_{01}\cosh[\sqrt{p_n}(\xi_1-\xi_h)]\right\}}{p_n}\sinh[\sqrt{p_n}(\xi-\xi_1)]..$$
$$..\frac{d\ln[\eta(\xi_1)]}{d\xi_1}d\xi_1\Big|_{p_n=-\frac{n^2\pi^2}{\xi_h^2}} \tag{2.4.30}$$

All residues of $e^{pt}I_2^*(\xi,p)$ are calculated now, summing them gives $I_2(\xi,t)$ such that

$$I_2(\xi,t)=\frac{T_{02}-T_{01}}{\xi_h}\int_0^{\xi}(\xi_1-\xi)\frac{d\ln[\eta(\xi_1)]}{d\xi_1}d\xi_1-\sum_{n=1}^{\infty}\frac{2(-1)^n n\pi i e^{-\frac{n^2\pi^2}{\xi_h^2}t}}{\xi_h^2}..$$
$$..\int_0^{\xi}\frac{\left\{T_{02}\cosh(\sqrt{p_n}\xi_1)-T_{01}\cosh[\sqrt{p_n}(\xi_1-\xi_h)]\right\}}{p_n}\sinh[\sqrt{p_n}(\xi-\xi_1)]..$$
$$..\frac{d\ln[\eta(\xi_1)]}{d\xi_1}d\xi_1\Big|_{p_n=-\frac{n^2\pi^2}{\xi_h^2}} \tag{2.4.31}$$

$\delta\tilde{T}_1(\xi,t)$ is then obtained by substituting (2.4.25) and (2.4.31) into (**??**)

$$\delta\tilde{T}_1(\xi,t) = \frac{T_{02}-T_{01}}{\xi_h}\int_0^{\xi}(\xi_1-\xi)\frac{d\ln[\eta(\xi_1)]}{d\xi_1}d\xi_1$$
$$+\xi\frac{\{T_{01}-T_{02}\}}{\xi_h^2}\int_0^{\xi_h}(\xi_1-\xi_h)\frac{d\ln[\eta(\xi_1)]}{d\xi_1}d\xi_1-\sum_{n=1}^{\infty}\frac{2(-1)^n n\pi i}{\xi_h^2}e^{p_n t}..$$
$$..\int_0^{\xi}\frac{\left\{T_{02}\cosh(\sqrt{p_n}\xi_1)-T_{01}\cosh[\sqrt{p_n}(\xi_1-\xi_h)]\right\}}{p_n}\sinh[\sqrt{p_n}(\xi-\xi_1)]..$$
$$..\frac{d\ln[\eta(\xi_1)]}{d\xi_1}\,d\xi_1\Big|_{p_n=-\frac{n^2\pi^2}{\xi_h^2}}+\sum_{n=1}^{\infty}\left\{-\frac{4n^2\pi^2}{\xi_h^4}t+\frac{2}{\xi_h^2}\right\}e^{p_n t}..$$
$$..\int_0^{\xi_h}\frac{\left\{T_{02}\cosh(\sqrt{p_n}\xi_1)-T_{01}\cosh[\sqrt{p_n}(\xi_1-\xi_h)]\right\}}{p_n}..$$
$$..\sinh[\sqrt{p_n}(\xi_h-\xi_1)]\sinh(\sqrt{p_n}\xi)\frac{d\ln[\eta(\xi_1)]}{d\xi_1}d\xi_1\Big|_{p_n=-\frac{n^2\pi^2}{\xi_h^2}}$$
$$-\frac{4n^2\pi^2}{\xi_h^4}e^{p_n t}\int_0^{\xi_h}\frac{\partial}{\partial p}\left\{\frac{\left\{T_{02}cosh(\sqrt{p_n}\xi_1)-T_{01}cosh[\sqrt{p_n}(\xi_1-\xi_h)]\right\}}{p_n}..\right.$$
$$\left..\sinh[\sqrt{p_n}(\xi_h-\xi_1)]\sinh(\sqrt{p_n}\xi)\frac{d\ln[\eta(\xi_1)]}{d\xi_1}d\xi_1\right\}\Big|_{p_n=-\frac{n^2\pi^2}{\xi_h^2}} \quad (2.4.32)$$

Summing up (2.4.14) and (2.4.32) transient temperature distribution change $\tilde{T}(\xi,t)$ is obtained in time domain for $m=0$ and $m=1$

$$\tilde{T}(\xi,t) = T_{01}+(T_{02}-T_{01})\frac{\xi}{\xi_h}+\sum_{n=1}^{\infty}2e^{-\frac{n^2\pi^2}{\xi_h^2}t}\frac{(-1)^n T_{02}-T_{01}}{n\pi}sin\left(n\pi\frac{\xi}{\xi_h}\right)$$
$$+\frac{T_{02}-T_{01}}{\xi_h}\int_0^{\xi}(\xi_1-\xi)\frac{d\ln[\eta(\xi_1)]}{d\xi_1}d\xi_1$$
$$+\xi\frac{\{T_{01}-T_{02}\}}{\xi_h^2}\int_0^{\xi_h}(\xi_1-\xi_h)\frac{d\ln[\eta(\xi_1)]}{d\xi_1}d\xi_1$$
$$-\sum_{n=1}^{\infty}\frac{2(-1)^n n\pi i}{\xi_h^2}e^{p_n t}..$$

$$
\begin{aligned}
&\cdot\cdot\int_0^{\xi}\frac{\left\{T_{02}\cosh(\sqrt{p_n}\xi_1)-T_{01}\cosh[\sqrt{p_n}(\xi_1-\xi_h)]\right\}}{p}\sinh[\sqrt{p_n}(\xi-\xi_1)]\cdot\cdot\\
&\cdot\cdot\frac{d\ln[\eta(\xi_1)]}{d\xi_1}\,d\xi_1\Big|_{p_n=-\frac{n^2\pi^2}{\xi_h^2}}\\
&+\sum_{n=1}^{\infty}\left\{-\frac{4n^2\pi^2}{\xi_h^4}t+\frac{2}{\xi_h^2}\right\}e^{p_nt}\cdot\cdot\\
&\cdot\cdot\int_0^{\xi_h}\frac{\left\{T_{02}\cosh(\sqrt{p_n}\xi_1)-T_{01}\cosh[\sqrt{p_n}(\xi_1-\xi_h)]\right\}}{p}\cdot\cdot\\
&\cdot\cdot\sinh[\sqrt{p_n}(\xi_h-\xi_1)]\sinh(\sqrt{p_n}\xi)\frac{d\ln[\eta(\xi_1)]}{d\xi_1}d\xi_1\Big|_{p_n=-\frac{n^2\pi^2}{\xi_h^2}}\\
&-\sum_{n=1}^{\infty}\frac{4n^2\pi^2}{\xi_h^4}e^{p_nt}\cdot\cdot\\
&\cdot\cdot\frac{\partial}{\partial p}\int_0^{\xi_h}\frac{\left\{T_{02}\cosh(\sqrt{p_n}\xi_1)-T_{01}\cosh[\sqrt{p_n}(\xi_1-\xi_h)]\right\}}{p_n}\cdot\cdot\\
&\cdot\cdot\sinh[\sqrt{p_n}(\xi_h-\xi_1)]\sinh(\sqrt{p_n}\xi)\frac{d\ln[\eta(\xi_1)]}{d\xi_1}d\xi_1\Big|_{p_n=-\frac{n^2\pi^2}{\xi_h^2}}
\end{aligned}
\tag{2.4.33}
$$

If the terms for $m \geq 2$ were inserted, that would require the calculations of Laplace and inverse Laplace transform of functions having poles of order of three and higher.

Since the equation of transient temperature distribution change has already been found, transient temperature distribution now may be calculated numerically. The equation is expressed here in terms of the variable ξ, but also since $\xi = \xi(x)$, we can change the variable ξ back to the x by using the chain rule. Recalling the chain rule one more time

$$
d\xi_1 = \frac{d\xi_1}{dx_1}dx_1 \tag{2.4.34}
$$

and

$$
\frac{d\xi_1}{dx_1}\frac{d}{d\xi_1} = \frac{d}{dx_1} \tag{2.4.35}
$$

Applying (2.4.34) to first integral in the (2.4.33) gives

$$\frac{T_{02}-T_{01}}{\xi_h}\int_0^{\xi}(\xi_1-\xi)\frac{d\ln[\eta(\xi_1)]}{d\xi_1}d\xi_1 = \frac{T_{02}-T_{01}}{\xi_h}\int_0^{x}(\xi_1-\xi)\frac{d\ln[\eta(\xi_1)]}{d\xi_1}\frac{d\xi_1}{dx_1}dx_1$$

Applying (2.4.35) gives

$$\frac{T_{02}-T_{01}}{\xi_h}\int_0^{x}(\xi_1-\xi)\underbrace{\frac{d\ln[\eta(\xi_1)]}{d\xi_1}\frac{d\xi_1}{dx_1}}_{d\ln[\eta(x_1)]/dx_1}dx_1 = \frac{T_{02}-T_{01}}{\xi_h}\int_0^{x}(\xi_1-\xi)\frac{d\ln[\eta(x_1)]}{dx_1}dx_1$$

The transformation of the first term is complete. Since all the subsequent integrals have $\frac{d}{d\xi_1}\ln[\eta(\xi_1)]d\xi_1$ in the integral sign, transformation trend will be same. Accordingly, evaluating gives the second integral in (2.4.33) gives

$$\xi\frac{\{T_{01}-T_{02}\}}{\xi_h^2}\int_0^{\xi_h}(\xi_1-\xi_h)\frac{d\ln[\eta(\xi_1)]}{d\xi_1}d\xi_1 = \xi\frac{\{T_{01}-T_{02}\}}{\xi_h^2}\int_0^{h}(\xi_1(x_1)-\xi_h)\frac{d\ln[\eta(x_1)]}{dx_1}dx_1$$

and the next summation as

$$-\sum_{n=1}^{\infty}\frac{2(-1)^n n\pi i}{\xi_h^2}e^{p_n t}..$$
$$..\int_0^{\xi}\frac{\{T_{02}\cosh(\sqrt{p_n}\xi_1)-T_{01}\cosh[\sqrt{p_n}(\xi_1-\xi_h)]\}}{p_n}\sinh[\sqrt{p_n}(\xi-\xi_1)]..$$
$$..\frac{d\ln[\eta(\xi_1)]}{d\xi_1}\,d\xi_1\Big|_{p_n=-\frac{n^2\pi^2}{\xi_h^2}} = -\sum_{n=1}^{\infty}\frac{2(-1)^n n\pi i}{\xi_h^2}e^{p_n t}..$$

$$.. \int_0^x \frac{\left\{T_{02}\cosh(\sqrt{p_n}\xi_1(x_1)) - T_{01}\cosh[\sqrt{p_n}(\xi_1(x_1)-\xi_h)]\right\}}{p_n} \sinh[\sqrt{p_n}(\xi-\xi_1)]..$$

$$.. \frac{d\ln[\eta(x_1)]}{dx_1} dx_1 \Big|_{p_n=-\frac{n^2\pi^2}{\xi_h^2}}$$

the next summation as

$$\sum_{n=1}^{\infty} \left\{ -\frac{4n^2\pi^2}{\xi_h^4} t + \frac{2}{\xi_h^2} \right\} e^{p_n t} ..$$

$$.. \int_0^{\xi_h} \frac{\left\{T_{02}\cosh(\sqrt{p_n}\xi_1) - T_{01}\cosh[\sqrt{p_n}(\xi_1-\xi_h)]\right\}}{p_n} ..$$

$$.. \sinh[\sqrt{p_n}(\xi_h-\xi_1)] \sinh(\sqrt{p_n}\xi) \frac{d\ln[\eta(\xi_1)]}{d\xi_1} d\xi_1 \Big|_{p_n=-\frac{n^2\pi^2}{\xi_h^2}}$$

$$= \sum_{n=1}^{\infty} \left\{ -\frac{4n^2\pi^2}{\xi_h^4} t + \frac{2}{\xi_h^2} \right\} e^{p_n t} ..$$

$$.. \int_0^{h} \frac{\left\{T_{02}\cosh(\sqrt{p_n}\xi_1(x_1)) - T_{01}\cosh[\sqrt{p_n}(\xi_1(x_1)-\xi_h)]\right\}}{p_n} ..$$

$$.. \sinh[\sqrt{p_n}(\xi_h-\xi_1(x_1))] \sinh(\sqrt{p_n}\xi) \frac{d\ln[\eta(x_1)]}{dx_1} dx_1 \Big|_{p_n=-\frac{n^2\pi^2}{\xi_h^2}}$$

finally, the last summation as

$$-\sum_{n=1}^{\infty} \frac{4n^2\pi^2}{\xi_h^4} e^{p_n t} ..$$

$$.. \int_0^{\xi_h} \frac{\partial}{\partial p} \left\{ \frac{\left\{T_{02}\cosh(\sqrt{p_n}\xi_1) - T_{01}\cosh[\sqrt{p_n}(\xi_1-\xi_h)]\right\}}{p_n} ..$$

$$.. \sinh[\sqrt{p_n}(\xi_h-\xi_1)] \sinh(\sqrt{p_n}\xi) \frac{d\ln[\eta(\xi_1)]}{d\xi_1} d\xi_1 \right\} \Big|_{p_n=-\frac{n^2\pi^2}{\xi_h^2}} = -\sum_{n=1}^{\infty} \frac{4n^2\pi^2}{\xi_h^4} e^{p_n t} ..$$

$$.. \int_0^h \frac{\partial}{\partial p} \Bigg\{ \frac{\left\{ T_{02} \cosh(\sqrt{p_n}\xi_1(x_1)) - T_{01} \cosh[\sqrt{p_n}(\xi_1(x_1) - \xi_h)] \right\}}{p_n} ..$$

$$.. \sinh[\sqrt{p_n}(\xi_h - \xi_1(x_1))] \sinh(\sqrt{p_n}\xi) \frac{d \ln[\eta(x_1)]}{dx_1} dx_1 \Bigg\} \Bigg|_{p_n = -\frac{n^2\pi^2}{\xi_h^2}}$$

Taking the derivative by using MATLAB® symbolic toolbox gives

$$\int_0^h \frac{\partial}{\partial p} \Bigg\{ \frac{\left\{ T_{02} \cosh(\sqrt{p_n}\xi_1(x_1)) - T_{01} \cosh[\sqrt{p_n}(\xi_1(x_1) - \xi_h)] \right\}}{p_n} ..$$

$$.. \sinh[\sqrt{p_n}(\xi_h - \xi_1(x_1))] \sinh(\sqrt{p_n}\xi) \frac{d \ln[\eta(x_1)]}{dx_1} dx_1 =$$

$$\int_0^h \sinh(\sqrt{p_n}\xi) \sinh(\sqrt{p_n}[\xi_1(x_1) - \xi_h]) ..$$

$$.. \frac{T_2 \cosh(\sqrt{p_n}\xi_1(x_1)) - T_1 \cosh(\sqrt{p_n}[\xi_1(x_1) - \xi_h])}{p_n^2}$$

$$- \sinh(\sqrt{p_n}\xi) \sinh(\sqrt{p_n}[\xi_1(x_1) - \xi_h]) ..$$

$$.. \frac{T_2 \xi_1(x_1) \sinh(\sqrt{p_n}\xi_1(x_1)) - T_1 (\xi_1(x_1) - \xi_h) \sinh(\sqrt{p_n}[\xi_1(x_1) - \xi_h])}{2p_n\sqrt{p_n}}$$

$$- \xi \cosh(\sqrt{p_n}\xi) \sinh(\sqrt{p_n}[\xi_1(x_1) - \xi_h]) ..$$

$$.. \frac{T_2 \cosh(\sqrt{p_n}\xi_1(x_1)) - T_1 \cosh(\sqrt{p_n}[\xi_1(x_1) - \xi_h])}{2p_n\sqrt{p_n}}$$

$$- (\xi_1(x_1) - \xi_h) \sinh(\sqrt{p_n}\xi) \cosh(\sqrt{p_n}[\xi_1(x_1) - \xi_h]) ..$$

$$.. \frac{T_2 \cosh(\sqrt{p_n}\xi_1(x_1)) - T_1 \cosh(\sqrt{p_n}[\xi_1(x_1) - \xi_h])}{2p_n\sqrt{p_n}} \frac{d \ln[\eta(x_1)]}{dx_1} dx_1 \Bigg\} \Bigg|_{p_n = -\frac{n^2\pi^2}{\xi_h^2}} \tag{2.4.36}$$

The script and output of the program are given in (D). The whole transient temperature change distribution equation along the FGM strip of thickness of h in terms of x is written as

$$\tilde{T}(x,t) = T_{01} + (T_{02} - T_{01}) \frac{\xi}{\xi_h} + \sum_{n=1}^{\infty} 2e^{-\frac{n^2\pi^2}{\xi_h^2}t} \frac{(-1)^n T_{02} - T_{01}}{n\pi} \sin\left(n\pi \frac{\xi}{\xi_h}\right)$$

$$+ \frac{T_{02} - T_{01}}{\xi_h} \int_0^x (\xi_1(x_1) - \xi) \frac{d \ln[\eta(x_1)]}{dx_1} dx_1$$

$$+\xi\frac{\{T_{01}-T_{02}\}}{\xi_h^2}\int_0^h(\xi_1(x_1)-\xi_h)\frac{d\ln[\eta(x_1)]}{dx_1}dx_1$$

$$-\sum_{n=1}^{\infty}\frac{2(-1)^n n\pi i}{\xi_h^2}e^{p_n t}..$$

$$..\int_0^x\frac{\left\{T_{02}\cosh(\sqrt{p_n}\xi_1(x_1))-T_{01}\cosh[\sqrt{p_n}(\xi_1(x_1)-\xi_h)]\right\}\sinh[\sqrt{p_n}(\xi-\xi_1(x_1))]}{p_n}..$$

$$..\frac{d\ln[\eta(x_1)]}{dx_1}dx_1+\sum_{n=1}^{\infty}\left\{-\frac{4n^2\pi^2}{\xi_h^4}t+\frac{2}{\xi_h^2}\right\}e^{p_n t}..$$

$$..\int_0^h\frac{\left\{T_{02}\cosh(\sqrt{p_n}\xi_1(x_1))-T_{01}\cosh[\sqrt{p_n}(\xi_1(x_1)-\xi_h)]\right\}}{p_n}..$$

$$..\sinh[\sqrt{p_n}(\xi_h-\xi_1(x_1))]\sinh(\sqrt{p_n}\xi)\frac{d\ln[\eta(x_1)]}{dx_1}dx_1-\sum_{n=1}^{\infty}\frac{4n^2\pi^2}{\xi_h^4}e^{p_n t}..$$

$$..\int_0^h\sinh(\sqrt{p_n}\xi)\sinh(\sqrt{p_n}[\xi_1(x_1)-\xi_h])..$$

$$..\frac{T_2\cosh(\sqrt{p_n}\xi_1(x_1))-T_1\cosh(\sqrt{p_n}[\xi_1(x_1)-\xi_h])}{p_n^2}$$

$$-\sinh(\sqrt{p_n}\xi)\sinh(\sqrt{p_n}[\xi_1(x_1)-\xi_h])..$$

$$..\frac{T_2\xi_1(x_1)\sinh(\sqrt{p_n}\xi_1(x_1))-T_1(\xi_1(x_1)-\xi_h)\sinh(\sqrt{p_n}[\xi_1(x_1)-\xi_h])}{2p_n\sqrt{p_n}}$$

$$-\xi\cosh(\sqrt{p_n}\xi)\sinh(\sqrt{p_n}[\xi_1(x_1)-\xi_h])..$$

$$..\frac{T_2\cosh(\sqrt{p_n}\xi_1(x_1))-T_1\cosh(\sqrt{p_n}[\xi_1(x_1)-\xi_h])}{2p_n\sqrt{p_n}}$$

$$-(\xi_1(x_1)-\xi_h)\sinh(\sqrt{p_n}\xi)\cosh(\sqrt{p_n}[\xi_1(x_1)-\xi_h])..$$

$$..\frac{T_2\cosh(\sqrt{p_n}\xi_1(x_1))-T_1\cosh(\sqrt{p_n}[\xi_1(x_1)-\xi_h])}{2p_n\sqrt{p_n}}\frac{d\ln[\eta(x_1)]}{dx_1}dx_1\Bigg|_{p_n=-\frac{n^2\pi^2}{\xi_h^2}}$$

(2.4.37)

Note that all formulation is made here considering the transient temperature change. So regarding (2.1.1), transient temperature distribution may be expressed by simply adding the initial temperature T_0 to (2.4.37).

CHAPTER 3

NUMERICAL RESULTS FOR THE TRANSIENT TEMPERATURE DISTRIBUTION

In this chapter, the temperature distribution in an FGM strip consisting of ceramic/ metal is to be analyzed. As specific examples, ZrO_2/Ti-6Al-4V and ZrO_2/Rene-41 will be studied respectively. Along the thickness, numerical values of Young's modulus in the ZrO_2/Ti-6Al-4V strip are continuously get smaller from the pure ceramic phase to the pure metal phase, whereas they get larger in the ZrO_2/Rene-41 strip. The numerical results obtained for ZrO_2/Ti-6Al-4V serve the purpose of verification since this case has already been considered in [1, 2, 28]. Transient temperature distribution is solved for exponential, linear and parabolic gradations in thermomechanical properties from $x = 0$ to $x = h$ for both FGM strip respectively. That means, the thermomechanical properties of the FGM strip at a given position in x-direction are obtained by the given functions. In the next section, mathematical calculations will be given in detail.

3.1 Material Properties and Gradation

At $x = 0$ the composition of the FGM is pure ceramic, and at $x = h$ it is pure metal. The thermal conductivity, specific heat, density, linear expansion coefficient, shear modulus and Young's modulus of ceramic are λ_0, C_0, ρ_0, α_0, μ_0, E_0 and those of metal are λ_h, C_h, ρ_h, α_h, μ_h, E_h respectively. Poisson's ratio, ν is taken as constant. Properties of ZrO_2, Ti-6Al-4V (or often Ti64) and Rene-41 are given in Table 3.1.

Table 3.1: Material properties of ZrO_2 [2], Ti-6Al-4V [2] and Rene-41 [1, 4]

	Thermal conductivity, λ [W/(mK)]	Specific heat, C [J/(kgK)]	Density, ρ [kg/m^3]	Young's modulus E [GPa]	Linear expansion, coefficient, α [1/K]	Poisson's ratio, ν [-]
ZrO_2	2.09	456.7	5331	151.0	10^{-5}	0.33
Ti-6Al-4V	7.50	537.0	4420	116.7	0.95×10^{-5}	0.33
Rene-41	25.50	452.0	8250	219.7	1.67×10^{-5}	0.33

3.1.1 Exponential Gradation

In the following, the expressions of thermomechanical properties are shown to be defined by exponential functions. This is basically a two parameters curve fit satisfying the values of thermomechanical properties at the boundaries exactly and giving the values of thermomechanical properties at intermediate points according to an exponential variation. Beginning with the gradation of Young's modulus

$$E(x) = B_1 e^{\beta_1 x} \tag{3.1.1}$$

B_1 and β_1 are material constants to be determined. At $x = 0$, since the phase is pure ceramic, it means that at $x = 0$, $E(0) = E_0$. Applying this condition to (3.1.1) gives

$$E(0) = B_1 \cancel{e^{\beta_1 0}}^{1} = E_0$$

which yields

$$B_1 = E_0$$

Updating (3.1.1) as

$$E(x) = E_0 e^{\beta_1 x} \tag{3.1.2}$$

At $x = h$ since the phase is pure metal, $E(h) = E_h$ condition should be satisfied. Applying it to (3.1.2)

$$E(h) = E_0 e^{\beta_1 h} = E_h$$

which gives

$$\beta_1 = \frac{\ln(E_h/E_0)}{h}$$

β_1 is actually referred to as the nonhomogeneity parameter of the Young's modulus. Final expression of the Young's modulus for exponential gradation is written by

$$E(x) = E_0 e^{\ln(E_h/E_0)x/h} \tag{3.1.3}$$

Here each thermomechanical property is assumed to change according to the exponential function from $x = 0$ to $x = h$; remaining thermomechanical properties may then be defined as below regarding the expression of Young's modulus. The linear expansion coefficient is

$$\alpha(x) = \alpha_0 e^{\ln(\alpha_h/\alpha_0)x/h} \tag{3.1.4}$$

The thermal conductivity is

$$\lambda(x) = \lambda_0 e^{\ln(\lambda_h/\lambda_0)x/h} \tag{3.1.5}$$

The specific heat is

$$C(x) = C_0 e^{\ln(C_h/C_0)x/h} \tag{3.1.6}$$

Finallly the density is

$$\rho(x) = \rho_0 e^{\ln(\rho_h/\rho_0)x/h} \tag{3.1.7}$$

The thermomechanical properties have now been expressed as a function of x. Then $\eta(x)$ may also be expressed. Considering (2.1.10), it may simply be written as

$$\eta(x) = \sqrt{\lambda(x)C(x)\rho(x)} \tag{3.1.8}$$

Using (3.1.5), (3.1.6), (3.1.7) and (3.1.8); the transient temperature distribution (2.4.37), is calculated by MATLAB® numerically. The related script is given in (E). In the calculations normalized time t_n, which is non-dimensional, is used, and it is defined by the following formula same as in [2]

$$t_n = \frac{\lambda_0}{C_0\rho_0 h^2}t$$

The thickness h is taken as unity for simplicity without losing generality. In order to validate the numerical results, transient temperature changes in the boundaries, i.e., the boundary conditions are considered to be the same as in [2], which are $T_{01} = -700\,K$ and $T_{02} = -600\,K$. This represents the sudden cooling of an FGM layer from its rather high processing temperature down to room temperature.

It may be seen that, in (2.4.37) the upper limits of the summation signs go to ∞. However during recursive calculations it is observed that setting the upper limits to 10 gives a converging solution. Tabulated transient temperature change in the strip through the thickness, i.e., $T(x,t) - T_0$ in Table 3.2 are normalized by the absolute value of T_{01} for the normalized time $t_n = 0.05$. Results for $m = 0$ refer to the solution of unperturbed temperature distribution i.e., to the numerical calculation of the terms that do not contain $d\ln(\eta(x))/dx$ in (2.4.37), whereas results for $m = 1$ refer to calculation of the transient thermal distribution change by using the full expression.

Table 3.2: Normalized results of the transient temperature change distribution solutions with different orders (m) at $t_n = 0.05$ for exponential gradation of material properties of ZrO_2/Ti-6Al-4V

x/h	$m = 0$	$m = 1$
0	-1.0000	-1.0000
0.1	-0.7896	-0.7718
0.2	-0.6217	-0.6006
0.3	-0.5107	-0.4966
0.4	-0.4585	-0.4569
0.5	-0.4588	-0.4703
0.6	-0.5010	-0.5225
0.7	-0.5728	-0.5988
0.8	-0.6624	-0.6863
0.9	-0.7599	-0.7749
1	-0.8571	-0.8571

Table 3.3: Comparison between the normalized temperature solutions with different orders (J) when $t_n = 0.05$, taken from [2] (ZrO_2/Ti-6Al-4V)

x/h	$J = 0$	$J = 1$	$J = 2$
0	-1.000	-1.000	-1.000
0.1	-0.790	-0.772	-0.772
0.2	-0.622	-0.601	-0.602
0.3	-0.511	-0.497	-0.499
0.4	-0.458	-0.457	-0.460
0.5	-0.459	-0.470	-0.473
0.6	-0.501	-0.523	-0.525
0.7	-0.573	-0.599	-0.600
0.8	-0.662	-0.686	-0.687
0.9	-0.730	-0.775	-0.775
1	-0.857	-0.857	-0.857

The normalized transient temperature distribution change calculated in [2] is also shown in Table 3.3 to compare with and verify our solutions. Note that, J corresponds to m in our notation. In Table 3.3, there is an extra column of results of calculation for $J = 2$. It refers to the solution for three terms expansion.

The normalized transient temperature distribution in Table 3.2 is tabulated with four significant digits, whereas in Table 3.3 it is three. When the values in Table 3.2 are to be rounded up to three decimal places, it may be seen that results are identical. It is the verification of the solution of the transient thermal distribution in an FGM strip with general thermomechanical properties.

Also for exponential gradation another script is written to find numerical results regarding the equation (2.4.33) by using MATLAB®. In (2.4.33) an analytical expression for transient temperature have been found in terms of ξ and the variable of the integrals is actually function of x_1, i.e., $\xi_1 = \xi_1(x_1)$. In (2.1.10), η is defined as a function of ξ. Since ξ and ξ_1 are independent from each other; $\eta(\xi_1)$ may then be defined as

$$\eta(\xi_1) = \sqrt{\lambda(\xi_1)C(\xi_1)\rho(\xi_1)} \tag{3.1.9}$$

By using (3.1.5), (3.1.6) and (3.1.7), since x and x_1 are independent variables, it may be shown that

$$\lambda(x_1) = \lambda_0 e^{\ln(\lambda_h/\lambda_0)x_1/h} \tag{3.1.10}$$

$$C(x_1) = C_0 e^{\ln(C_h/C_0)x_1/h} \tag{3.1.11}$$

$$\rho(x_1) = C_0 e^{\ln(\rho_h/\rho_0)x_1/h} \tag{3.1.12}$$

Therefore, the multiplier $d\ln[\eta(\xi_1)]/d\xi_1$ in the integrals in (2.4.33) may then be handled such as follows

Table 3.4: Normalized results of the transient temperature change distribution solutions with different orders (m) at $t_n = 2$ and at steady state for exponential gradation of material properties of ZrO_2/Ti-6Al-4V

x/h	$m = 0$	$m = 1$	t_∞
0	-1.0000	-1.0000	-1.0000
0.1	-0.9812	-0.9765	-0.9765
0.2	-0.9635	-0.9556	-0.9556
0.3	-0.9470	-0.9370	-0.9370
0.4	-0.9315	-0.9206	-0.9206
0.5	-0.9170	-0.9061	-0.9061
0.6	-0.9034	-0.8934	-0.8934
0.7	-0.8907	-0.8823	-0.8823
0.8	-0.8788	-0.8727	-0.8727
0.9	-0.8676	-0.8643	-0.8643
1	-0.8571	-0.8571	-0.8571

* First the expression for ξ_1 is found in terms of x_1 according to (3.1.8) as below

$$\xi_1(x_1) = \int_0^{x_1} \frac{1}{\sqrt{\kappa(r)}} dr \tag{3.1.13}$$

* Then the inverse function of $\xi_1(x_1)$, i.e., $x_1(\xi_1)$ is found.

* Lastly expressing (3.1.10), (3.1.11) and (3.1.12) in terms of $x_1(\xi_1)$ and substituting them into (3.1.9), the analytical expression for $\eta(\xi_1)$ is found. Taking its derivative by MATLAB® symbolic toolbox is straightforward.

Other mathematical manipulations are also straightforward. The script and the output of the program are given in (F) for the same x/h points provided in Table 3.2. It may be necessary to check that the chain rule is applied to (2.4.36) correctly. It is observed that the results are identical with those in Table 3.2.

In Table 3.4 the normalized transient temperature distribution change is tabulated at $t_n = 2$ and normalized steady state temperature distribution. It is seen there is no difference between the results at $t_n = 2$ and steady state. Therefore it may be said that when $t_n = 2$ temperature distribution has reached steady state.

The transient temperature change distribution at different normalized times are depicted in Figure 3.1.

3.1.2 Power Law Gradation

The expressions of thermomechanical properties are shown to be this time defined by power law functions. Similar to exponential gradation, here the gradation is also defined by a two parameters curve fit satisfying the values of thermomechanical properties at the boundaries and giving the values of thermomechanical properties at intermediate points according to power law functions. Definition of thermomechanical properties are written below. Note that i can have values of $1, 2, \cdots$. For $i = 1$ the gradation in the material properties is linear, whereas for $i = 2$ it is parabolic. Beginning with the gradation of Young's modulus

$$E(x) = U_1(x/h)^i + \upsilon_1 \tag{3.1.14}$$

U_1 and υ_1 are constants to be determined. At $x = 0$ since the phase is pure ceramic, it means that at $x = 0$, $E(0) = E_0$. Applying this condition to (3.1.14) gives

$$E(0) = U_1\cancelto{0}{(0/h)^i} + \upsilon_1 = E_0 \rightarrow \upsilon_1 = E_0$$

giving

$$\upsilon_1 = E_0$$

Updating (3.1.14) as

$$E(x) = U_1(x/h)^i + E_0 \tag{3.1.15}$$

At $x = h$ the phase is pure metal, so $E(h) = E_h$ condition should be satisfied. Applying it to (3.1.2) gives

$$E(h) = U_1 \cancel{(h/h)^i}^{1} + E_0 = E_h$$

which leads to

$$U_1 = E_h - E_0$$

Final expression of Young's modulus for power law gradation is then written by

$$E(x) = (E_h - E_0)(x/h)^i + E_0 \tag{3.1.16}$$

Here each thermomechanical property is assumed to change according to the power law functions from x to h; remaining thermomechanical properties may then be defined as below regarding the expression of Young's modulus. The linear expansion coefficient is

$$\alpha(x) = (\alpha_h - \alpha_0)(x/h)^i + \alpha_0 \tag{3.1.17}$$

The thermal conductivity is

$$\lambda(x) = (\lambda_h - \lambda_0)(x/h)^i + \lambda_0 \tag{3.1.18}$$

Table 3.5: Normalized results of the transient temperature change distribution solutions with different orders (m) at $t_n = 0.01$ for linear gradation of material properties of ZrO_2/Ti-6Al-4V

x/h	$m = 0$	$m = 1$
0	-1.0000	-1.0000
0.1	-0.5051	-0.4774
0.2	-0.2053	-0.1848
0.3	-0.0709	-0.0617
0.4	-0.0293	-0.0272
0.5	-0.0387	-0.0414
0.6	-0.0937	-0.1011
0.7	-0.2051	-0.2172
0.8	-0.3794	-0.3937
0.9	-0.6060	-0.6170
1	-0.8571	-0.8571

Table 3.6: Normalized results of the transient temperature change distribution solutions with different orders (m) at $t_n = 0.01$ for parabolic gradation of material properties of ZrO_2/Ti-6Al-4V

x/h	$m = 0$	$m = 1$	t_∞
0	-1.0000	-1.0000	-1.000
0.1	-0.4814	-0.4758	-0.9776
0.2	-0.1642	-0.1590	-0.9563
0.3	-0.0412	-0.0388	-0.9366
0.4	-0.0116	-0.0117	-0.9192
0.5	-0.0213	-0.0250	-0.9041
0.6	-0.0710	-0.0812	-0.8911
0.7	-0.1817	-0.2011	-0.8802
0.8	-0.3640	-0.3894	-0.8711
0.9	-0.6013	-0.6217	-0.8635
1	-0.8571	-0.8571	-0.8571

Table 3.7: Normalized results of the transient temperature change distribution solutions with different orders (m) when $t_n = 0.01$ for linear gradation of material properties of ZrO_2/Rene-41

x/h	$m = 0$	$m = 1$	t_∞
0	-1.0000	-1.0000	-1.000
0.1	-0.4936	-0.4777	-0.9765
0.2	-0.1849	-0.1731	-0.9556
0.3	-0.0550	-0.0500	-0.9370
0.4	-0.0186	-0.0180	-0.9206
0.5	-0.0277	-0.0312	-0.9061
0.6	-0.0795	-0.0889	-0.8934
0.7	-0.1904	-0.2076	-0.8823
0.8	-0.3695	-0.3917	-0.8727
0.9	-0.6029	-0.6208	-0.8643
1	-0.8571	-0.8571	-0.8571

Table 3.8: Normalized results of the transient temperature change distribution solutions with different orders (m) at $t_n = 0.01$ for linear gradation of material properties of ZrO_2/Rene-41

x/h	$m = 0$	$m = 1$	t_∞
0	-1.0000	-1.0000	-1.000
0.1	-0.5632	-0.5309	-0.9693
0.2	-0.3139	-0.2850	-0.9475
0.3	-0.1902	-0.1742	-0.9302
0.4	-0.1537	-0.1511	-0.9156
0.5	-0.1813	-0.1900	-0.9031
0.6	-0.2587	-0.2755	-0.8920
0.7	-0.3756	-0.3962	-0.8820
0.8	-0.5217	-0.5412	-0.8730
0.9	-0.6862	-0.6988	-0.8647
1	-0.8571	-0.8571	-0.8571

Table 3.9: Normalized results of the transient temperature change distribution solutions with different orders (m) at $t_n = 0.01$ for parabolic gradation of material properties of ZrO_2/Rene-41

x/h	$m = 0$	$m = 1$	t_∞
0	-1.0000	-1.0000	-1.000
0.1	-0.4872	-0.4813	-0.9723
0.2	-0.1861	-0.1805	-0.9475
0.3	-0.0735	-0.0730	-0.9268
0.4	-0.0636	-0.0715	-0.9100
0.5	-0.1147	-0.1336	-0.8964
0.6	-0.2125	-0.2422	-0.8853
0.7	-0.3476	-0.3839	-0.8762
0.8	-0.5085	-0.5434	-0.8687
0.9	-0.6825	-0.7055	-0.8624
1	-0.8571	-0.8571	-0.8571

The specific heat is

$$C(x) = (C_h - C_0)(x/h)^i + C_0 \tag{3.1.19}$$

Finally the density is

$$\rho(x) = (\rho_h - \rho_0)(x/h)^i + \rho_0 \tag{3.1.20}$$

By giving $i = 1$ and $i = 2$, linear and parabolic variation of the thermomechanical properties are provided. Transient temperature change distribution is calculated for these variations with the same boundary conditions of temperature changes, i.e., for the same thermal shock conditions as those used to find numerical solution for exponential property variation. Results of different orders for the linear and parabolic gradation of material properties are given in Table 3.5 and Table 3.6 at $t_n = 0.01$

and they are depicted also at different normalized time values also in Figure 3.2 and Figure 3.3, respectively.

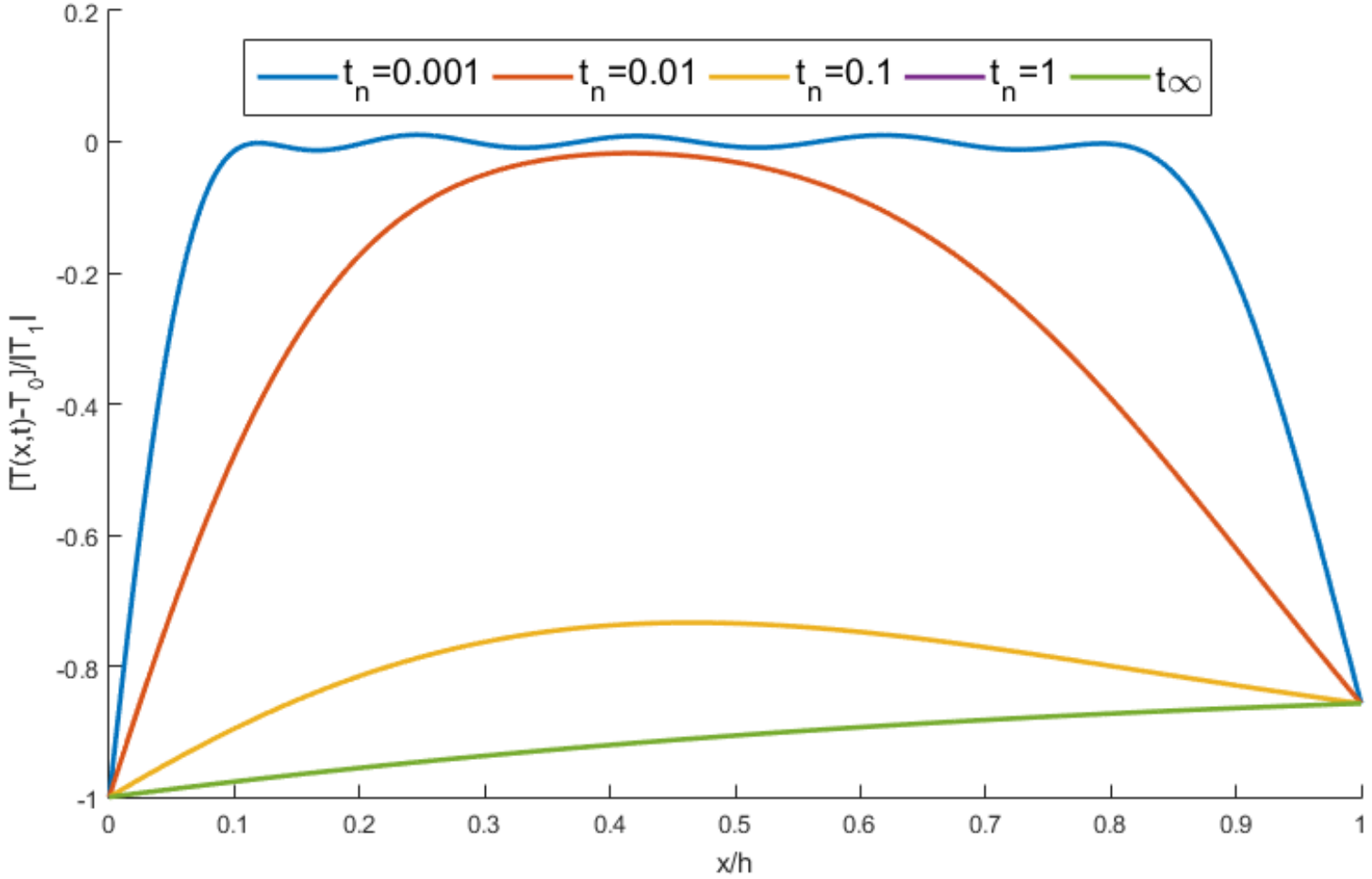

Figure 3.1: Normalized transient temperature change distributions for different time values in ZrO_2/Ti-6Al-4V FGM strip under thermal shock for exponential gradation of material properties

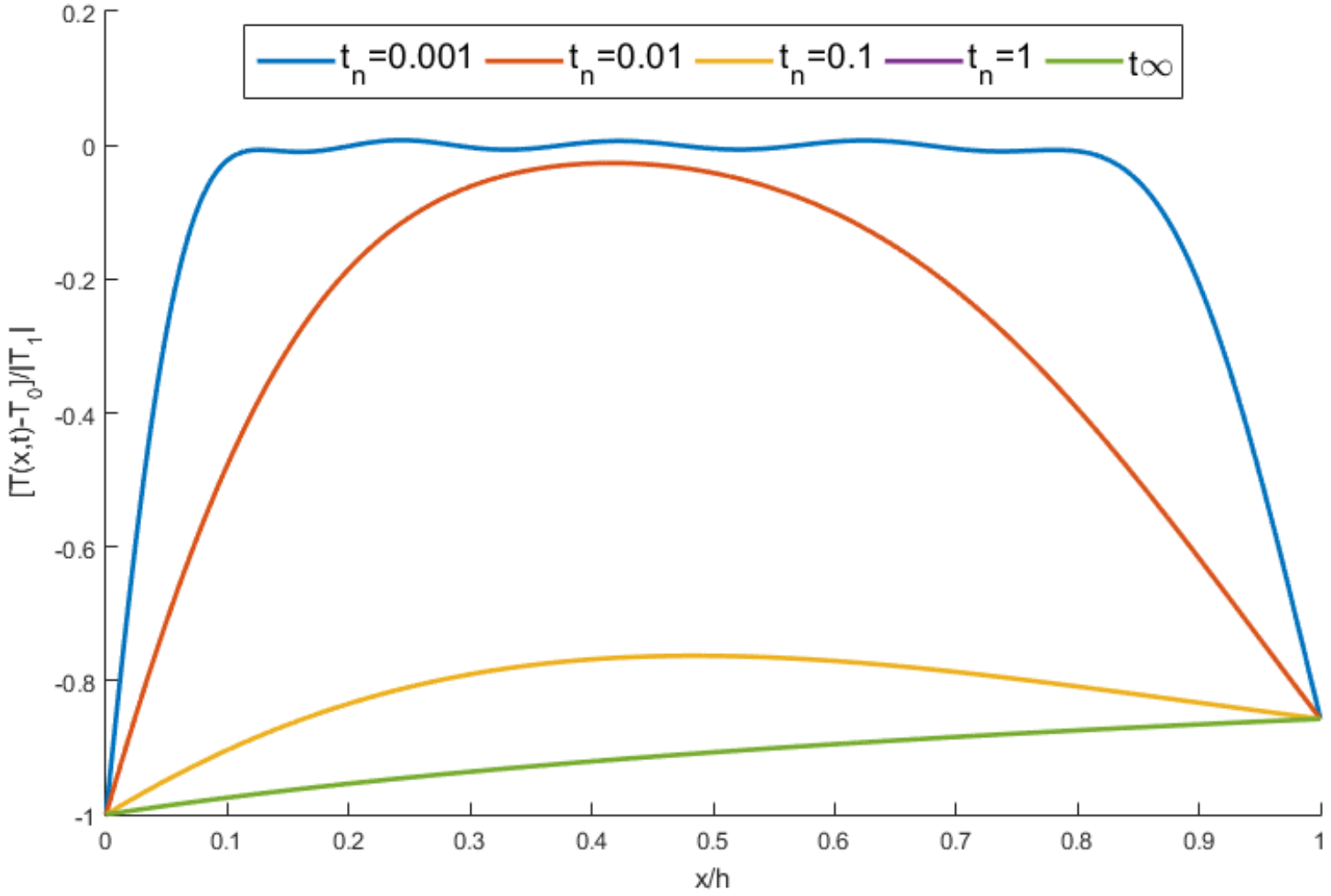

Figure 3.2: Normalized transient temperature change distributions for different time values in ZrO_2/Ti-6Al-4V FGM strip under thermal shock for linear gradation of material properties ($i = 1$)

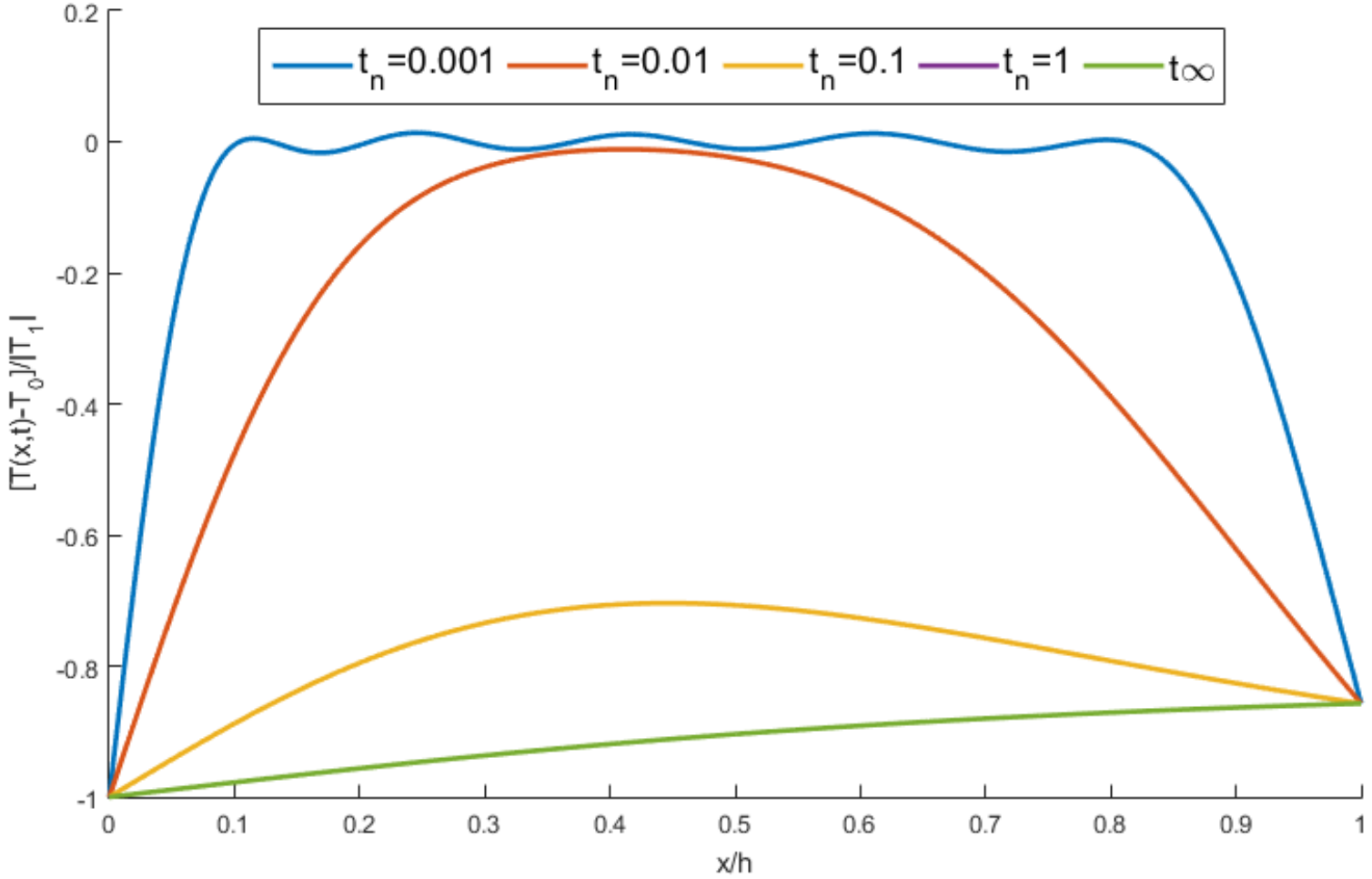

Figure 3.3: Normalized transient temperature change distributions for different time values in ZrO_2/Ti-6Al-4V FGM strip under thermal shock for parabolic gradation of material properties ($i = 2$)

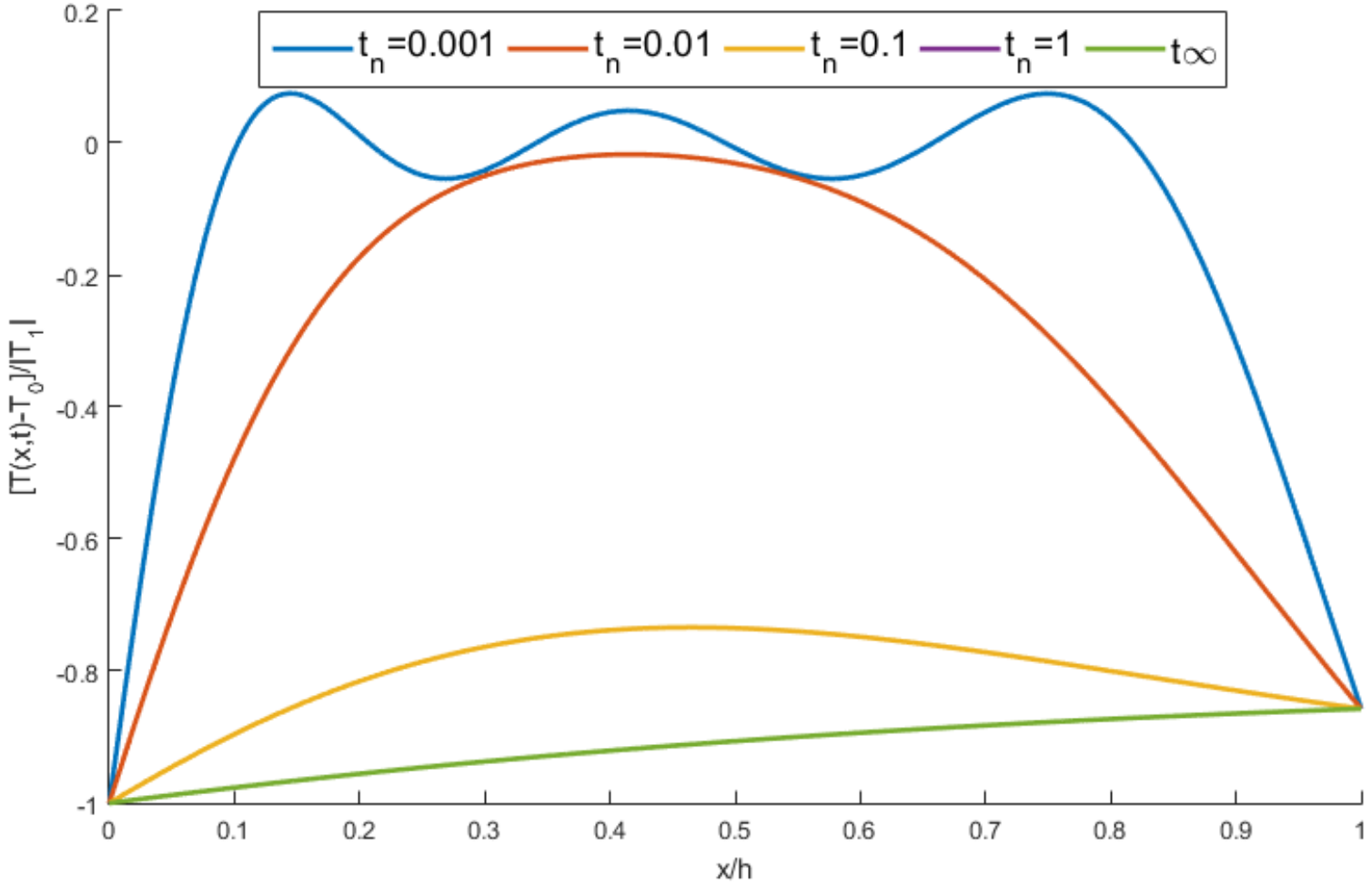

Figure 3.4: Normalized transient temperature change distributions for different time values in ZrO_2/Rene-41 FGM strip under thermal shock for exponential gradation of material properties

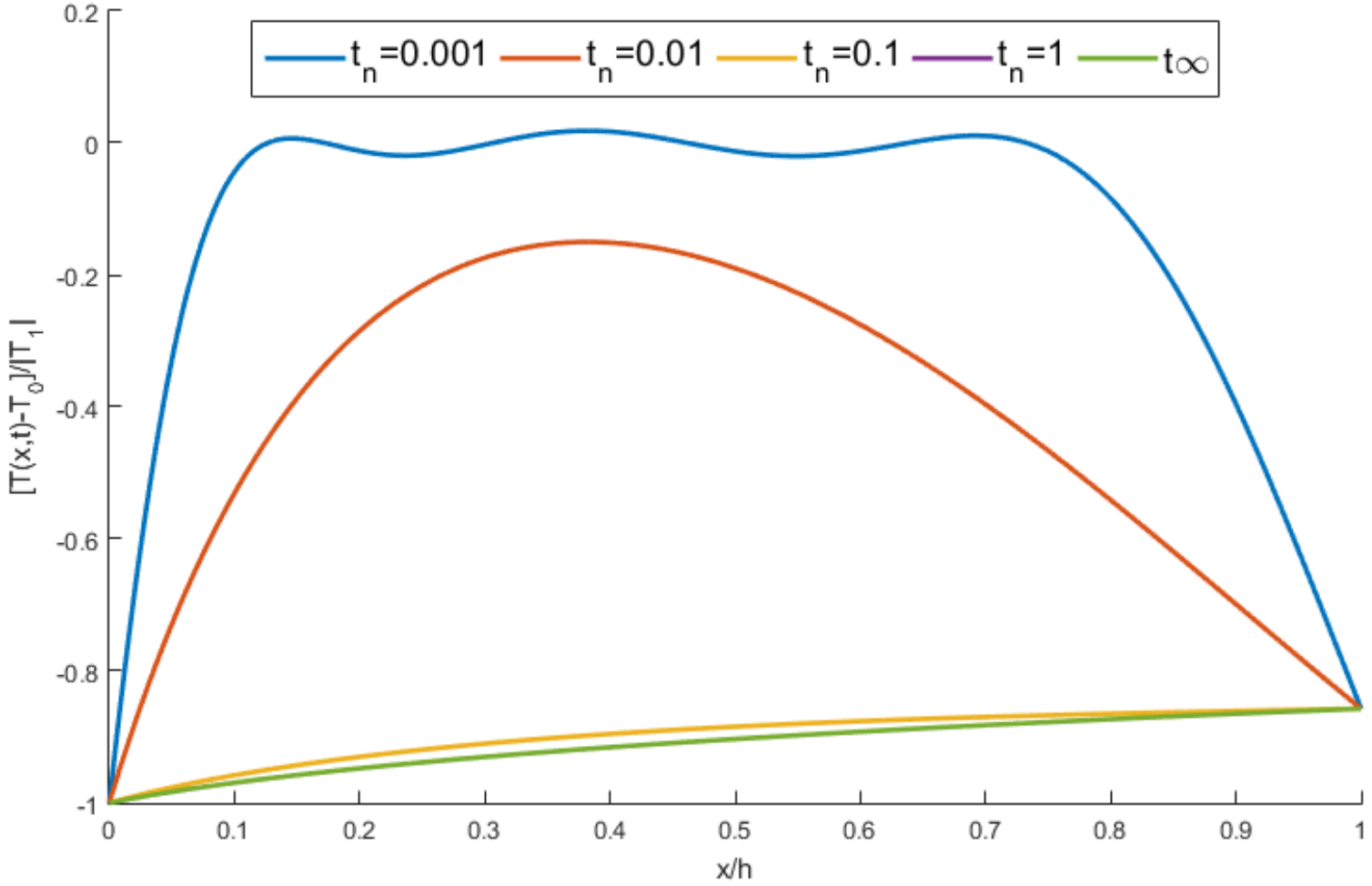

Figure 3.5: Normalized transient temperature change distributions for different time values in ZrO_2/Rene-41 FGM strip under thermal shock for linear gradation of material properties ($i = 1$)

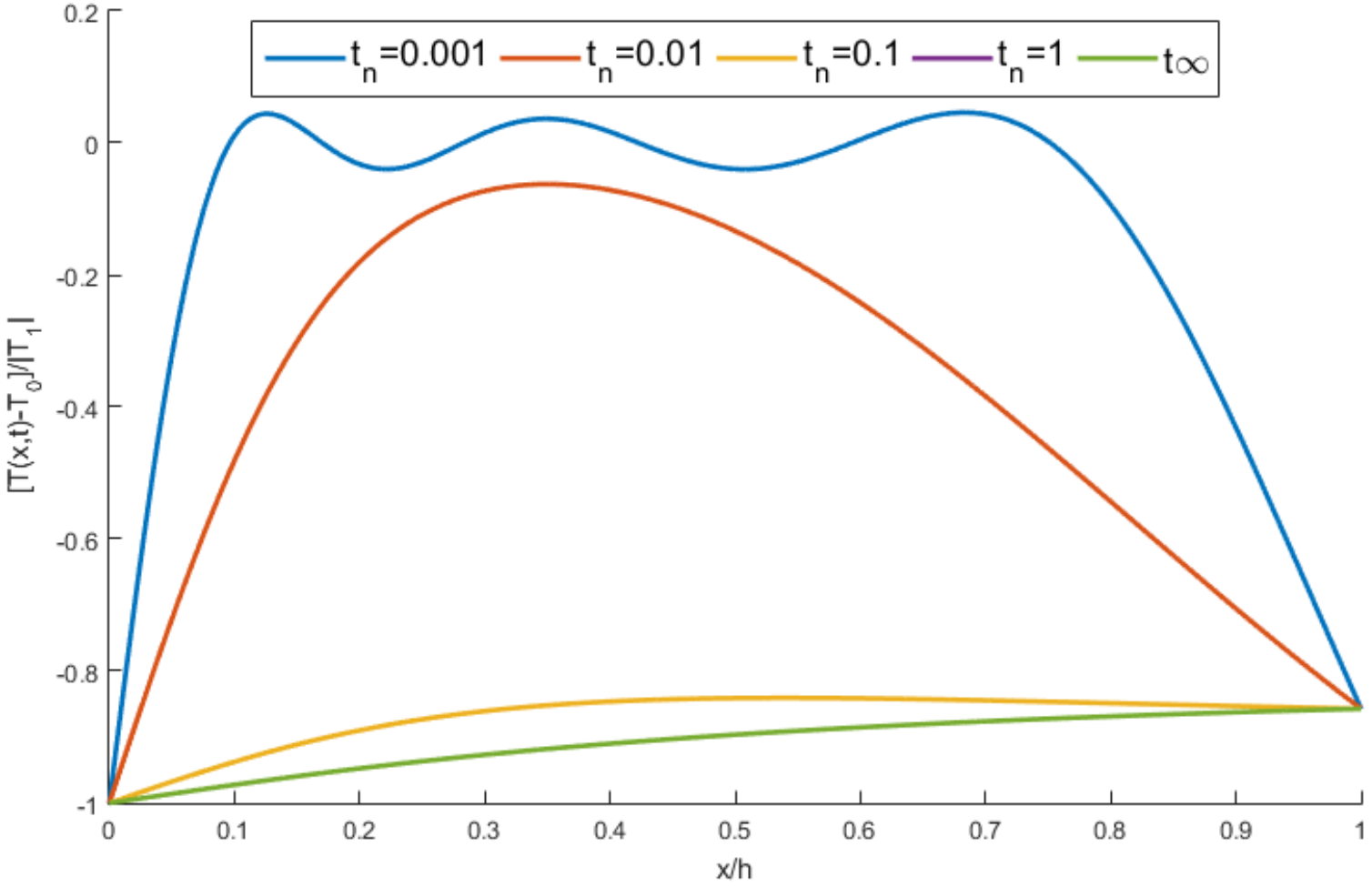

Figure 3.6: Normalized transient temperature change distributions for different time values in ZrO_2/Rene-41 FGM strip under thermal shock for parabolic gradation of material properties ($i = 2$)

CHAPTER 4

TRANSIENT THERMAL STRESSES AND THERMAL STRESS INTENSITY FACTORS

4.1 Thermal Stresses

When the material properties are changing only in thickness direction, the problem is one of mode-I plane strain crack problem [49]. For an infinitely long FGM strip of a thickness h (i.e., $-\infty < y < \infty$, $0 < x < h$) if the strip is free of surface tractions at $x = 0$ and $x = h$ and subjected to transient temperature distribution, following conditions could be applied [1, 49]

$$\begin{aligned} &\sigma_{xx} = 0 \\ &\epsilon_{zz} = 0 \\ &\sigma_{ij} = 0 \quad i \neq j \quad (i, j = x, y) \end{aligned} \tag{4.1.1}$$

Also all nonvanishing field quantities are independent of y and z in this case. Thus the only compatibility equation that needs to be satisfied is

$$\frac{\partial \epsilon_{yy}(x,t)}{\partial x^2} = 0 \tag{4.1.2}$$

which gives

$$\epsilon_{yy}(x,t) = A_t x + B_t \tag{4.1.3}$$

Thus the transient thermal stress distribution may be obtained as for plane strain approach [1, 49]

$$\sigma_{yy}^{T}(x,t) = \frac{E(x)}{1-\nu^2}\left\{A_t x + B_t - (1+\nu)\alpha(x)\tilde{T}(x,t)\right\} \tag{4.1.4}$$

where A_t and B_t are the time dependent coefficients to be determined from the boundary conditions at the edges.

If the surfaces of the strip are assumed to be insulated and it has a small width, w (i.e., $w \to 0$ in z-direction) then the plane stress approach is considered. The transient thermal stress distribution may be written [1, 49]

$$\sigma_{yy}^{T}(x,t) = E(x)\left\{A_t x + B_t - \alpha(x)\tilde{T}(x,t)\right\} \tag{4.1.5}$$

where the following conditions apply

$$\begin{aligned} &\sigma_{xx} = 0 \\ &\sigma_{zz} = 0 \\ &\sigma_{ij} = 0 \quad i \neq j \quad (i,j = x,y) \end{aligned} \tag{4.1.6}$$

Such as in [1, 2, 28], here also a plane strain (or cylindrical bending [49]) approach is considered. Note that these equations apply in the absence of any cracks. If the plate is unconstrained along its far away edges A_t and B_t may be solved from the following conditions

$$\begin{aligned} \int_0^h \sigma_{yy}^{T}(x,t)dx = 0 \\ \int_0^h x\sigma_{yy}^{T}(x,t)dx = 0 \end{aligned} \tag{4.1.7}$$

These conditions ensure that there is no net force in y-direction and there is no net bending moment about z-axis, hence the strip is free of constraints. Coefficient A_t and B_t may be calculated by solving (4.1.7) simultaneously. Substituting (4.1.4) into (4.1.7) gives

$$\int_0^h \left[E(x)\left\{A_t x + B_t - \alpha(x)[1+\nu]\tilde{T}(x,t)\right\}/(1-\nu^2)\right]dx = 0$$

$$\int_0^h \left[xE(x)\left\{A_t x + B_t - \alpha(x)[1+\nu]\tilde{T}(x,t)\right\}/(1-\nu^2)\right]dx = 0$$

With mathematical manipulations the following equations also hold

$$\int_0^h \frac{E(x)\Big\{A_t x + B_t\Big\}}{1-\nu^2}dx = \int_0^h \frac{E(x)\alpha(x)[1+\nu^2]\tilde{T}(x,t)}{1-\nu^2}dx$$
$$\int_0^h \frac{xE(x)\Big\{A_t x + B_t\Big\}}{1-\nu^2}dx = \int_0^h \frac{xE(x)\alpha(x)[1+\nu^2]\tilde{T}(x,t)}{1-\nu^2}dx \tag{4.1.8}$$

To calculate the coefficients A_t and B_t numerically, MATLAB® is used. Since ν is constant, the denominators may be canceled in both sides in (4.1.8) and it expands then as follows

$$A_t\int_0^h xE(x)dx + B_t\int_0^h E(x)dx = \int_0^h E(x)\alpha(x)[1+\nu^2]\tilde{T}(x,t)dx$$
$$A_t\int_0^h x^2E(x)dx + B_t\int_0^h xE(x)dx = \int_0^h xE(x)\alpha(x)[1+\nu^2]\tilde{T}(x,t)dx \tag{4.1.9}$$

For a certain material property change; numerical calculations of $\int_0^h xE(x)dx$, $\int_0^h E(x)dx$, $\int_0^h x^2E(x)dx$, $\int_0^h E(x)\alpha(x)[1+\nu^2]\tilde{T}(x,t)dx$ and $\int_0^h xE(x)\alpha(x)[1+\nu^2]\tilde{T}(x,t)dx$ are possible. Only unknowns in this group of equations are A_t and B_t. Actually $\int_0^h xE(x)dx$, $\int_0^h E(x)dx$ and $\int_0^h x^2E(x)dx$ are the known coefficients of A_t and B_t. Therefore, this group of equations becomes a system of linear equations. The solution of this system of equations gives A_t and B_t at a certain time corresponding to transient temperature distribution at that instant. This solution may then be found by using MATLAB®. The point to note here is that, since the limits of the integrals are from 0 to h, the whole transient temperature distribution along the thickness, i.e., from 0 to h must be calculated. Otherwise it may not be possible to obtain a solution by numerical methods.

After calculating the coefficients A_t and B_t, substituting the results into (4.1.4), transient thermal stress distribution for plane strain case may be obtained. The temperature boundary conditions remain the same as in calculations of transient temperature

distribution, which are $T_{01} = -700\,K$ and $T_{02} = -600\,K$. Tabulated values of transient thermal stress distribution are normalized by as in [1, 2, 28]

$$\sigma_0 = \frac{E_0 \alpha_0 |T_{01}|}{1 - \nu} \tag{4.1.10}$$

Transient thermal stress distributions for particular values of normalized time are given in Tables 4.1, 4.2, 4.3, 4.4, 4.5 for ZrO_2/Ti-6Al-4V and in Tables 4.6, 4.7, 4.8 for ZrO_2/Rene-41 material combinations. Also the thermal stress curves are plotted for particular values of normalized time with different gradations in material properties in Figures 4.1, 4.2, 4.3 for ZrO_2/Ti-6Al-4V and 4.4, 4.5, 4.6 for ZrO_2/Rene-41. In any published paper since there is no transient stress distribution table, the exact numerical results could not be compared. However as the curves in Figures 4.1, 4.2, 4.3 are compared with those in [1, 28], it is seen that the curves overlap each other.

Table 4.1: Normalized results of the transient thermal stress distribution solutions with different orders (m) at $t_n = 0.05$ and at steady state for exponential gradation of material properties in ZrO_2/Ti-6Al-4V under thermal shock

x/h	$m = 0$	$m = 1$	t_∞
0	0.3501	0.3692	0.0169
0.1	0.1404	0.1373	0.0066
0.2	−0.0168	−0.0272	0.0005
0.3	−0.1127	−0.1216	−0.0048
0.4	−0.1506	−0.1515	−0.0068
0.5	−0.1411	−0.1348	−0.0069
0.6	−0.0972	−0.0867	−0.0054
0.7	−0.0320	−0.0220	−0.0026
0.8	0.0434	0.0476	−0.0014
0.9	0.1202	0.1137	0.0062
1	0.1922	0.1713	0.0118

Table 4.2: Normalized results of the transient thermal stress distribution solutions with different orders (m) at $t_n = 0.05$ and at steady state for linear gradation in material properties of ZrO_2/Ti-6Al-4V under thermal shock

x/h	$m = 0$	$m = 1$	t_∞
0	0.3133	0.3446	0.0183
0.1	0.1218	0.1205	0.0061
0.2	−0.0160	−0.0273	0.0012
0.3	−0.0981	−0.1075	−0.0052
0.4	−0.1307	−0.1336	−0.0067
0.5	−0.1233	−0.1198	−0.0063
0.6	−0.0864	−0.0792	−0.0046
0.7	−0.0301	−0.0229	−0.0019
0.8	0.0366	0.0402	−0.0016
0.9	0.1063	0.1032	0.0057
1	0.1731	0.1610	0.0101

Table 4.3: Normalized results of the transient thermal stress distribution solutions with different orders (m) at $t_n = 0.05$ and at steady state for linear gradation in thermomechanical properties and exponential gradation in Young's modulus $E(x)$ of ZrO_2/Ti-6Al-4V under thermal shock

x/h	$m = 0$	$m = 1$	t_∞
0	0.3186	0.3493	0.0269
0.1	0.1262	0.1244	0.0137
0.2	−0.0117	−0.0233	0.0055
0.3	−0.0937	−0.1033	0.0007
0.4	−0.1265	−0.1295	−0.0016
0.5	−0.1195	−0.1161	−0.0020
0.6	−0.0834	−0.0762	−0.0011
0.7	−0.0280	−0.0206	0.0009
0.8	0.0379	0.0417	0.0037
0.9	0.1070	0.1043	0.0071
1	0.1738	0.1622	0.0109

Table 4.4: Normalized results of the transient thermal stress distribution solutions with different orders (m) at $t_n = 0.01$ and at steady state for parabolic gradation in material properties of ZrO_2/Ti-6Al-4V under thermal shock

x/h	$m = 0$	$m = 1$	t_∞
0	0.7624	0.7715	0.0088
0.1	0.2370	0.2373	0.0046
0.2	−0.0850	−0.0873	0.0004
0.3	−0.2102	−0.2128	−0.0028
0.4	−0.2410	−0.2442	−0.0046
0.5	−0.2326	−0.2354	−0.0049
0.6	−0.1873	−0.1869	−0.0038
0.7	−0.0910	−0.0855	−0.0018
0.8	0.0570	0.0644	0.0011
0.9	0.2328	0.2332	0.0042
1	0.3993	0.3821	0.0074

Table 4.5: Normalized results of the transient thermal stress distribution solutions with different orders (m) at $t_n = 0.01$ and at steady state for parabolic gradation in thermomechanical properties and exponential gradation in Young's modulus $E(x)$ of ZrO_2/Ti-6Al-4V under thermal shock

x/h	$m = 0$	$m = 1$	t_∞
0	0.7554	0.7644	0.0087
0.1	0.2251	0.2253	0.0044
0.2	−0.0874	−0.0897	0.0003
0.3	−0.2041	−0.2066	−0.0027
0.4	−0.2307	−0.2337	−0.0044
0.5	−0.2214	−0.2240	−0.0046
0.6	−0.1789	−0.1786	−0.0037
0.7	−0.0893	−0.0841	−0.0017
0.8	0.0508	0.0580	0.0009
0.9	0.2231	0.2237	0.0040
1	0.3965	0.3795	0.0073

Table 4.6: Normalized results of the transient thermal stress distribution solutions with different orders (m) at $t_n = 0.01$ and at steady state for exponential gradation in thermomechanical properties and exponential gradation in Young's modulus $E(x)$ of ZrO_2/Rene-41 under thermal shock

x/h	$m = 0$	$m = 1$	t_∞
0	0.9344	0.9528	0.0309
0.1	0.4049	0.4014	0.0160
0.2	0.0122	0.0071	−0.0033
0.3	−0.2165	−0.2193	−0.0070
0.4	−0.3470	−0.3499	−0.0142
0.5	−0.4217	−0.4245	−0.0179
0.6	−0.4275	−0.4262	−0.0173
0.7	−0.3130	−0.3031	−0.0119
0.8	−0.0275	0.0121	0.0007
0.9	0.4417	0.4436	0.0169
1	1.0566	1.0099	0.0421

Table 4.7: Normalized results of the transient thermal stress distribution solutions with different orders (m) at $t_n = 0.01$ and at steady state for linear gradation in thermomechanical properties and exponential gradation in Young's modulus $E(x)$ of ZrO_2/Rene-41 under thermal shock

x/h	$m = 0$	$m = 1$	t_∞
0	0.8061	0.8370	0.0124
0.1	0.3472	0.3366	0.0026
0.2	−0.0181	0.0018	−0.0014
0.3	−0.2051	−0.2144	−0.0031
0.4	−0.3362	−0.3350	−0.0034
0.5	−0.3799	−0.3686	−0.0029
0.6	−0.3342	−0.3159	−0.0019
0.7	−0.1956	−0.1763	−0.0006
0.8	0.0360	0.0464	0.0010
0.9	0.3540	0.3420	0.0027
1	0.7442	0.6927	0.0045

Table 4.8: Normalized results of the transient thermal stress distribution solutions with different orders (m) at $t_n = 0.01$ and at steady state for parabolic gradation in thermomechanical properties and exponential gradation in Young's modulus $E(x)$ of ZrO_2/Rene-41 under thermal shock

x/h	$m = 0$	$m = 1$	t_∞
0	0.9494	0.9580	0.1265
0.1	0.3720	0.3689	0.0618
0.2	−0.0245	−0.0335	0.0084
0.3	−0.2435	−0.2532	−0.0315
0.4	−0.3562	−0.3620	−0.0571
0.5	−0.3917	−0.3885	−0.0675
0.6	−0.3464	−0.3313	−0.0619
0.7	−0.2086	−0.1852	−0.0392
0.8	0.0309	0.0498	0.0018
0.9	0.3751	0.3665	0.0628
1	0.8215	0.7529	0.1456

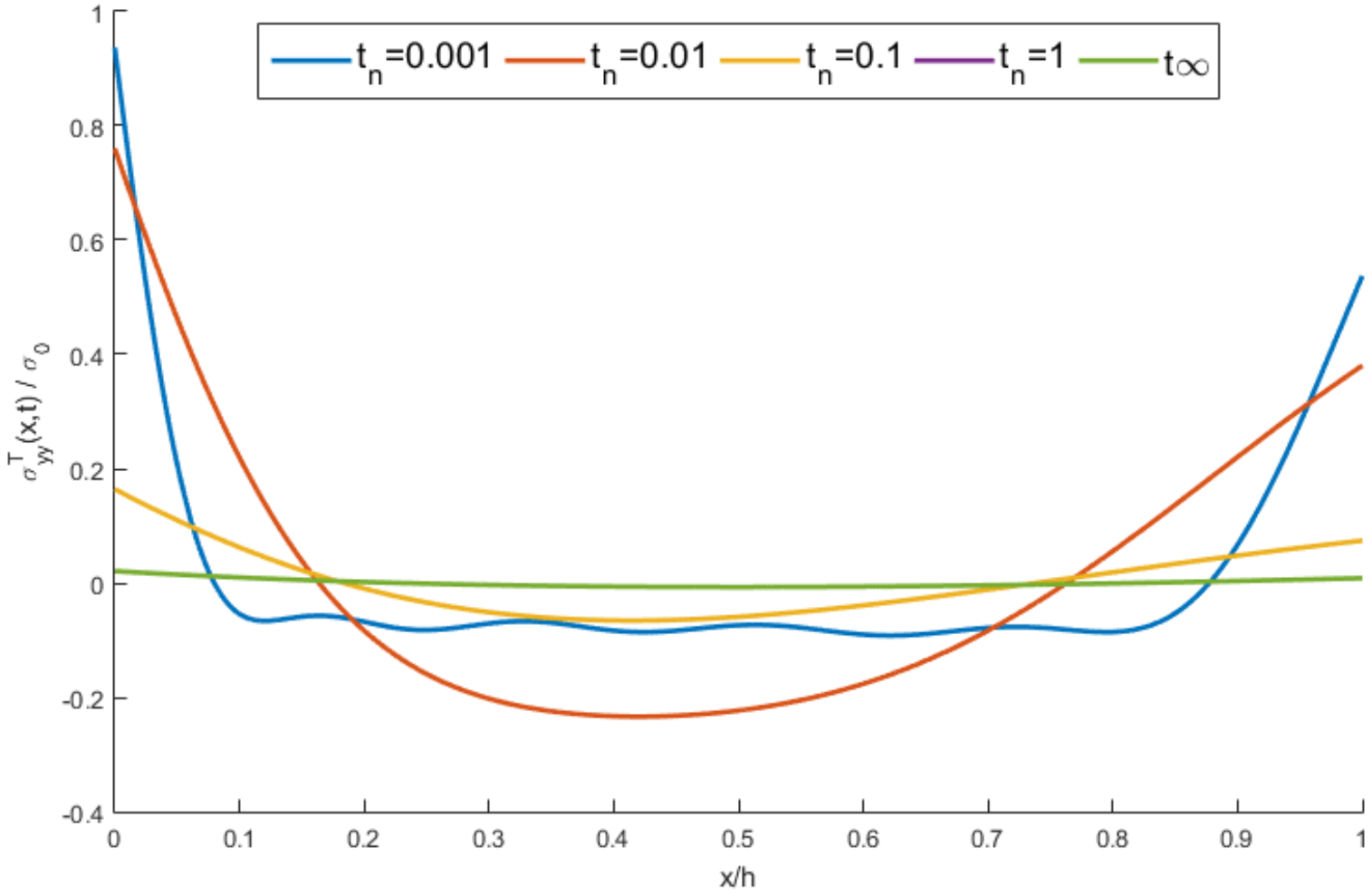

Figure 4.1: Normalized transient thermal stress distributions for different time values in ZrO_2/Ti-6Al-4V FGM strip under thermal shock for exponential gradation of material properties

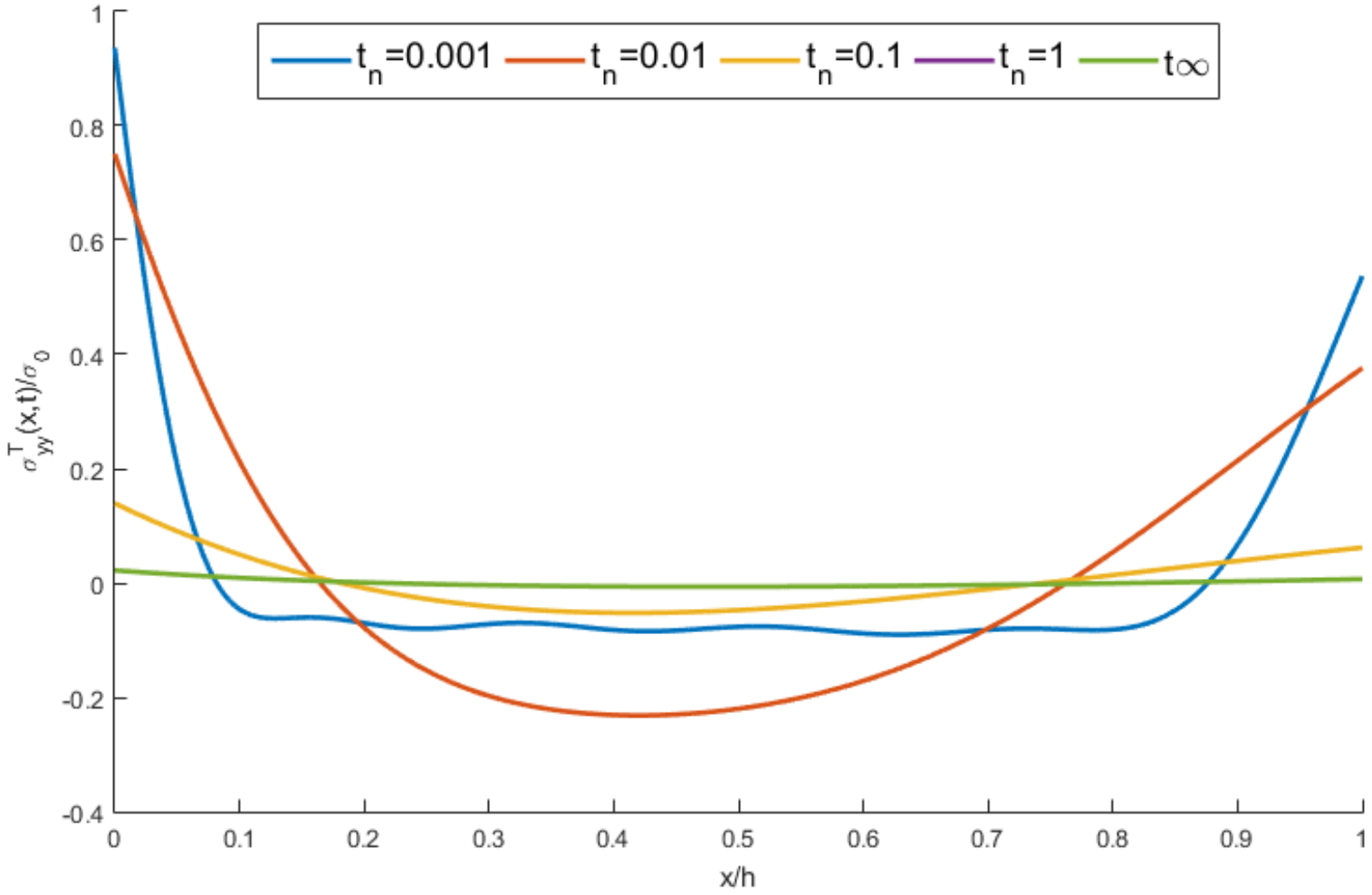

Figure 4.2: Normalized transient thermal stress distributions for different time values in ZrO_2/Ti-6Al-4V FGM strip under thermal shock for linear gradation in thermomechanical properties ($i = 1$) and exponential gradation in Young's modulus $E(x)$

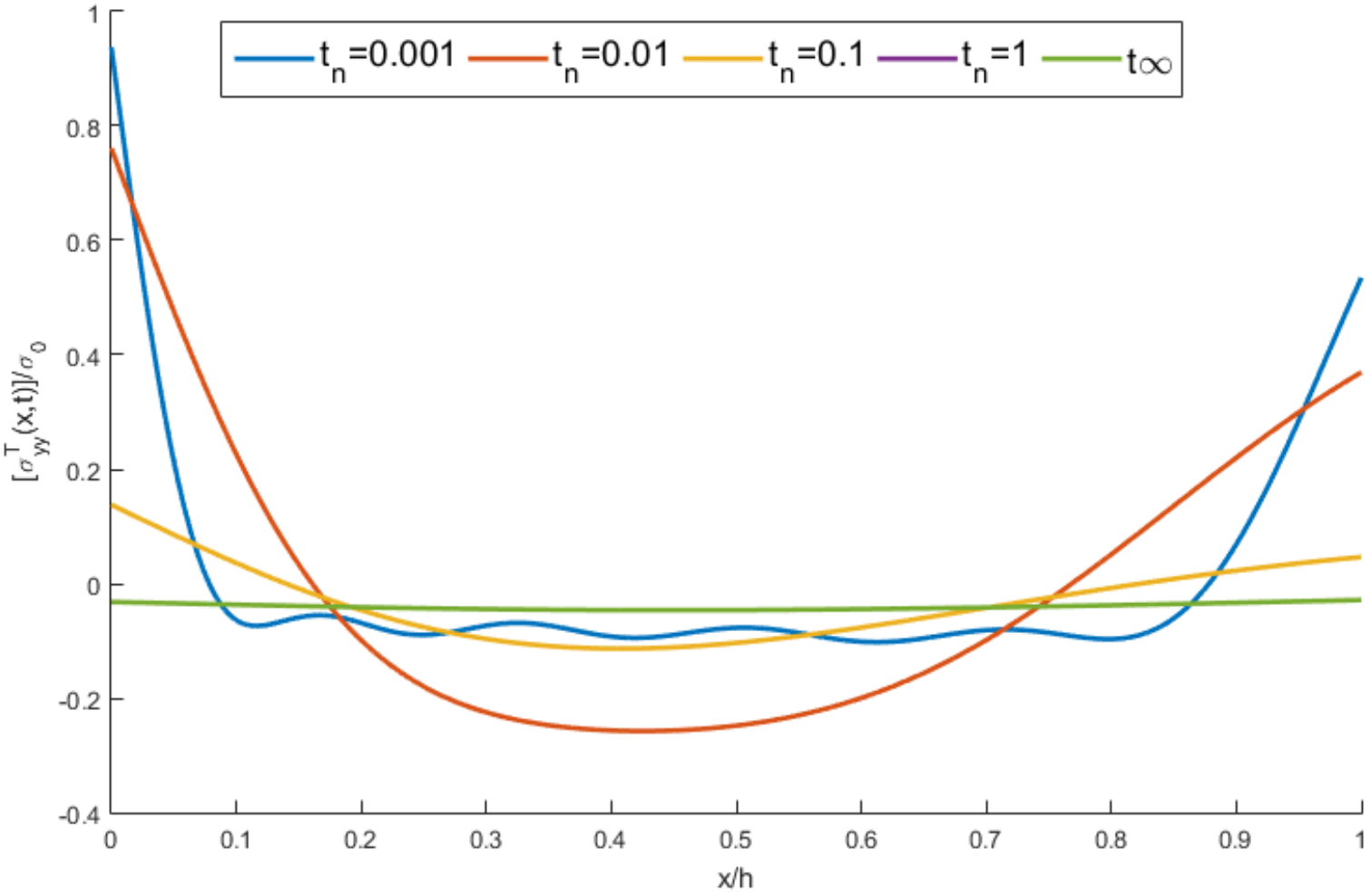

Figure 4.3: Normalized transient thermal stress distributions for different time values in ZrO_2/Ti-6Al-4V FGM strip under thermal shock for parabolic gradation in thermomechanical properties ($i = 2$) and exponential gradation in Young's modulus $E(x)$

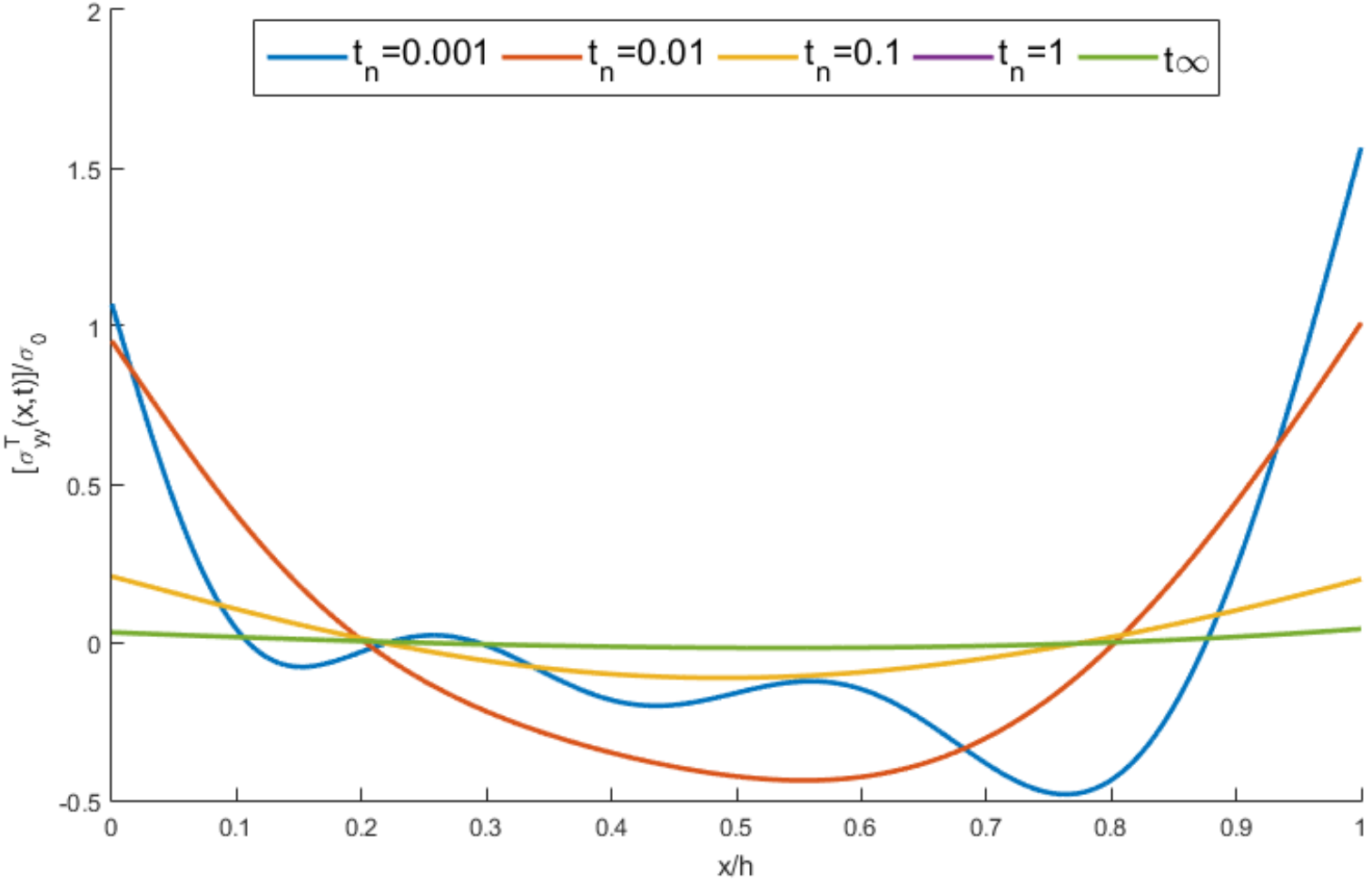

Figure 4.4: Normalized transient thermal stress distributions for different time values in ZrO_2/Rene-41 FGM strip under thermal shock for exponential gradation of material properties

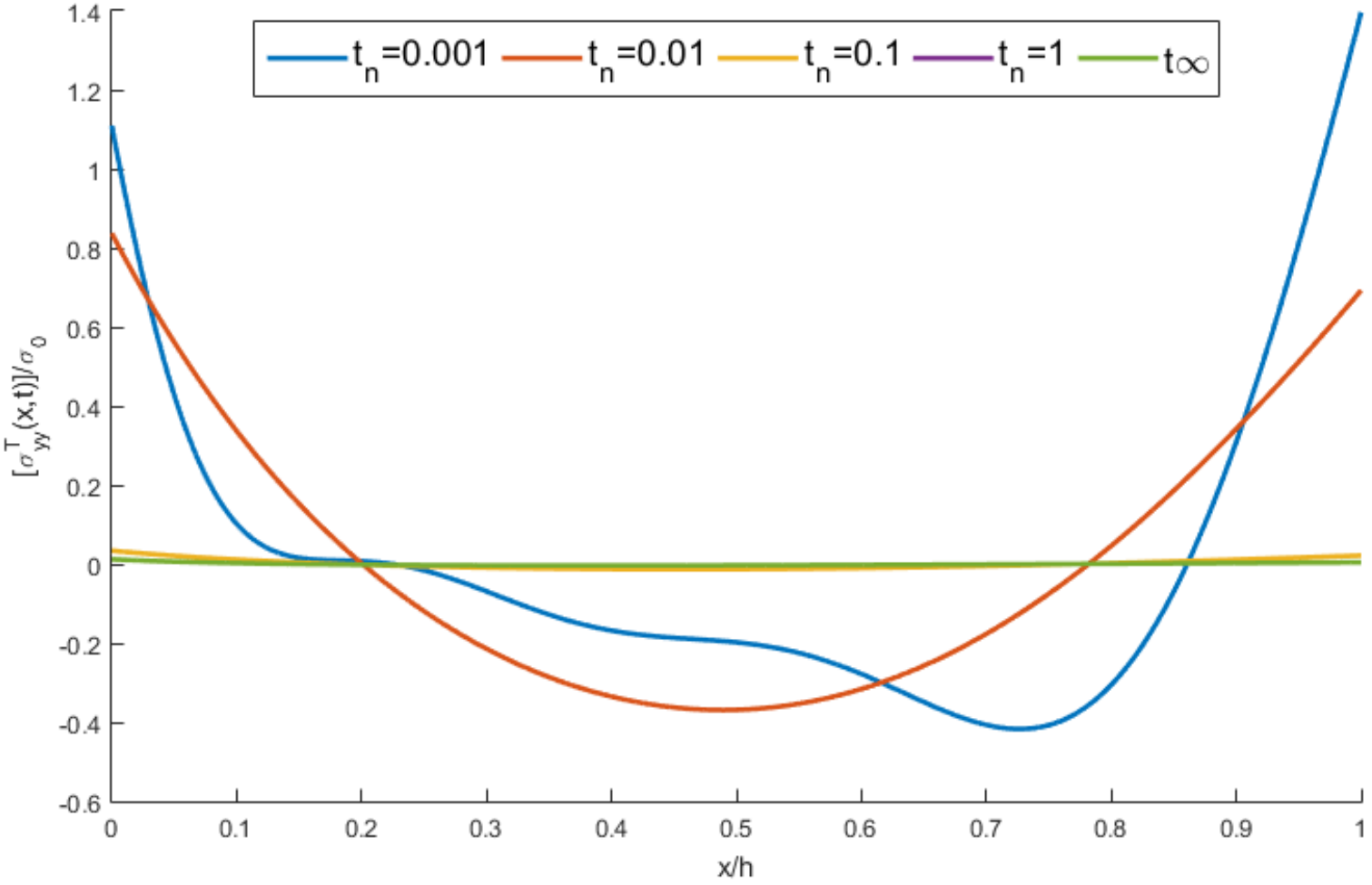

Figure 4.5: Normalized transient thermal stress distributions for different time values in ZrO_2/Rene-41 FGM strip under thermal shock for linear gradation in thermomechanical properties ($i = 1$) and exponential gradation in Young's modulus $E(x)$

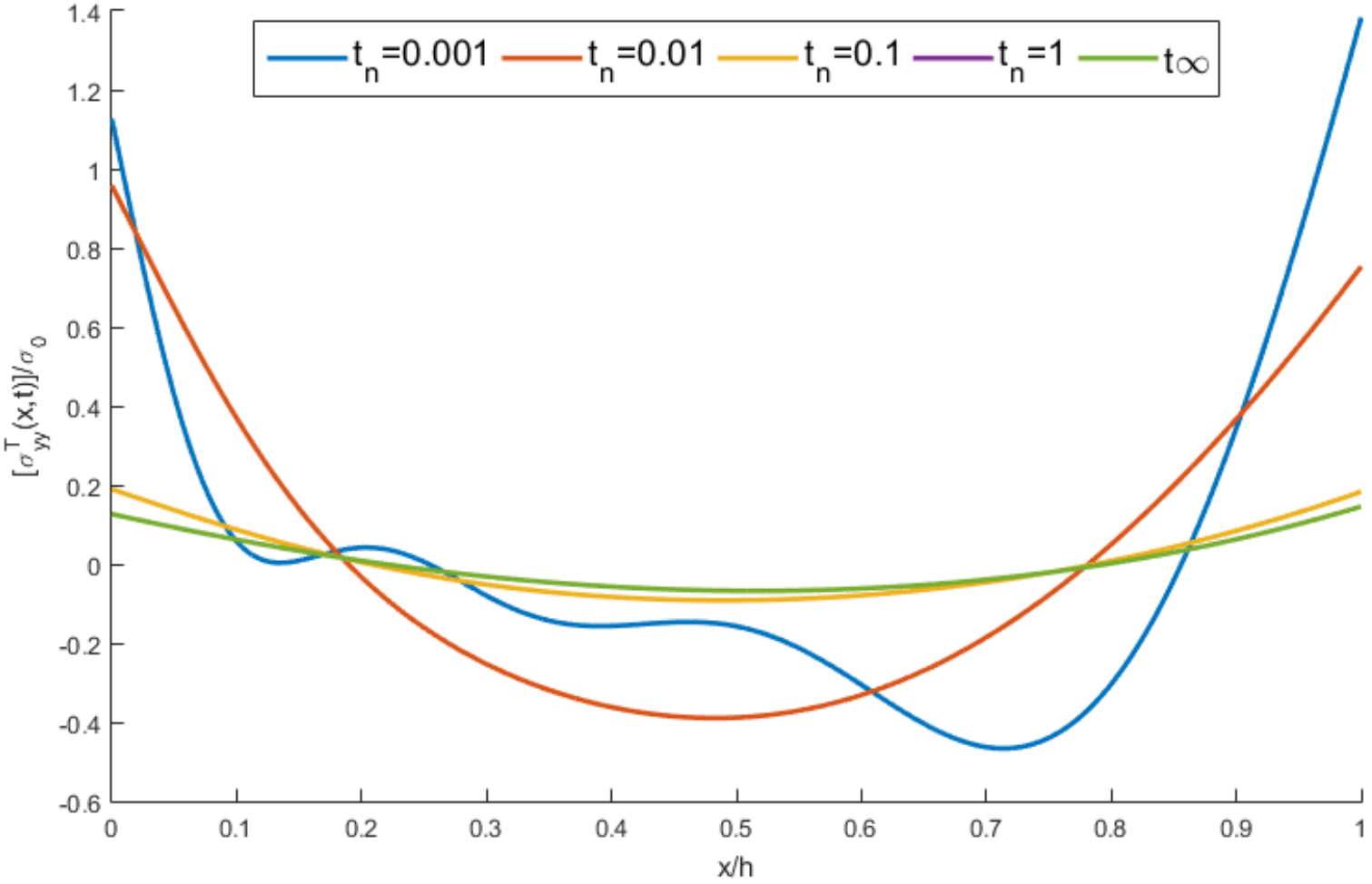

Figure 4.6: Normalized transient thermal stress distributions for different time values in ZrO_2/Rene-41 FGM strip under thermal shock for parabolic gradation of thermomechanical properties ($i = 2$) and exponential gradation in Young's modulus $E(x)$

4.2 TSIFs for Periodic Cracks

In [3] the TSIFs of an FGM strip containing periodic edge cracks are determined by solving a singular integral equation under the assumption of exponentially varying Young's modulus and thermal conductivity and of constant Poisson's ratio and constant thermal diffusivity, κ. In other words, in that study temperature distribution is found under constant thermal diffusivity assumption and the thermal stresses are based on that temperature distribution, i.e. the coefficient of leading term becomes constant in (2.1.7).

In current study, TSIF formulation in [3] will be utilized however by replacing the crack surface tractions with the current thermal stresses. The formulation is birefly discussed below. Geometry of elasticity problem of periodic cracks is depicted in Figure 2.2b. Since the shear modulus, $\mu(x)$, is considered varying exponentially it may be written as

$$\mu(x) = \mu_0 e^{\beta x} \tag{4.2.1}$$

where μ_0 is the shear modulus (or modulus of rigidity) at $x = 0$, i.e., of ceramic. Here β is called as nonhomogeneity parameter of the material. To consider an exponentially varying shear modulus is very common in literature [2]. The constitutive equations for such an FGM are stated below as

$$\sigma_{xx}(x,y) = \frac{\mu(x)}{\gamma - 1}\left[(1+\gamma)\frac{\partial u(x,y)}{\partial x} + (3-\gamma)\frac{\partial v(x,y)}{\partial y}\right] \tag{4.2.2a}$$

$$\sigma_{yy}(x,y) = \frac{\mu(x)}{\gamma - 1}\left[(1+\gamma)\frac{\partial v(x,y)}{\partial y} + (3-\gamma)\frac{\partial u(x,y)}{\partial x}\right] \tag{4.2.2b}$$

$$\sigma_{xy}(x,y) = \mu(x)\left[\frac{\partial u(x,y)}{\partial y} + \frac{\partial v(x,y)}{\partial x}\right] \tag{4.2.2c}$$

where $u(x,y)$ and $v(x,y)$ are displacements respectively in x and y directions and γ is Kolosov's constant which equals to $\gamma = 3 - 4\nu$ in plane strain approach and

$\gamma = (3-\nu)/(1+\nu)$ in plane stress approach. Also the equilibrium equations in the absence of any body forces may be written as

$$\frac{\partial \sigma_{xx}}{\partial x} + \frac{\partial \sigma_{xy}}{\partial y} = 0 \tag{4.2.3a}$$

$$\frac{\partial \sigma_{xy}}{\partial x} + \frac{\partial \sigma_{yy}}{\partial y} = 0 \tag{4.2.3b}$$

for the plane elasticity problem under consideration. By using (4.2.2) and (4.2.3), it may be shown that the governing equations of the problem in terms of displacements u and v are as follows

$$(\gamma+1)\frac{\partial^2 u}{\partial x^2} + (\gamma-1)\frac{\partial^2 u}{\partial y^2} + 2\frac{\partial^2 v}{\partial x \partial y} + \beta(\gamma+1)\frac{\partial u}{\partial x} + \beta(3-\gamma)\frac{\partial v}{\partial y} = 0 \tag{4.2.4a}$$

$$(\gamma-1)\frac{\partial^2 v}{\partial x^2} + (\gamma+1)\frac{\partial^2 v}{\partial y^2} + 2\frac{\partial^2 u}{\partial x \partial y} + \beta(\gamma-1)\frac{\partial u}{\partial y} + \beta(\gamma-1)\frac{\partial v}{\partial x} = 0 \tag{4.2.4b}$$

The FGM strip containing periodic cracks is subjected to the following boundary conditions

$$v(x,0) = 0 \qquad b < x < h \tag{4.2.5a}$$

$$\sigma_{yy}(x,0) = -\sigma_{yy}^{T}(x,t) \qquad 0 < x < b \tag{4.2.5b}$$

$$\sigma_{xy}(x,0) = 0 \qquad 0 < x < h \tag{4.2.5c}$$

$$\sigma_{xy}(x,c) = 0 \qquad 0 < x < h \tag{4.2.5d}$$

$$v(x,c) = 0 \qquad 0 < x < h \tag{4.2.5e}$$

$$\sigma_{xx}(0,y) = 0 \qquad 0 < y < c \tag{4.2.5f}$$

$$\sigma_{xy}(0,y) = 0 \qquad 0 < y < c \tag{4.2.5g}$$

$$\sigma_{xx}(h,y) = 0 \qquad 0 < y < c \tag{4.2.5h}$$

$$\sigma_{xy}(h,y) = 0 \qquad 0 < y < c \tag{4.2.5i}$$

By defining an auxiliary unknown

$$g(x) = \frac{\partial}{\partial x} v(x,0)$$

After a rather lengthy procedure [3], all the unknown field variables (displacements, strains, stresses) of the problem can be expressed in terms of this auxiliary unknown by using the boundary conditions. The last remaining boundary condition (4.2.5b) can then be used to obtain a singular integral equation for solving $g(t)$. Singular integral equation whose solution of which gives $g(x)$, is given as follows

$$\int_0^b \Big[h_1(x,t) + h_2(x,t)\Big] g(t)dt = -\frac{\sigma_{yy}^T(x,t)(\gamma - 1)}{\mu(x)} \tag{4.2.6}$$

$h_1(x,t)$ and $h_2(x,t)$ are known and given in [3]. Here the only unknown is $g(t)$. This singular integral equation was solved in order to find the solution for the periodic edge cracks. For the edge cracks mode-I SIF is defined as follows

$$k(b) = \lim_{x \to b^+} \sqrt{2(x-b)}\sigma_{yy}(x,0) = -\frac{4\mu(+1)}{\gamma + 1}\sqrt{b}\varphi(+1)$$

where

$$G(s) = g(t(s)) = \frac{\varphi(s)}{\sqrt{1-s}}$$

and

$$t = \frac{b}{2}(s+1) \qquad\qquad -1 \leq s \leq 1$$

Further details regarding the derivation and solution of the singular integral equation may be found in [3].

In this study the transient thermal stresses with the opposite signs at certain points along a crack are to be applied as the crack surface traction to calculate the corre-

sponding TSIFs numerically. Since in [3] TSIFs are calculated by using Fortran, another script is written in MATLAB® to replace the crack surface tractions with the current transient thermal stresses, i.e., to give the transient thermal stresses as input to the program in Fortran to calculate the TSIFs in the FGM under the thermal shock strip along the periodic cracks.

TSIFs are normalized by [17]

$$k_0(b) = \frac{k(b)}{\sigma_0\sqrt{b}}$$

where b is crack length. The normalized transient and steady TSIFs results of both FGM strips ZrO_2/Ti-6Al-4V and ZrO_2/Rene-41 for different gradation in material properties are tabulated below for different crack spacing and different crack lengths.

The variation of the TSIFs for various crack lengths, crack spacings and gradation types are graphically shown as a function of normalized time in Figures 4.7,4.8,4.9 and 4.10, 4.11, 4.12 respectively for ZrO_2/Ti-6Al-4V and ZrO_2/Rene-41.

Table 4.9: Normalized results of TSIF solutions of ZrO_2/Ti-6Al-4V strip under thermal shock with exponential gradation in material properties with different orders (m) at $t_n = 0.01$ and steady state

$C/b = 10$			
b/h	$m = 0$	$m = 1$	t_∞
0.1	0.4610	0.4623	0.0116
0.2	0.2347	0.2328	0.0069
0.3	0.1109	0.1093	0.0037
$C/b = 5$			
b/h	$m = 0$	$m = 1$	t_∞
0.1	0.4222	0.4231	0.0106
0.2	0.1870	0.1850	0.0056
0.3	0.0665	0.0650	0.0024
$C/b = 2$			
b/h	$m = 0$	$m = 1$	t_∞
0.1	0.2921	0.2919	0.0075
0.2	0.0908	0.0887	0.0023
0.3	-0.0047	-0.0060	0.0005

Table 4.10: Normalized results of TSIF solutions of ZrO_2/Ti-6Al-4V strip under thermal shock for linear gradation in material properties with different orders (m) at $t_n = 0.01$ and steady state

$C/b = 10$			
b/h	$m = 0$	$m = 1$	t_∞
0.1	0.4521	0.4510	0.0116
0.2	0.2335	0.2284	0.0064
0.3	0.1112	0.1077	0.0031
$C/b = 5$			
b/h	$m = 0$	$m = 1$	t_∞
0.1	0.4141	0.4126	0.0107
0.2	0.1865	0.1816	0.0052
0.3	0.0672	0.0642	0.0020
$C/b = 2$			
b/h	$m = 0$	$m = 1$	t_∞
0.1	0.2867	0.2841	0.0074
0.2	0.0919	0.0874	0.0027
0.3	-0.0033	-0.0054	0.0001

Table 4.11: Normalized results of TSIF solutions of ZrO_2/Ti-6Al-4V strip under thermal shock for parabolic gradation in material properties with different orders (m) at $t_n = 0.01$ and steady state

$C/b = 10$			
b/h	$m = 0$	$m = 1$	t_∞
0.1	0.4828	0.4866	0.0070
0.2	0.2450	0.2458	0.0046
0.3	0.1153	0.1150	0.0026
$C/b = 5$			
b/h	$m = 0$	$m = 1$	t_∞
0.1	0.4423	0.4457	0.0065
0.2	0.1951	0.1955	0.0039
0.3	0.0690	0.0685	0.0018
$C/b = 2$			
b/h	$m = 0$	$m = 1$	t_∞
0.1	0.3068	0.3089	0.0047
0.2	0.0947	0.0944	0.0027
0.3	−0.0051	−0.0060	0.0001

Table 4.12: Normalized results of TSIF solutions of ZrO_2/Rene-41 FGM strip under thermal shock for exponential gradation in material properties with different orders (m) at $t_n = 0.01$ and steady state

$C/b = 10$			
b/h	$m = 0$	$m = 1$	t_∞
0.1	0.6662	0.6695	0.0239
0.2	0.4070	0.4055	0.0163
0.3	0.2502	0.2482	0.0106
$C/b = 5$			
b/h	$m = 0$	$m = 1$	t_∞
0.1	0.6201	0.6230	0.0223
0.2	0.3446	0.3429	0.0140
0.3	0.1830	0.1810	0.0080
$C/b = 2$			
b/h	$m = 0$	$m = 1$	t_∞
0.1	0.4489	0.4500	0.0163
0.2	0.2090	0.2068	0.0090
0.3	0.0660	0.0640	0.0035

Table 4.13: Normalized results of TSIF solutions of ZrO_2/Rene-41 FGM strip under thermal shock for linear gradation in material properties with different orders (m) at $t_n = 0.01$ and steady state

$C/b = 10$			
b/h	$m = 0$	$m = 1$	t_∞
0.1	0.5665	0.5683	0.0063
0.2	0.3522	0.3434	0.0029
0.3	0.2099	0.1994	0.0013
$C/b = 5$			
b/h	$m = 0$	$m = 1$	t_∞
0.1	0.5273	0.5285	0.0059
0.2	0.2987	0.2901	0.0024
0.3	0.1522	0.1428	0.0008
$C/b = 2$			
b/h	$m = 0$	$m = 1$	t_∞
0.1	0.3817	0.3807	0.0040
0.2	0.1828	0.1743	0.0011
0.3	0.0519	0.0441	−0.0002

Table 4.14: Normalized results of TSIF solutions of ZrO_2/Rene-41 FGM strip under thermal shock for parabolic gradation in material properties with different orders (m) at $t_n = 0.01$ and steady state

$C/b = 10$			
b/h	$m = 0$	$m = 1$	t_∞
0.1	0.6468	0.6481	0.0948
0.2	0.3741	0.3700	0.0622
0.3	0.2139	0.2069	0.0387
$C/b = 5$			
b/h	$m = 0$	$m = 1$	t_∞
0.1	0.6013	0.6023	0.0884
0.2	0.3141	0.3100	0.0531
0.3	0.1514	0.1449	0.0287
$C/b = 2$			
b/h	$m = 0$	$m = 1$	t_∞
0.1	0.4319	0.4322	0.0646
0.2	0.1838	0.1798	0.0335
0.3	0.0426	0.0371	0.0113

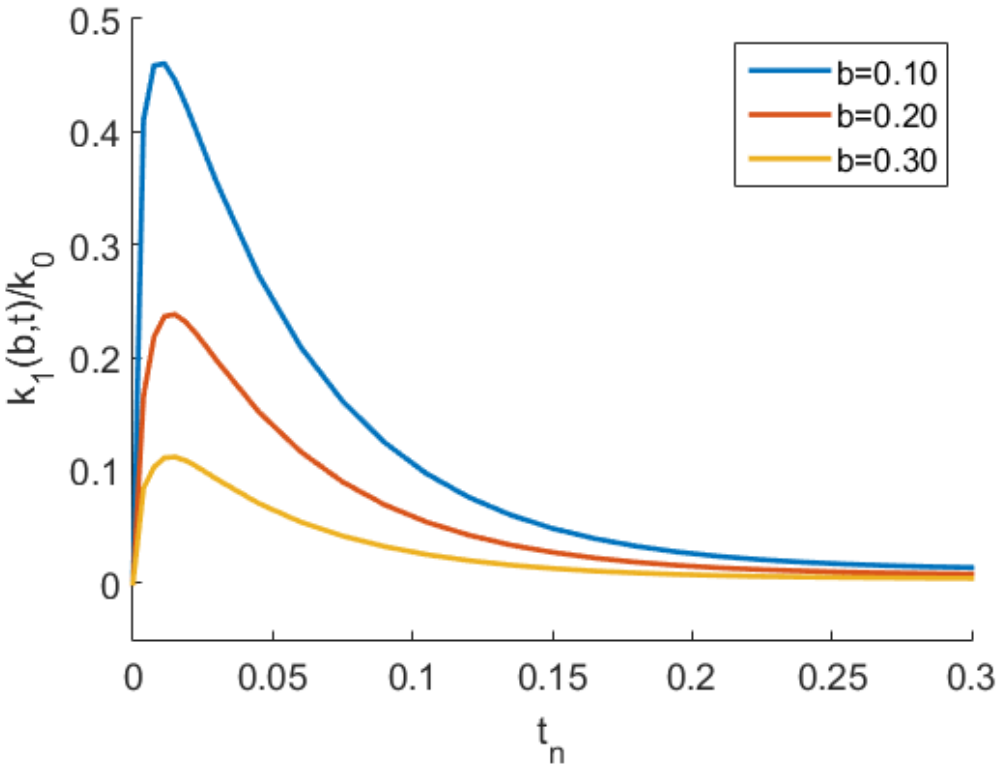
0.5
0.4
0.3
0.2
0.1
0
k1(b,t)/k0
0
0.05
0.1
0.15
0.2
0.25
0.3
tn
b=0.10
b=0.20
b=0.30

(a) $c/b = 10$

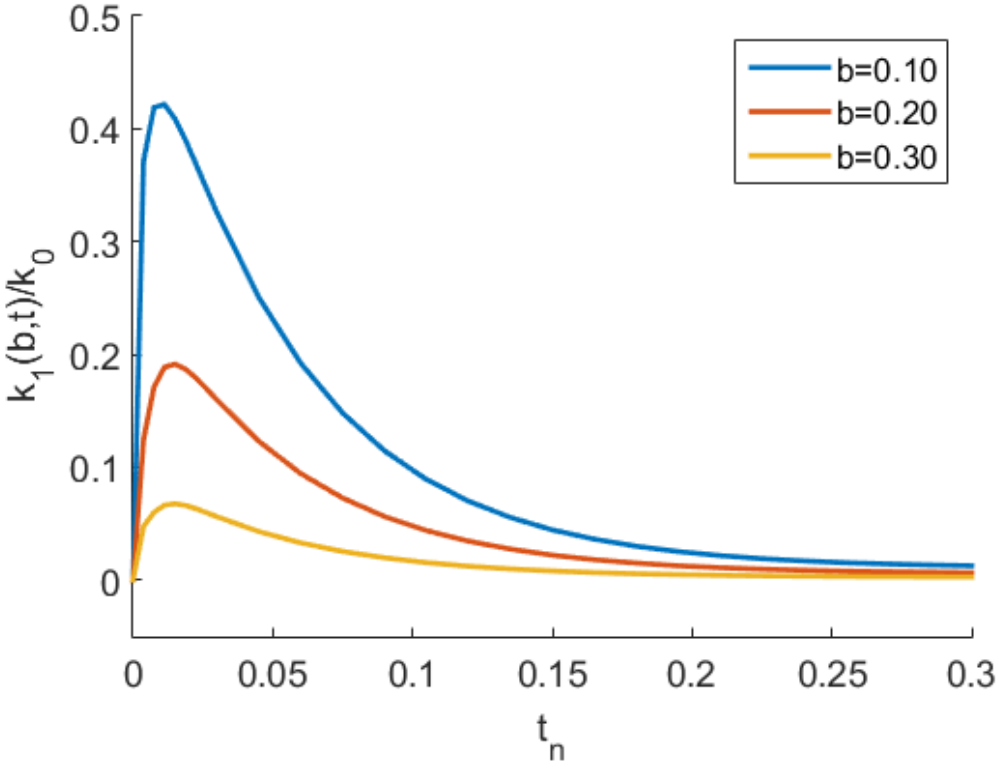
0.5
0.4
0.3
0.2
0.1
0
k1(b,t)/k0
0
0.05
0.1
0.15
0.2
0.25
0.3
tn
b=0.10
b=0.20
b=0.30

(b) $c/b = 5$

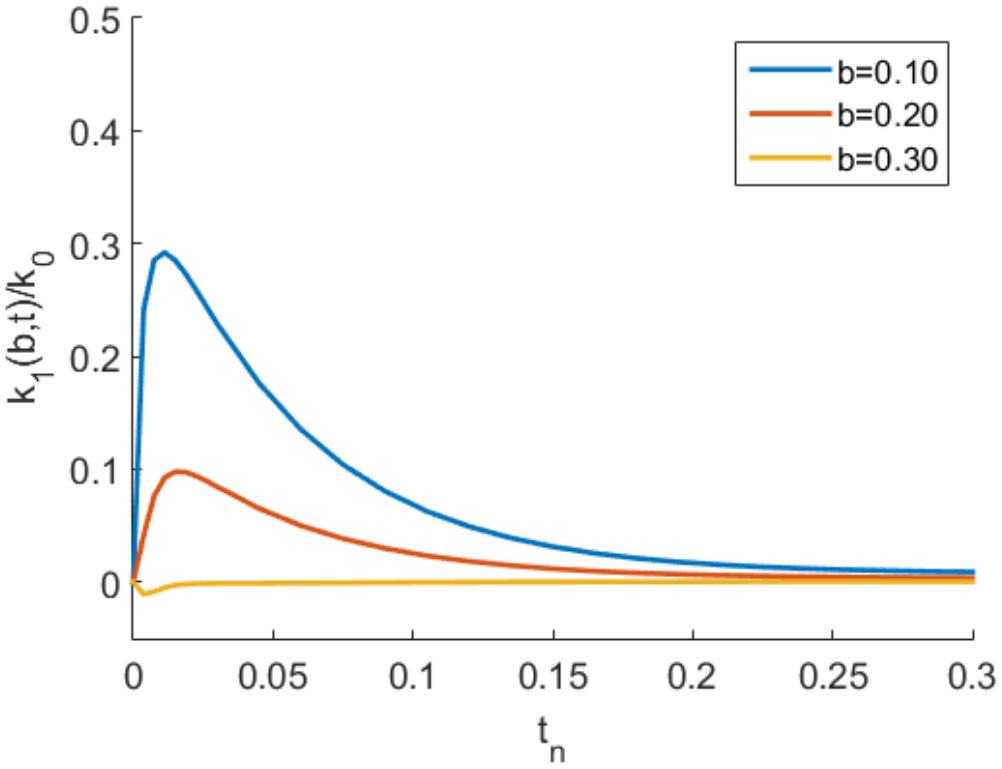

(c) $c/b = 2$

Figure 4.7: Normalized transient TSIF values of periodically cracked ZrO_2/Ti-6Al-4V strip under thermal shock for exponential gradation in material properties, with varying crack spacings c/b and varying crack lengths b

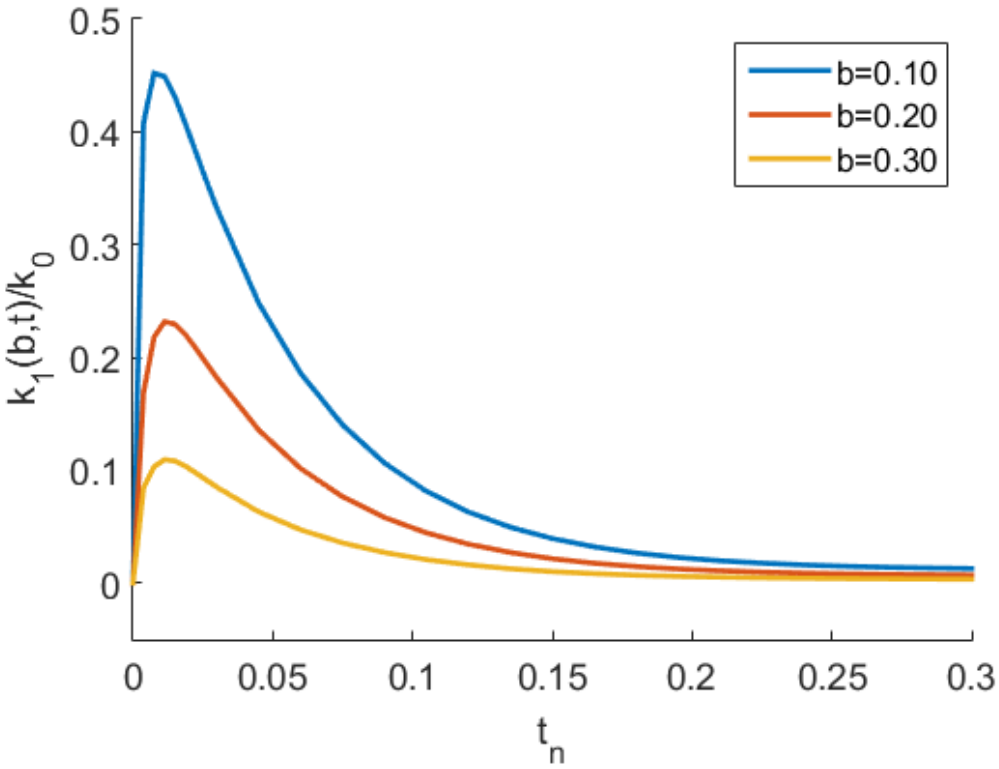
0.5
0.4
0.3
0.2
0.1
0
k1(b,t)/k0
0
0.05
0.1
0.15
0.2
0.25
0.3
tn
b=0.10
b=0.20
b=0.30

(a) $c/b = 10$

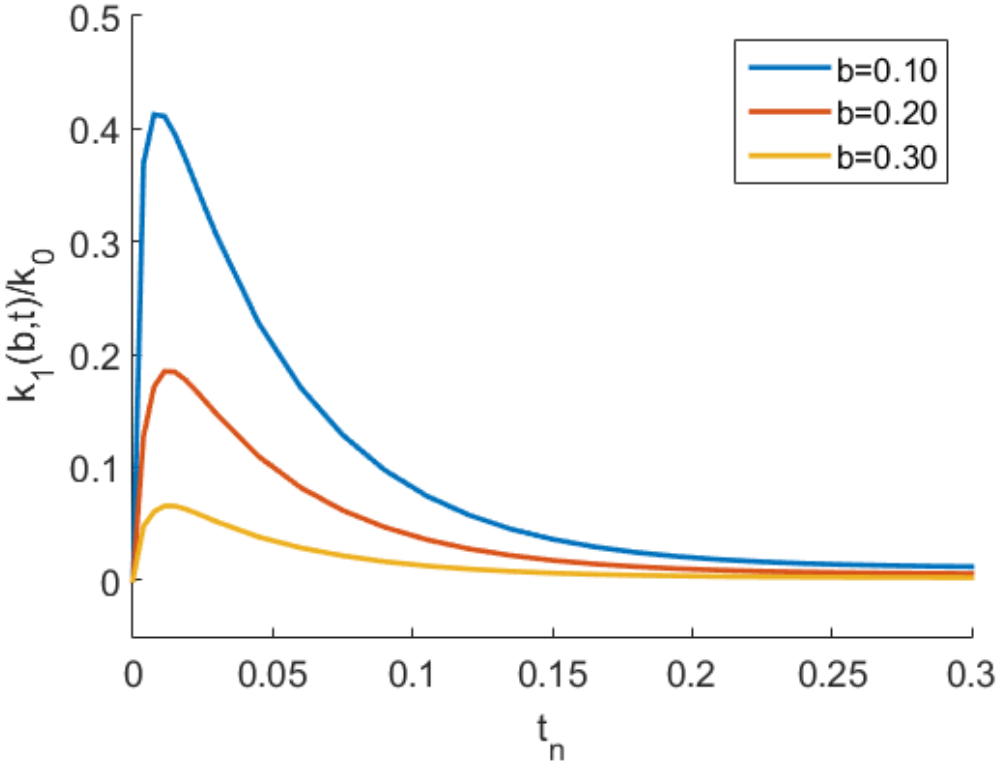
0.5
0.4
0.3
0.2
0.1
0
k1(b,t)/k0
0
0.05
0.1
0.15
0.2
0.25
0.3
tn
b=0.10
b=0.20
b=0.30

(b) $c/b = 5$

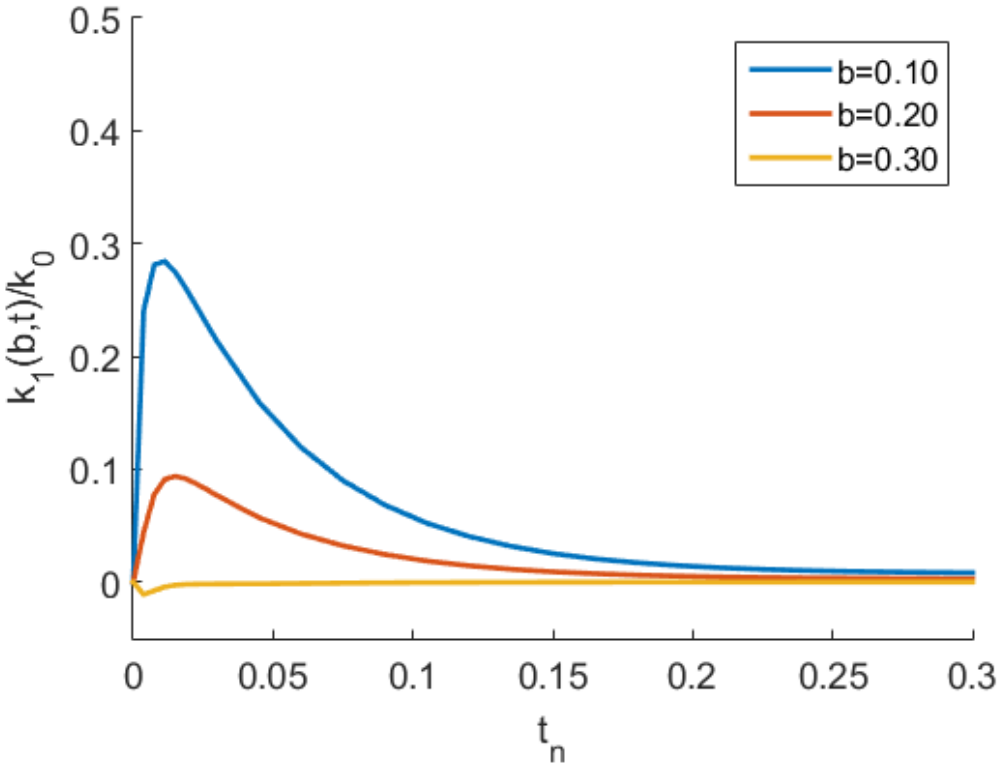

(c) $c/b = 2$

Figure 4.8: Normalized transient TSIF values of periodically cracked ZrO_2/Ti-6Al-4V strip under thermal shock for linear gradation in material properties, with varying crack spacings c/b and varying crack lengths b

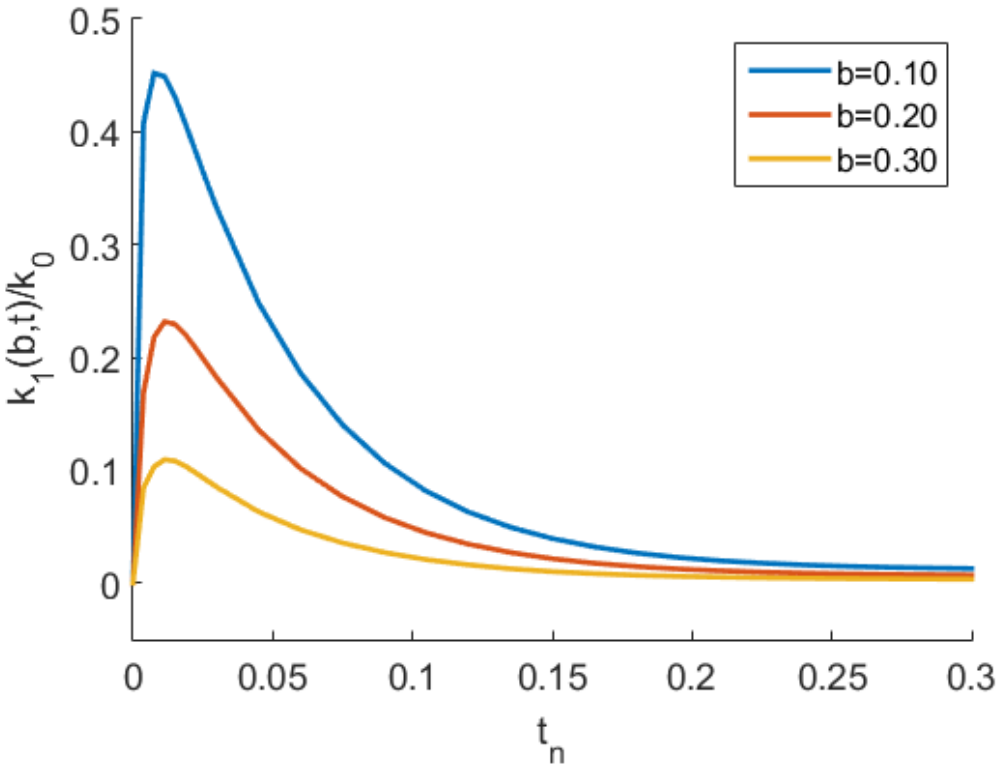
0.5
0.4
0.3
0.2
0.1
0
k1(b,t)/k0
0
0.05
0.1
0.15
0.2
0.25
0.3
tn
b=0.10
b=0.20
b=0.30

(a) $c/b = 10$

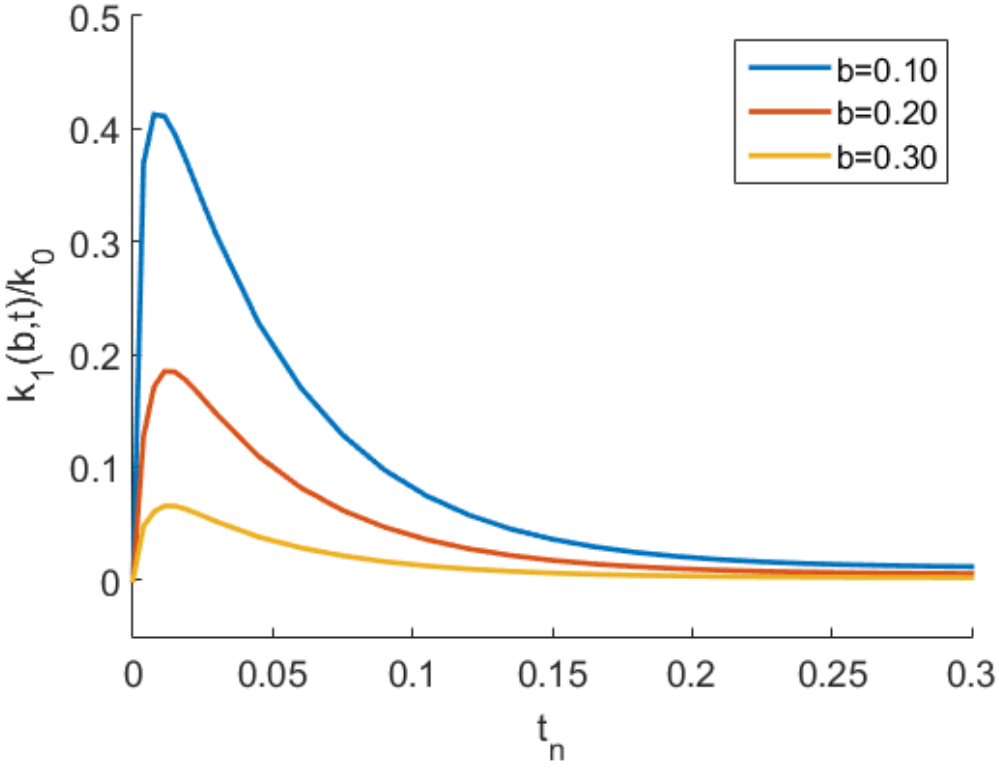
0.5
0.4
0.3
0.2
0.1
0
k1(b,t)/k0
0
0.05
0.1
0.15
0.2
0.25
0.3
tn
b=0.10
b=0.20
b=0.30

(b) $c/b = 5$

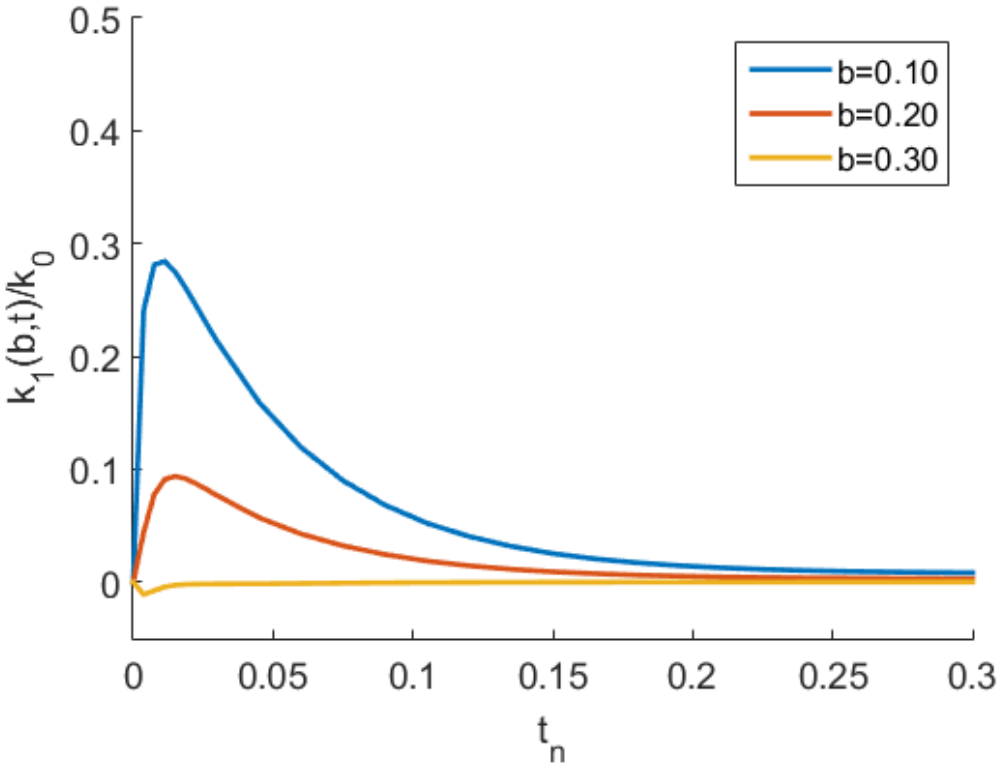

(c) $c/b = 2$

Figure 4.9: Normalized transient TSIF values of periodically cracked ZrO_2/Ti-6Al-4V strip under thermal shock for parabolic gradation in material properties, with varying crack spacings c/b and varying crack lengths b

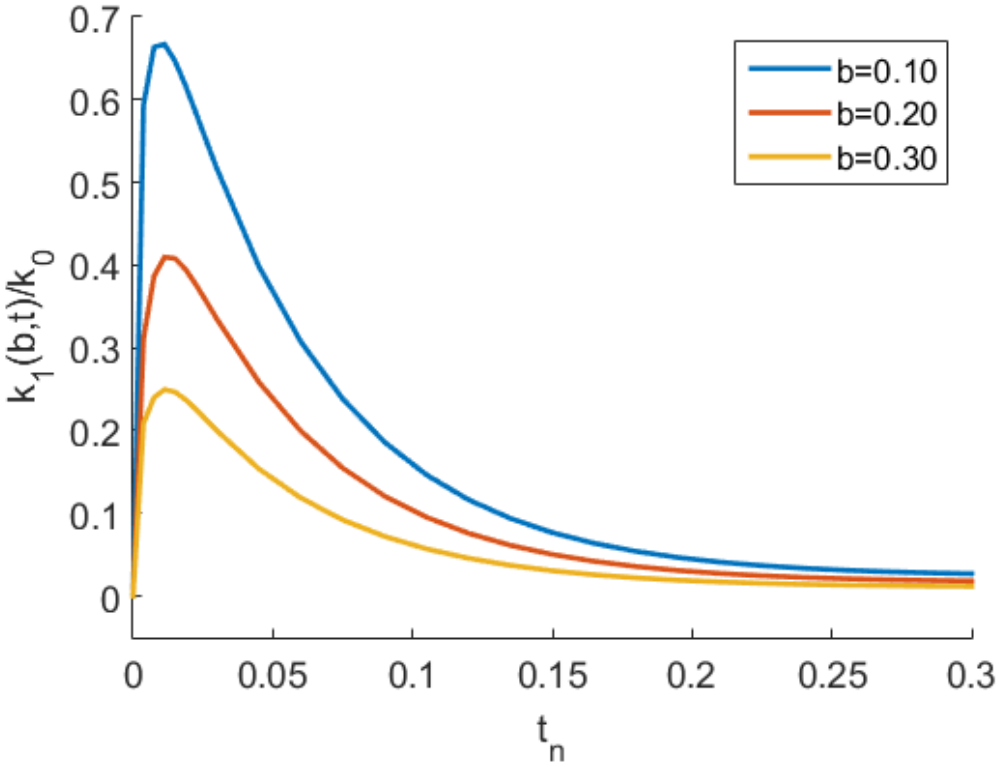
0.7
0.6
0.5
0.4
0.3
0.2
0.1
0
k1(b,t)/k0
0
0.05
0.1
0.15
0.2
0.25
0.3
tn
b=0.10
b=0.20
b=0.30

(a) $c/b = 10$

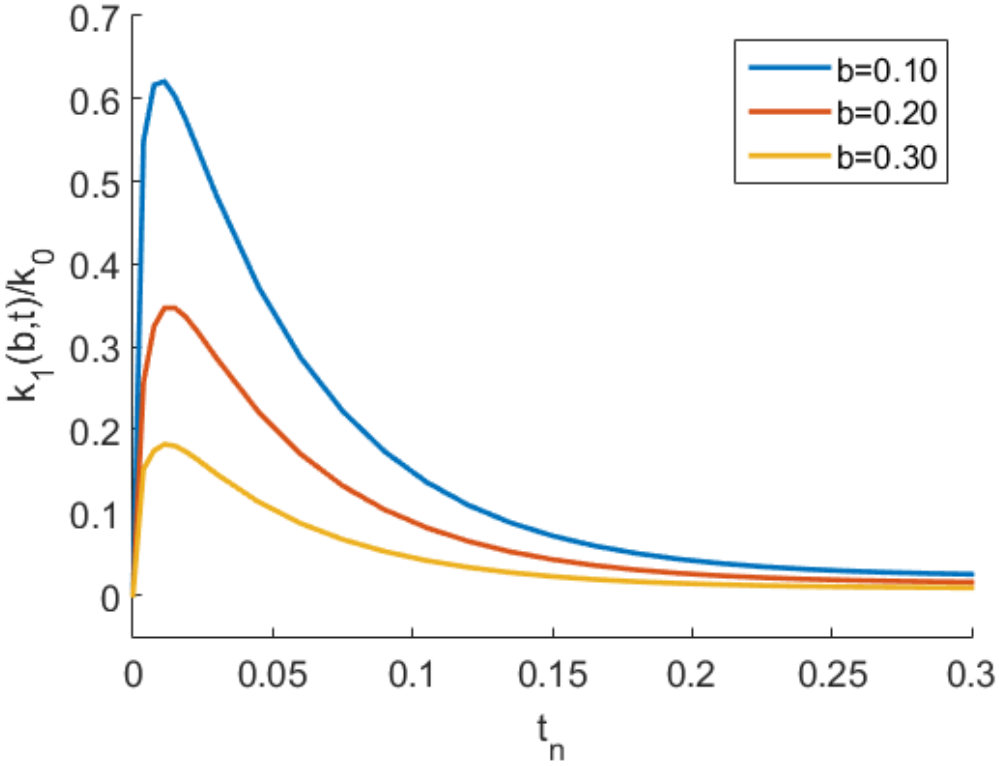
0.7
0.6
0.5
0.4
0.3
0.2
0.1
0
k1(b,t)/k0
0
0.05
0.1
0.15
0.2
0.25
0.3
tn
b=0.10
b=0.20
b=0.30

(b) $c/b = 5$

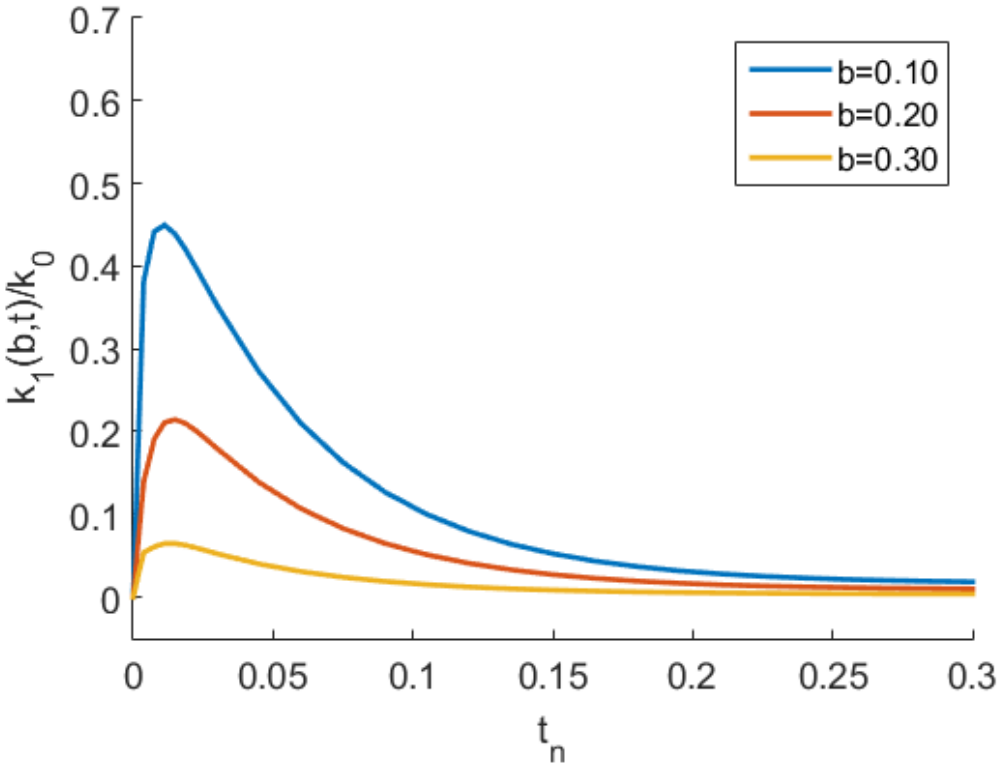

(c) $c/b = 2$

Figure 4.10: Normalized transient TSIF values of periodically cracked ZrO_2/Rene-41 strip under thermal shock for exponential gradation in material properties, with varying crack spacings c/b and varying crack lengths b

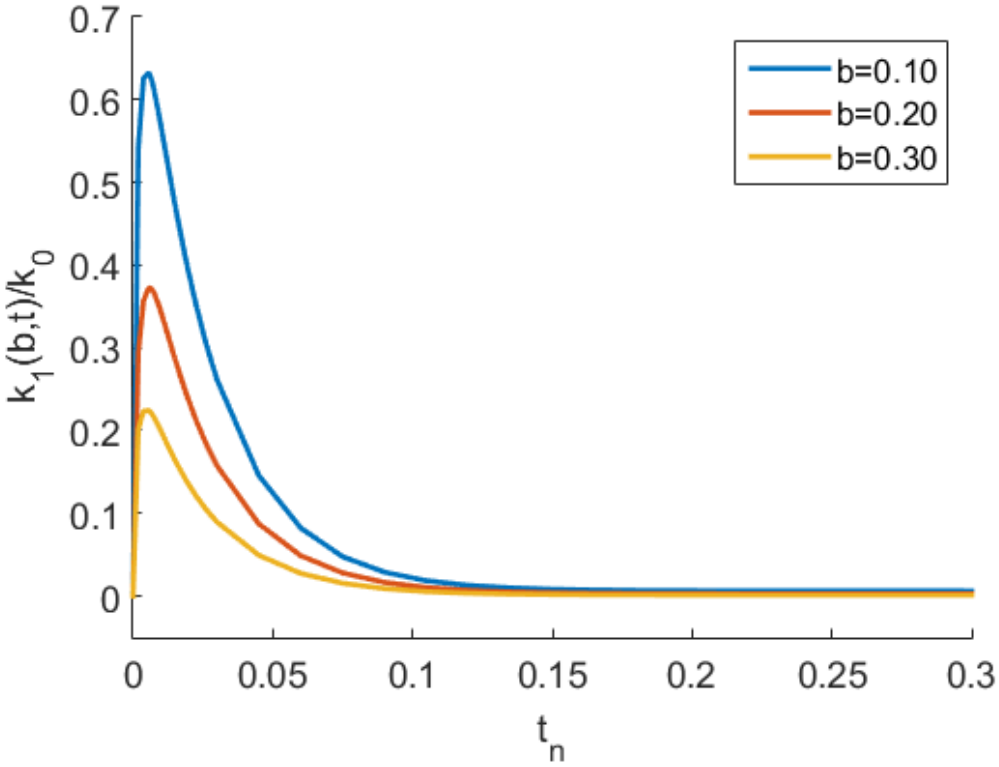
b=0.10
b=0.20
b=0.30
k1(b,t)/k0
tn
0.7
0.6
0.5
0.4
0.3
0.2
0.1
0
0
0.05
0.1
0.15
0.2
0.25
0.3

(a) $c/b = 10$

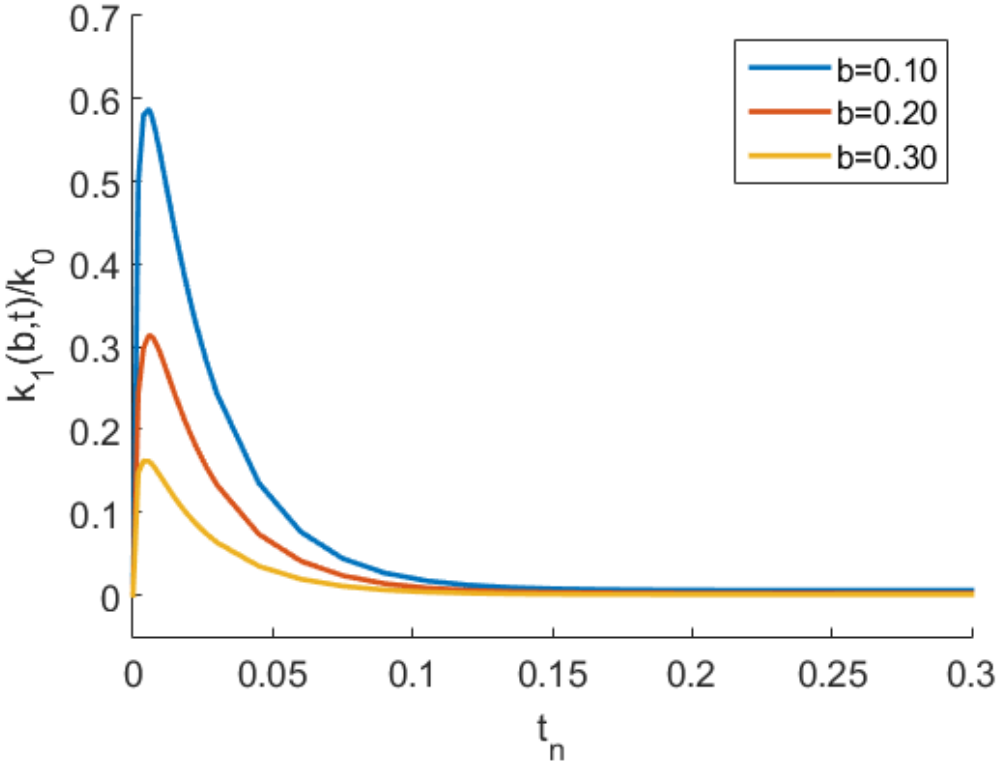
b=0.10
b=0.20
b=0.30
k1(b,t)/k0
tn
0.7
0.6
0.5
0.4
0.3
0.2
0.1
0
0
0.05
0.1
0.15
0.2
0.25
0.3

(b) $c/b = 5$

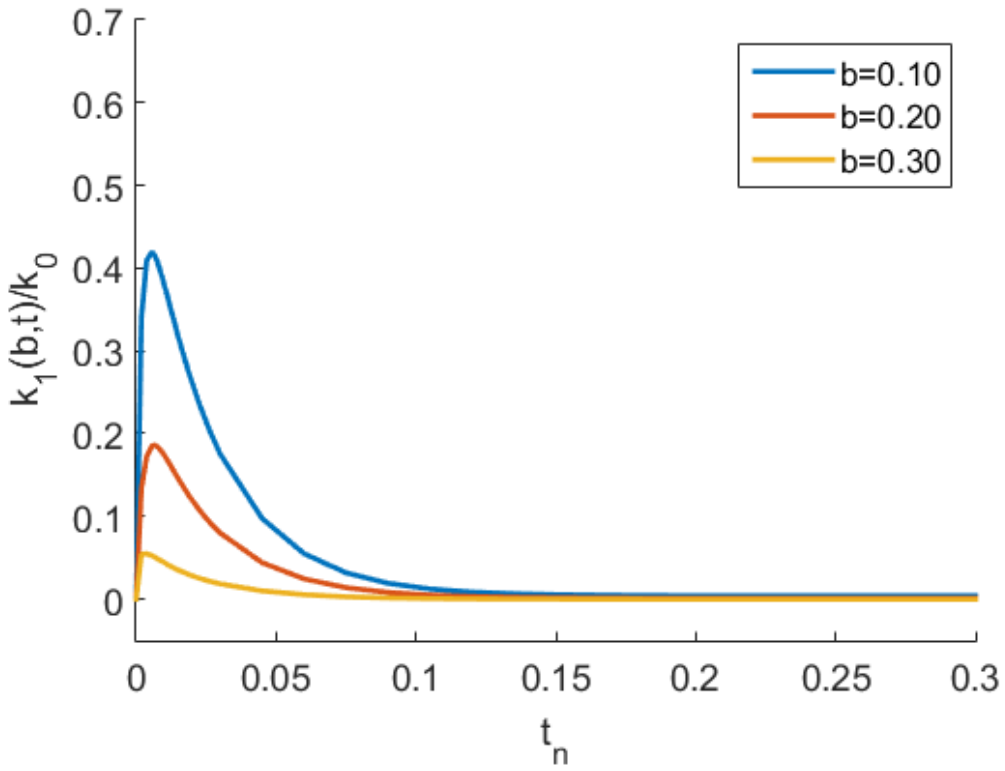

(c) $c/b = 2$

Figure 4.11: Normalized transient TSIF values of periodically cracked ZrO_2/Rene-41 strip under thermal shock for linear gradation in material properties, with varying crack spacings c/b and varying crack lengths b

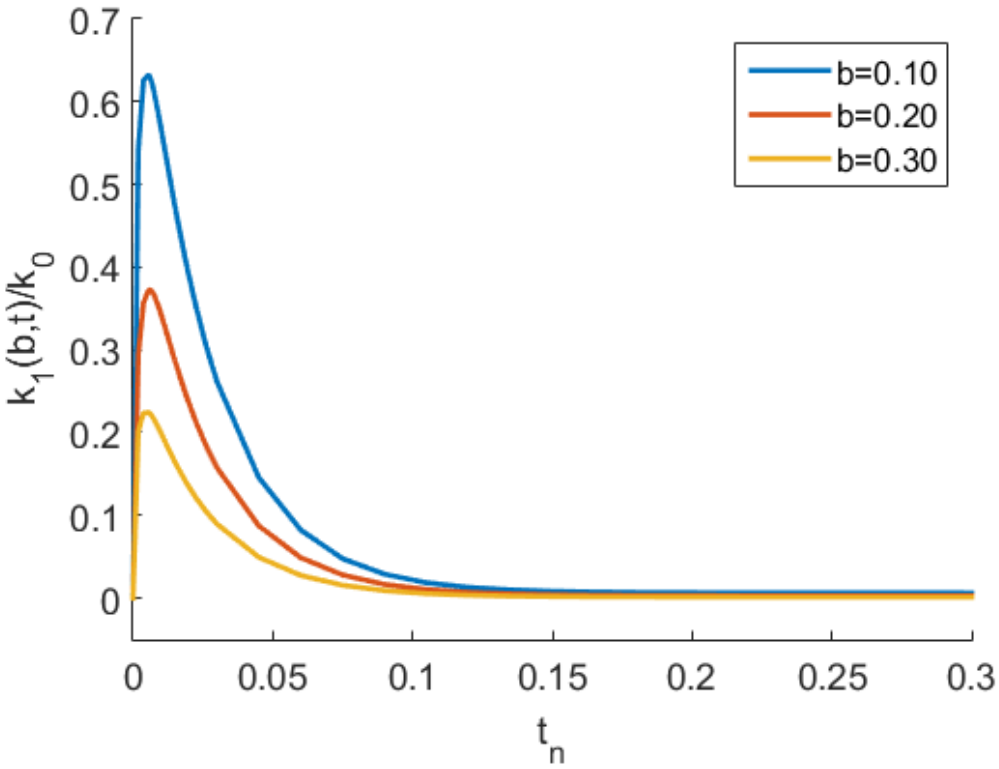
0.7
0.6
0.5
0.4
0.3
0.2
0.1
0
k1(b,t)/k0
0
0.05
0.1
0.15
0.2
0.25
0.3
tn
b=0.10
b=0.20
b=0.30

(a) $c/b = 10$

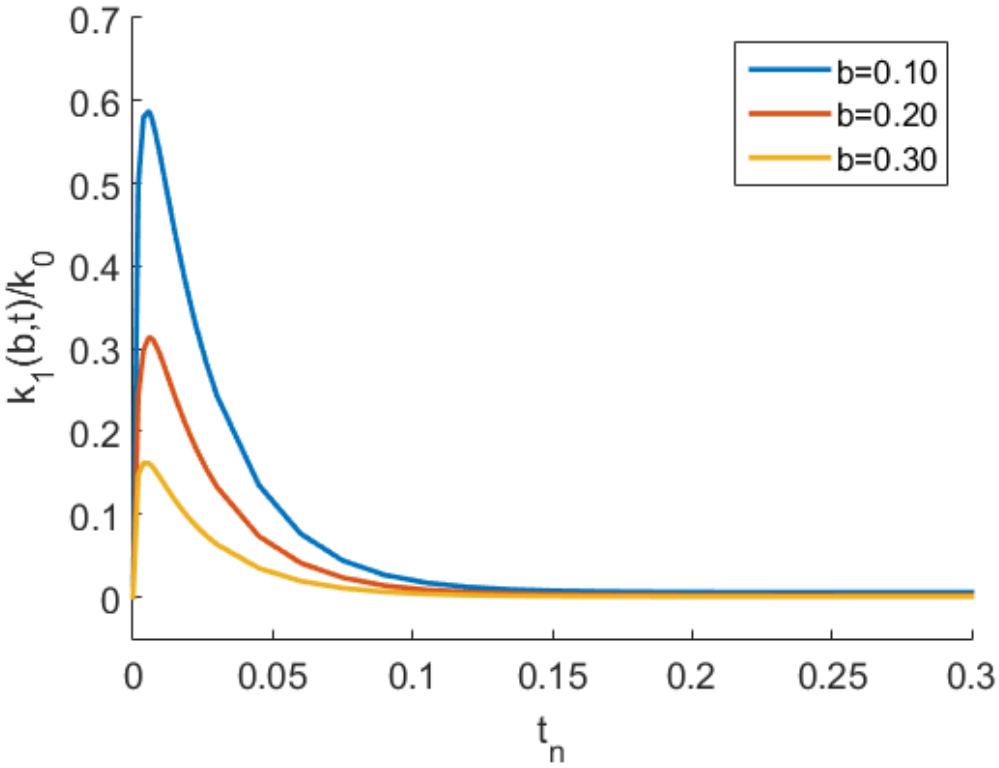
0.7
0.6
0.5
0.4
0.3
0.2
0.1
0
k1(b,t)/k0
0
0.05
0.1
0.15
0.2
0.25
0.3
tn
b=0.10
b=0.20
b=0.30

(b) $c/b = 5$

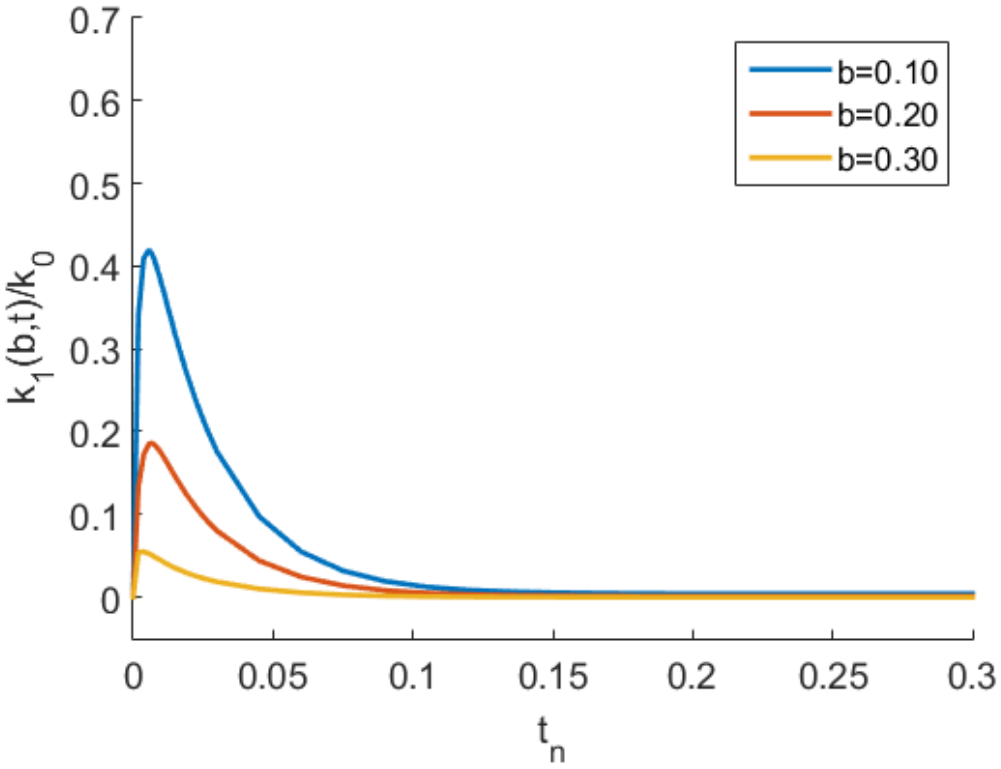

(c) $c/b = 2$

Figure 4.12: Normalized transient TSIF values of periodically cracked ZrO_2/Rene-41 strip under thermal shock for parabolic gradation in material properties, with varying crack spacings c/b and varying crack lengths b

4.3 Discussion and Conclusion

In this study, analytical solution for 1D transient temperature distribution and the resulting thermal stress distribution of the infinitely long FGM strips (ZrO_2/Ti-6Al-4V and ZrO_2/Rene-41) under thermal shock are found with general thermomechanical properties in the absence of any crack. Since the general thermomechanical properties are used; the analytical solution works actually for any definition of thermomechanical property variation through the thickness. Numerical calculations are performed by using MATLAB®. Although the results for only exponential, linear and parabolic gradation in material properties of each strip for different normalized times are shown in relevant sections; by changing the definition of material properties i.e., of thermal conductivity, specific heat, density, Young's modulus, linear expansion coefficient in the scripts in the sections (E) and (F) for any gradation of transient temperature distribution and resulting thermal stresses may also be calculated. Furthermore, if any FGM other than ZrO_2/Ti-6Al-4V and ZrO_2/Rene-41 is to be used; the thermoemechanical properties at $x = 0$ and $x = h$ i.e., λ_0, C_0, ρ_0, α_0, E_0 and λ_h, C_h, ρ_h, α_h, E_h should be changed in the formulation. Poisson's ratio ν is considered to be constant, however it may also be defined by a function of position if it is required. The results are compared with those in [28] to validate the solution and it is seen that, the results fit very well with each other. In any published paper since there is no transient stress distribution table, the exact numerical results could not been compared. However as the plotted curves are compared with those in [1, 28], it is seen that they overlap with each other.

After calculating the transient thermal stress distribution, corresponding thermal stress intensity factors (TSIFs) are calculated for the FGM strips containing periodic edge cracks by using the program written in Fortran in [3]. This program is intended to use exponentially varying Young's modulus, i.e., $E(x) = E_0 e^{\ln(E_h/E_0)x/h}$. So thermal stress distribution is calculated by using exponentially varying Young's modulus in particular. Since the program in [3] is written in Fortran language, another script is also prepared in MATLAB® to provide the results of transient thermal stress distribution as crack surface tractions to calculate corresponding TSIFs for different crack lengths b and crack spacings c/b. Since in the literature, the periodic cracking of an

FGM strip under thermal shock with general thermomechanical properties has not been studied yet, it may not be possible to compare the exact results with any other studies. However as the crack spacing increases sufficiently, periodic cracks are expected to behave as a single crack. Therefore TSIF values are calculated by increased crack spacing, and curves for t_n-TSIFs are then obtained. These curves are compared with those in [28] obtained for a single crack, and it is seen that trend of curves are very similar.

Numerical results show that;

* Near the surfaces, the temperature difference is very large in the strip when the normalized time t_n is very small (e.g., 0.001), and also the corresponding values of the thermal stress near the surfaces are also very large. [28]
* As t_n increases, i.e., as the temperature distribution approaches its steady state, the temperature difference decreases, and so do the resulting thermal stresses as well. [28]
* The temperature distribution in the FGM strip is almost linear as it reaches steady state.
* From figures it is seen that in the ZrO_2/Ti-6Al-4V strip, the thermal stress is larger at the pure ceramic (ZrO_2) surface than those at the pure metal (Ti-6Al-4V) surface whereas in ZrO_2/Rene-41 the thermal stress is larger at the pure metal (Rene-41) surface than those at the pure ceramic surface. Since the Young's moduli are $E_{Ti-6Al-4V} < E_{ZrO_2} < E_{Rene-41}$, this may be attributed to the fact that in an FGM strip consisting of two materials, at (or also near) the surface that Young's modulus is larger, the thermal stress is also larger at that surface.
* As periodic crack length b increases, TSIF values decrease. This conclusion is observed also in [28] for a single crack.
* As periodic crack spacing c increases, TSIF values also increase [20].
* TSIF values of periodic cracks in the FGM strip increase to a peak at an early normalized time, and then decrase quickly. This conclusion is observed also in [28] for a single crack.

* In some cases, especially for small crack spacing and deep cracks, TSIF values of the FGM strips under thermal shock are negative and these results actually have no physical meaning. This phenomenon observed also in [19]. The negative TSIF results are meaningful only when they are combined with the mechanical loads.

4.4 Future Work

In this study the analytic form of transient heat conduction equation is found by solving only the two terms expansion of perturbed equation. In future it may be calculated by using three terms. This perturbation method can be applied to problems with different thermal boundary conditions, such as time dependent boundary temperatures, surface heat flux or convective boundary conditions. Such boundary conditions could be more realistic than the thermal shock implementation here.

Furthermore, this perturbation method could be extended to different types of domains such as semi-infinite planes or composite domains such as a strip with varying thermomechanical properties perfectly bonded to another strip or semi-infinite half plane with uniform thermomechanical properteis. These cases would be realistic since FGMs are usually used as coatings. Possibility of solution for temperature dependent thermomechanical properties and heat generation within the domain could be explored.

REFERENCES

[1] L. Guo and N. Noda, "Investigation methods for thermal shock crack problems of functionally graded materials-part: I, analytical method," *Journal of Thermal Stresses*, vol. 37, p. 292–324, 2014.

[2] L. Guo and N. Noda, "An analytical method for thermal stresses of a functionally graded material cylindrical shell under a thermal shock," *Acta Mech*, vol. 214, pp. 71–78, 2010.

[3] A. Köse, "Thermal stress problems for an fgm strip containing periodic cracks," *METU*, 2013.

[4] SubsTech, "Heat-treatable nickel-chromium-iron alloy rene 41." "http://www.substech.com/dokuwiki/doku.php?id=heat-treatable_nickel-chromium-iron_alloy_rene_41", 2012.

[5] R. M. Mahamood and E. T. Akinlabi, "Functionally graded materials," *Springer International Publishing*, 2017.

[6] Y. Miyamoto, "Functionally graded materials: design, processing and applications," *Material technology series*, 1999.

[7] F. Erdoğan and M. Öztürk, "Diffusion problems in bonded nonhomogeneous materials with an interface cut," *Final project report*, 1992.

[8] I. Shiota and M. Y. Miyamoto, "Functionally graded materials," *Elsevier Science*, 1996.

[9] F. Ebrahimi, "Advances in functionally graded materials and structuress," *ExLi4EvA*, 2016.

[10] Z. H. Jin and R. C. Batra, "Some basic fracture mechanics concepts in functionally graded materials," *J.Mech.Phys.Solids*, vol. 44, no. 8, 1996.

[11] K. Ichikawa, “Functionally graded materials in the 21st century: a workshop on trends and forecasts,” *Kluwer Academic Publisher*, 2001.

[12] P. Gu and R. J. Asaro, “Cracks in functionally graded materials,” *Int.J.Solids Structures*, vol. 34, no. 1, 1995.

[13] F. Erdoğan, “Fracture mechanics of functionally graded materials,” *Composite Engineering*, vol. 5, no. 7, 1995.

[14] G. Bao and L. Wang, “Multiple cracking in functionally graded ceramic/metal coating,” *Int.J.Solids Structures*, vol. 32, no. 19, 1994.

[15] Z.-H. Jin and N. Noda, “Crack-tip singular fields in nonhomogeneous materials,” *Journal of Applied Mechanics*, vol. 61, pp. 738–740, 1994.

[16] Y. Tanigawa, “Some basic thermoelastic problems for nonhomogeneous structural materials,” *Applied Mechanics Reviews*, vol. 48, no. 6, 1995.

[17] N. Noda, “Thermal stresses intensity factor for functionally gradient plate with an edge crack,” *Journal of Thermal Stresses*, vol. 20, no. 3, 1997.

[18] N. Noda, “Thermal stress in functionally graded materials,” *Journal of Thermal Stresses*, vol. 22, no. 4, 1999.

[19] S. Ueda, “Thermally induced fracture of a functionally grade piezoelectric layer,” *Journal of Thermal Stresses*, vol. 27, no. 4, 2004.

[20] S. Ueda, “A cracked functionally graded piezoelectric material strip under transient thermal loading,” *Acta Mech*, vol. 199, pp. 53–70, 2008.

[21] S. Ueda and Y. Ashida, “Infinite row of parallel cracks in a functionally graded piezoelectric material strip under mechanical and transient thermal loading conditions,” *Journal of Thermal Stresses*, vol. 32, no. 11, 2009.

[22] S. Ueda and Y. Nakano, “A normal crack in a functionally graded thermal barrier coating bonded to a homogeneous elastic substrate under transient thermal loading,” *Journal of Thermal Stresses*, vol. 41, no. 10, 2018.

[23] S. Dag, B. Yıldırım, and D. Sarıkaya, “Mixed-mode fracture analysis of orthotropic functionally graded materials under mechanical and thermal loads,” *International Journal of Solids and Structures*, vol. 44, pp. 7816–7840, 2007.

[24] S.-H. Ding and X. Li, "Thermal stress intensity factors for an interface crack in functionally graded layered structures," *Arch Appl Mech*, vol. 81, pp. 943–955, 2010.

[25] B. Yıldırım, O. Kutlu, and S. Kadıoğlu, "Periodic crack problem for a functionally graded half-plane an analytic solution," *International Journal of Solids and Structures*, vol. 48, pp. 3020–3031, 2011.

[26] A. Yıldırım, D. Yarımpabuç, and K. Çelebi, "Thermal stress analysis of functionally graded annular fin," *Journal of Thermal Stresses*, 2019.

[27] Y. Obata and N. Noda, "Unsteady thermal stresses in a functionally gradient material plate," *Transactions of the Japan Society of Mechanical Engineers Series A*, vol. 59, no. 560, 1992.

[28] N. Noda and L. Guo, "Thermal shock analysis for a functionally graded plate with a surface crack," *Acta Mech*, vol. 195, pp. 157–166, 2008.

[29] Z. Jun, A. Xing, H. Chuanzhen, Z. Jianhua, and D. Jianxin, "An analysis of unsteady thermal stresses in a functionally gradient ceramic plate with symmetrical structure," *Ceramics International*, vol. 29, pp. 279–285, 2002.

[30] B. L. Wang and Y. W. Mai, "On thermal shock behavior of functionally graded material," *Journal of Thermal Stresses*, vol. 30, no. 6, 2007.

[31] Z.-H. Jin and G. H. Paulino, "Transient thermal stress analysis of an edge crack in a functionally graded material," *International Journal of Fracture*, vol. 107, pp. 73–98, 2001.

[32] H. Pan, T. Song, and Z. Wang, "Thermal fracture model for a functionally graded material with general thermomechanical properties and collinear cracks," *Journal of Thermal Stresses*, vol. 39, no. 7, 2016.

[33] Y. Zhang, L. Guo, and N. Noda, "Investigation methods for thermal shock problems of functionally graded materials-part ii: Combined analytical-numerical method," *Journal of Thermal Stresses*, vol. 37, pp. 325—-339, 2014.

[34] A. M. Nikolarakis and E. E. Theotokoglou, "Thermal shock problem of a three-layered functionally graded zirconia/titanium alloy strip based on a unified gen-

eralized thermoelasticity theory," *Journal of Thermal Stresses*, vol. 40, no. 5, 2016.

[35] C. B. Liu, Z. G. Bian, W. Q. Chen, and C. F. Lü, "Three-dimensional pyroelectric analysis of a functionally graded piezoelectric hollow sphere," *Journal of Thermal Stresses*, vol. 35, no. 6, 2012.

[36] A. Alibeigloo, "Three-dimensional semi-analytical thermo-elasticity solution for a functionally graded solid and an annular circular plate," *Journal of Thermal Stresses*, vol. 35, no. 8, 2012.

[37] M. Ohmici, N. Noda, and N. Sumi, "Plane heat conduction problems in functionally graded orthotropic materials," *Journal of Thermal Stresse*, vol. 40, no. 6, 2016.

[38] F. Guo, L. Guo, H. Yu, and L. Zhang, "Thermal fracture analysis of nonhomogeneous piezoelectric materials using an interaction energy integral method," *International Journal of Solids and Structures*, vol. 51, pp. 910–921, 2013.

[39] Y. Tokovyy and C.-C. Ma, "Three-dimensional temperature and thermal stress analysis of an inhomogeneous layer," *Journal of Thermal Stresses*, vol. 36, no. 8, 2013.

[40] S. P. Pawar, K. C. Deshmukh, and J. Verma, "Thermal behavior of functionally graded solid sphere with nonuniform heat generation," *Journal of Thermal Stresses*, vol. 40, no. 1, 2016.

[41] Y. Z. Feng and Z.-H. Jin, "Thermal shock damage and residual strength behavior of a functionally graded plate with surface cracks of alternating lengths," *Journal of Thermal Stresses*, vol. 35, no. 1, 2012.

[42] Afgrow, "Section 2.3. residual strength methodology." "`https://www.afgrow.net/applications/DTDHandbook/sections/page2_3.aspx`", 2019.

[43] J. R. Zuiker, "Functionally graded materials: Choice of micromechanics model and limitations in property variation," *Composite Engineering*, vol. 5, no. 7, 1995.

[44] Wolfram-Mathworld, “Fundamental theorems of calculus.” "http://140.177.205.23/FundamentalTheoremsofCalculus.html", 2019.

[45] M. D. Greenberg, “Advanced engineering mathematics,” *Prentice Hall*, 1998.

[46] F. Hildebrand, “Advanced calculus for applications,” *Prentice Hall*, 1962.

[47] A. D. Wunsch, “Complex variables with applications,” *Pearson Education*, 2005.

[48] IPFS, “Leibniz integral rule.” "https://ipfs.io/ipfs/QmXoypizjW3WknFiJnKLwHCnL72vedxjQkDDP1mXWo6uco/wiki/Leibniz_integral_rule.html", 2016.

[49] F. Erdogan and B. Wu, “Crack problems in fgm layers under thermal stresses,” *Journal of Thermal Stresses*, 1996.

APPENDIX A

SELECTED FORMULAS

$$\ln(xy) = \ln(x) + \ln(y) \tag{A.1}$$

$$\sinh(x) = \frac{e^x - e^{-x}}{2} \tag{A.2}$$

$$\cosh(x) = \frac{e^x + e^{-x}}{2} \tag{A.3}$$

$$\sinh(x \pm y) = \sinh(x)\cosh(y) \pm \cosh(x)\sinh(y) \tag{A.4}$$

$$\cosh(x \pm y) = \cosh(x)\cosh(y) \pm \sinh(x)\sinh(y) \tag{A.5}$$

$$\sinh(x) = -i\sin(ix) \tag{A.6}$$

$$\cosh(x) = \cos(ix) \tag{A.7}$$

$$\sinh(ix) = i\sin(x) \tag{A.8}$$

$$\cosh(ix) = \cos(x) \tag{A.9}$$

APPENDIX B

SERIES EXPANSION OF (2.4.8)

Source File

```
Element[p, Complex]
Series[(T02 Sinh[Sqrt[p]*xi] - T01 Sinh[Sqrt[p] (xi -
 ↪  xih)])/ Sinh[Sqrt[p] xih], {p, 0, 3}]
```

Output

```
1/(15120 xih) (-T01 (xi - xih) (15120 + 2520 p xi (xi -
 ↪  2 xih) +
42 p^2 xi (3 xi^3 - 12 xi^2 xih + 8 xi xih^2 + 8 xih^3)
 ↪  +
p^3 xi (3 xi^5 - 18 xi^4 xih + 24 xi^3 xih^2 + 24 xi^2
 ↪  xih^3 -
32 xi xih^4 - 32 xih^5)) +
T02 xi (15120 + 2520 p (xi^2 - xih^2) +
42 p^2 (3 xi^4 - 10 xi^2 xih^2 + 7 xih^4) +
p^3 (3 xi^6 - 21 xi^4 xih^2 + 49 xi^2 xih^4 - 31
 ↪  xih^6)))
```

APPENDIX C

EVALUATION THE RESIDUE OF $I_1(\xi)$

Source File

```
syms p t k(p) xih
res_I1 =
 ↪  2*diff(exp(p*t)*k(p),p)/diff((sinh(sqrt(p)*xih))^2,
 ↪  p,2)-2/3*exp(p*t)*k(p)*diff((sinh(sqrt(p)*xih))^2,
p,3)/(diff((sinh(sqrt(p)*xih))^2,p,2))^2
```

Output

```
(2*exp(p*t)*diff(k(p), p) +
 ↪  2*t*exp(p*t)*k(p))/((xih^2*cosh(p^(1/2)*xih)^2)
 ↪  /(2*p) + (xih^2*sinh(p^(1/2)*xih)^2)/(2*p) -
 ↪  (xih*cosh(p^(1/2)*xih)*sinh(p^(1/2)*xih))/
 ↪  (2*p^(3/2)))+(2*exp(p*t)*k(p)*((3*xih^2
 ↪  *cosh(p^(1/2)* xih)^2)/(4*p^2) +
 ↪  (3*xih^2*sinh(p^(1/2)*xih)^2)/(4*p^2)
 ↪  -(xih^3*cosh(p^(1/2)*xih)*sinh(p^(1/2)*xih))/p^(3/2)
 ↪  - (3*xih*cosh(p^(1/2)*xih)*sinh(p^(1/2)*xih))
 ↪  /(4*p^(5/2))))/(3*((xih^2*cosh(p^(1/2)*xih)^2)
 ↪  /(2*p) + (xih^2*sinh(p^(1/2)*xih)^2)/(2*p) -
 ↪  (xih*cosh(p^(1/2)*xih)*sinh(p^(1/2)*xih))
 ↪  /(2*p^(3/2)))^2)
```

APPENDIX D

DERIVATION IN (2.4.24)

Source File

```
syms xi1 xi xih p T1 T2
perturbed_4 = (T2*cosh(sqrt(p)*xi1)-T1 *
 ↪  cosh(sqrt(p)*(xi1-xih))) * sinh(sqrt(p) *
 ↪  (xih-xi1)) * sinh(sqrt(p)*xi) / p;
perturbed_5 = diff(perturbed_4,p);
```

Output

```
perturbed_5 =
(sinh(p^(1/2)*xi)*sinh(p^(1/2)*(xi1 -
 ↪  xih))*(T2*cosh(p^(1/2)*xi1) - T1*cosh(p^(1/2)*(xi1
 ↪  - xih))))/p^2 - (sinh(p^(1/2)*xi)*sinh(p^(1/2)*(xi1
 ↪  - xih))*((T2*xi1*sinh(p^(1/2)*xi1)) /(2*p^(1/2)) -
 ↪  (T1*sinh(p^(1/2)*(xi1 - xih))* (xi1 -
 ↪  xih))/(2*p^(1/2))))/p -
 ↪  (xi*cosh(p^(1/2)*xi)*sinh(p^(1/2)*(xi1 -
 ↪  xih))*(T2*cosh(p^(1/2)*xi1) - T1*cosh(p^(1/2)*(xi1
 ↪  - xih))))/(2*p^(3/2)) -
 ↪  (sinh(p^(1/2)*xi)*cosh(p^(1/2)*(xi1 -
 ↪  xih))*(T2*cosh(p^(1/2)*xi1) - T1*cosh(p^(1/2)*(xi1
 ↪  - xih)))*(xi1 - xih))/(2*p^(3/2))
```

APPENDIX E

FORMULATION OF TRANSIENT TEMPERATURE AND STRESS DISTRIBUTION IN TERMS OF x FOR EXPONENTIAL, LINEAR AND PARABOLIC GRADATIONS IN MATERIAL PROPERTIES

Source File

```
clear
clc
T1=-700; T2=-600;
E0=151; a0=1e-5; L0=2.09; C0=456.7; d0=5331;     %for
 ↪  ZrO2
Eh=116.7; ah=0.95*1e-5; Lh=7.5; Ch=537; dh=4420;
 ↪  %for Ti-6Al-4V
%Eh = 219.7; ah=1.67*1e-5; Lh=25.5; Ch=452; dh=8250;
 ↪  %for Rene-41

E = @(x) E0.*exp(x.*log(Eh/E0));     %exponential
 ↪  gradation in E(x)
%E = @(x) (Eh-E0).*x+E0;  %linear gradation in E(x)
%E = @(x) (Eh-E0).*x.^2+E0;  %parabolic gradation in
 ↪  E(x)
alpha = @(x) a0.*exp(x.*log(ah/a0)); %exponential
 ↪  gradation in \alpha(x)
%alpha = @(x) (ah-a0).*x+a0; %linear gradation in
 ↪  \alpha(x)
```

```
%alpha = @(x) (ah-a0).*x.^2+a0; %parabolic gradation in
 ↪  \alpha(x)
v=0.33;
x = 0:0.001:1;
tnArray = [0.01];
nMax = 5;

%%\xi_1(x1) and \eta(x1) for Exponential Gradation
xi1 = @(r) integral(@(s) (sqrt((C0*exp(s.*log(Ch/C0)))
 ↪  .*(d0*exp(s.*log(dh/d0)))
 ↪  ./(L0*exp(s.*log(Lh/L0))))),0,r);
%Where log(eta1(x1)) = log(sqrt((C0*exp(s.*log(Ch/C0)))
 ↪  .*(d0*exp(s.*log(dh/d0)))
 ↪  .*(L0*exp(s.*log(Lh/L0)))));
diff_log_eta = 22559632782886229/36028797018963968;

%%\xi_1(x1) and \eta(x1) for Linear Gradation
xi1 = @(r) integral(@(s) (sqrt((C0+(Ch-C0).*s)
 ↪  .*(d0+(dh-d0).*s)./(L0+(Lh-L0).*s))),0,r);
diff_log_eta = @(r)
 ↪  (-(1187278059.*r.^2+175663802.*r-13196685761)
 ↪  /(-791518706.*r.^3-175663802.*
 ↪  r.^2+26393371522.*r+10176910986));
%Where log(eta(x1)) = log(sqrt((C0+(Ch-C0).*x1)
 ↪  .*(d0+(dh-d0).*x1) .*(L0+(Lh-L0).*x1))));

%%\xi_1(x1) and \eta(x1) for Parabolic Gradation
xi1 = @(r) integral(@(s) (sqrt((C0+(Ch-C0).*s.^2)
 ↪  .*(d0+(dh-d0).*s.^2)./(L0+(Lh-L0).*s.^2))),0,r);
```

```
diff_log_eta = @(r) ((1822.*r.*((541.*r.^2)./100 +
 ↪  209./100).*((803.*r.^2)./10 + 4567./10) +
 ↪  (803.*r.*((541.*r.^2)./100 + 209./100).*(911.*r.^2
 ↪  - 5331))./5 + (541.*r.*((803.*r.^2)./10 +
 ↪  4567./10).*(911.*r.^2 -
 ↪  5331))./50)./(2.*((541.*r.^2)./100 +
 ↪  209./100).*((803.*r.^2)./10 + 4567./10).*(911.*r.^2
 ↪  - 5331)));
%Where log(eta(x1)) = log(sqrt((C0+(Ch-C0).*x1.^2)
 ↪  .*(d0+(dh-d0).*x1.^2) .*(L0+(Lh-L0).*x1.^2))));

TD = zeros(length(x),length(tnArray));
TS = zeros(length(x),length(tnArray));
for timeCounter = 1:length(tnArray)
t_n = tnArray(timeCounter);
fprintf('// Calculating for time =%10.3f
 ↪  ////////////////////////////////\n',t_n);
t = t_n*C0*d0/L0;

xi = zeros(length(x),1);
%\xi(n) for exponential gradation
for n = 1:length(x)
xi(n) = integral(@(x) sqrt(C0.*exp((Ch-C0).*x)
 ↪  .*d0.*exp((dh-d0).*x)./(L0.*exp((Lh-L0).*x))),0,
 ↪  x(n));    %Defining \xi(x)
end

%\xi(n) for linear gradation
for n = 1:length(x)
xi(n) = integral(@(x) sqrt((C0+(Ch-C0).*x)
 ↪  .*(d0+(dh-d0).*x)./(L0+(Lh-L0).*x)),0,x(n));
 ↪  %Defining \xi(x)
```

```
end

%\xi(n) for parabolic gradation
for n = 1:length(x)
xi(n) = integral(@(x) sqrt((C0+(Ch-C0).*x.^2)
 ↪  .*(d0+(dh-d0).*x.^2)./(L0+(Lh-L0).*x.^2)),0,x(n));
 ↪  %Defining \xi(x)
end
xiEnd = xi(end);

unperturbed_1 = zeros(1,length(x));
for k = 1:length(x)
unperturbed_1(k) = T1+(T2-T1)*xi(k)/xiEnd;
end

unperturbed_2 = zeros(nMax,length(x));
p = zeros(nMax,1);
for n=1:nMax
p(n) = -n^2*pi^2/(xiEnd)^2;
for j = 1:length(x)
unperturbed_2(n,j) =
 ↪  2*exp(p(n)*t)/(n*pi)*((-1)^n*T2-T1)*sin(n*pi*xi(j)
 ↪  /xiEnd);
end
end

parfor j = 1:length(x)
coef_1(j) = (T2-T1)/xiEnd;
coef_2(j) = (T1-T2)/xiEnd.*(xi(j)/xiEnd);
perturbed_1(j) =
 ↪  coef_1(j).*integral(@(r)((xi1(r)-xi(j))
 ↪  .*diff_log_eta(r)), 0,x(j),'ArrayValued',true);
```

```
perturbed_2(j) =
 ↪  coef_2(j).*integral(@(r)((xi1(r)-xiEnd)
 ↪  .*diff_log_eta(r)), 0,1,'ArrayValued',true);
end

for n=1:nMax
tic
fprintf('** Calculating for n=%d
 ↪  ******************************
 ↪  **********************\n',n)
pN = p(n);
coef_3 = -2*(-1)^n*n*pi*i/xiEnd/xiEnd.*exp(pN*t);
coef_4 = (-4*n^2*pi^2*t/xiEnd/xiEnd/xiEnd/xiEnd+2/xiEnd
 ↪  /xiEnd) .*exp(pN*t);
coef_5 = -4*n^2*pi^2/xiEnd/xiEnd/xiEnd/xiEnd*exp(pN*t);
parfor k=1:length(x)
perturbed_3(n,k) = coef_3.*integral(@(r)
 ↪  (T2.*cosh(sqrt(pN).*xi1(r))-T1.*cosh(sqrt(pN)
 ↪  .*(xi1(r)-xiEnd))) .*sinh(sqrt(pN).*(xi(k)-xi1(r)))
 ↪  ./pN.*diff_log_eta(r), 0,x(k),'ArrayValued',true);
perturbed_4(n,k) = coef_4.*integral(@(r)
 ↪  (sinh(sqrt(pN).*xi(k)).*sinh(sqrt(pN)
 ↪  .*(xiEnd-xi1(r))).* (T2.*cosh(sqrt(pN).*xi1(r)) -
 ↪  T1.*cosh(sqrt(pN).*(xi1(r) -
 ↪  xiEnd)))).*diff_log_eta(r),0,1,
 ↪  'ArrayValued',true);
```

```
perturbed_5(n,k) = coef_5.*integral(@(r)
 ↪  ((sinh(pN.^(1./2).*xi(k)).*sinh(pN.^(1./2).*(xi1(r)
 ↪  - xiEnd)).*(T2.*cosh(pN.^(1./2).*xi1(r)) -
 ↪  T1.*cosh(pN.^(1./2).*(xi1(r) - xiEnd)))./pN.^2 -
 ↪  (sinh(pN.^(1./2).*xi(k)).*sinh(pN.^(1./2).*(xi1(r)
 ↪  -xiEnd)).*((T2.*xi1(r).*sinh(pN.^(1./2).*xi1(r))./
 ↪  (2.*pN.^(1./2)) - (T1.*sinh(pN.^(1./2) .*(xi1(r) -
 ↪  xiEnd)).*(xi1(r) - xiEnd))./(2.*pN.^(1./2))))./pN -
 ↪  (xi(k).*cosh(pN.^(1./2).*xi(k)).*sinh(pN.^(1./2)
 ↪  .*(xi1(r) - xiEnd)).*(T2.*cosh(pN.^(1./2).*xi1(r))
 ↪  - T1.*cosh(pN.^(1./2).*(xi1(r) -
 ↪  xiEnd))))./(2.*pN.^(3./2)) -
 ↪  (sinh(pN.^(1./2).*xi(k)) .*cosh(pN.^(1./2).*(xi1(r)
 ↪  - xiEnd)).*(T2.*cosh(pN.^(1./2).*xi1(r)) -
 ↪  T1.*cosh(pN.^(1./2).*(xi1(r) - xiEnd))).*(xi1(r) -
 ↪  xiEnd))./(2.*pN.^(3./2))).*diff_log_eta(r),0,1,
 ↪  'ArrayValued',true);
end
toc
end
T_0 = (unperturbed_1 + sum(unperturbed_2)); %transient
 ↪  temperature distribution for m=0
T = (unperturbed_1+sum(unperturbed_2)+perturbed_1
 ↪  +perturbed_2 +sum(perturbed_3)+sum(perturbed_4)
 ↪  +sum(perturbed_5)); %transient temperature
 ↪  distribution for m=1
T_inf = (unperturbed_1 + perturbed_1 + perturbed_2); %
 ↪  steady state temperature distribution



first = trapz(x,E(x).*alpha(x)*(1+v).*T);
second = trapz(x,x.*E(x).*alpha(x)*(1+v).*T);
```

```
syms A B D F
first_var = trapz(x,E(x).*(A*x+B));
second_var = trapz(x,x.*E(x).*(A*x+B));

A = 1; B = 0;
a1 = eval(first_var)

A = 0; B = 1;
b1 = eval(first_var)

A = 1; B = 0;
a2 = eval(second_var)

A = 0; B = 1;
b2 = eval(second_var)

eqn1 = a1*D + b1*F == first;
eqn2 = a2*D + b2*F == second;

sol = solve([eqn1, eqn2], [D, F]);
A = sol.D;
B = sol.F;
s_0 = E0*a0*abs(T1)/(1-v);
sigma = E(x).*(A*x+B-alpha(x)*(1+v).*T)/(1-v^2);

TS_lin(:, timeCounter) = eval(sigma)';
TD_lin(:, timeCounter) = T';
end
```

APPENDIX F

FORMULATION OF TRANSIENT TEMPERATURE AND STRESS DISTRIBUTION IN TERMS OF $\xi(x)$ FOR EXPONENTIAL GRADATIONS IN MATERIAL PROPERTIES

Source File

```
clear
clc
%% Solution of transient temperature distribution
% Boundary conditions:
T1=-700; T2=-600;
E0=151; a0=1e-5; L0=2.09; C0=456.7; d0=5331;    %for
 ↪  ZrO2
Eh=116.7; ah=0.95*1e-5; Lh=7.5; Ch=537; dh=4420;
 ↪  %for Ti-6Al-4V
%Eh = 219.7; ah=1.67*1e-5; Lh=25.5; Ch=452; dh=8250;
 ↪  %for Rene-41

E = @(x) E0.*exp(x.*log(Eh/E0)); alpha = @(x)
 ↪  a0.*exp(x.*log(ah/a0)); v=0.33;
% Numerical Calculations
x = 0:0.001:1;  %h is taken as unity
tnArray = [0.01];
nMax = 5;
xi1 = @(r) integral(@(s) (sqrt((C0+(Ch-C0).*s)
 ↪  .*(d0+(dh-d0).*s)./(L0+(Lh-L0).*s))),0,r);
```

```
diff_log_eta = @(xi1) -37977257148335060102614381383391
 ↪  /(23475764654379020*(1683416459559779*xi1 -
 ↪  27884848395006771120));
%Where log(eta(x1)) = log(sqrt((C0+(Ch-C0).*x1)
 ↪  .*(d0+(dh-d0).*x1) .*(L0+(Lh-L0).*x1))));
TD = zeros(length(x),length(tnArray));
TS = zeros(length(x),length(tnArray));
for timeCounter = 1:length(tnArray)
t_n = tnArray(timeCounter);
fprintf('// Calculating for time =%10.3f
 ↪  ////////////////////////////////\n',t_n);
t = t_n*C0*d0/L0;
xi = zeros(length(x),1);
for j = 1:length(x)
xi(j) = 8282/5 - (8282*exp(-(1629*x(j))/2500))/5;
 ↪  %calculation of xi(x)
end
xiEnd = xi(end);

unperturbed_1 = zeros(1,length(x));
for k = 1:length(x)
unperturbed_1(k) = T1+(T2-T1)*xi(k)/xiEnd;    %solution
 ↪  of first unperturbed equation
end

unperturbed_2 = zeros(nMax,length(x));
p = zeros(nMax,1);
for n=1:5
p(n) = -n^2*pi^2/(xiEnd)^2;        %defining p_n
for j = 1:length(x)
```

```
unperturbed_2(n,j) = 2*exp(p(n)*t)/(n*pi)
 ↪  *((-1)^n*T2-T1)*sin(n*pi*xi(j)/xiEnd);    %solution
 ↪  of first unperturbed equation
end
end

perturbed_1  = zeros(1,length(x)); perturbed_2  =
 ↪  zeros(1,length(x));
for k = 1:length(xi)
coef_1 = (T2-T1)/xiEnd;     %coefficient of first
 ↪  perturbed term
coef_2 = (T1-T2)/xiEnd .* (xi(k)/xiEnd);    %coefficient
 ↪  of second perturbed term
perturbed_1(k) = coef_1 .* integral(@(xi1) (xi1-xi(k))
 ↪  .* diff_log_eta(xi1),0,xi(k),'ArrayValued',true);
 ↪  %solution of first perturbed equation
perturbed_2(k) = coef_2 .* integral(@(xi1) (xi1-xiEnd)
 ↪  .* diff_log_eta(xi1),0,xiEnd,'ArrayValued',true);
 ↪  %solution of second perturbed equation
end

for n=1:nMax
tic
fprintf('** Calculating for n=%d
 ↪  ********************************
 ↪  **********************\n',n)
pN = p(n);
coef_3 = -2*(-1)^n*n*pi*i/(xiEnd)^2 * exp(pN*t);
 ↪  %coefficient of third perturbed equation
coef_4 = (-4*n^2*pi^2*t/(xiEnd)^4+2 /
 ↪  (xiEnd)^2)*exp(pN*t);  %coefficient of forth
 ↪  perturbed equation
```

```
coef_5 = -4*n^2*pi^2/(xiEnd)^4 * exp(pN*t);
 ↪  %coefficient of fifth perturbed equation
%since following terms are under the summation sign, we
 ↪  need to form a matrix, and sum the terms in same
 ↪  columns to
%calculate the contributions of these terms. Summing
 ↪  the terms in same columns gives an array
%corresponding to x/h values
parfor k=1:length(x)
perturbed_3(n,k) = coef_3.*integral(@(xi1)
 ↪  (T2.*cosh(sqrt(pN).*xi1) - T1.*cosh(sqrt(pN).*(xi1
 ↪  - xiEnd))).*sinh(sqrt(pN).*(xi(k) -
 ↪  xi1))./pN.*diff_log_eta(xi1),0,xi(k),
 ↪  'ArrayValued',true); %Third perturbed equation
 ↪  calculation from n=1 to n=10 since it is in the
 ↪  summation sign.
perturbed_4(n,k) = coef_4.*integral(@(xi1)
 ↪  (T2*cosh(sqrt(pN).*xi1) - T1.*cosh(sqrt(pN).*(xi1 -
 ↪  xiEnd))).*sinh(sqrt(pN).*(xiEnd -
 ↪  xi1)).*sinh(sqrt(pN).*xi(k))./pN .*
 ↪  diff_log_eta(xi1),0,xiEnd,'ArrayValued',true);
 ↪  %Forth perturbed equation calculation from n=1 to
 ↪  n=10 since it is in the summation sign.
```

```
perturbed_5(n,k) = coef_5.*integral(@(xi1)
 ↪  ((sinh(pN.^(1./2).*xi(k)).*sinh(pN.^(1./2) .*(xi1 -
 ↪  xiEnd)).*(T2.*cosh(pN.^(1./2).*xi1) -
 ↪  T1.*cosh(pN.^(1./2).*(xi1 - xiEnd)))./pN.^2 -
 ↪  (sinh(pN.^(1./2).*xi(k)).*sinh(pN.^(1./2).*(xi1 -
 ↪  xiEnd)).*((T2.*xi1.*sinh(pN.^(1./2).*xi1))
 ↪  ./(2.*pN.^(1./2)) - (T1.*sinh(pN.^(1./2).*(xi1 -
 ↪  xiEnd)).*(xi1 - xiEnd))./(2.*pN.^(1./2))))./pN -
 ↪  (xi(k).*cosh(pN.^(1./2).*xi(k)).*sinh(pN.^(1./2)
 ↪  .*(xi1 - xiEnd)).*(T2.*cosh(pN.^(1./2).*xi1) -
 ↪  T1.*cosh(pN.^(1./2).*(xi1 -
 ↪  xiEnd))))./(2.*pN.^(3./2)) -
 ↪  (sinh(pN.^(1./2).*xi(k)).*cosh(pN.^(1./2).*(xi1 -
 ↪  xiEnd)) .*(T2.*cosh(pN.^(1./2).*xi1) -
 ↪  T1.*cosh(pN.^(1./2).*(xi1 - xiEnd))).*(xi1 -
 ↪  xiEnd))./(2.*pN.^(3./2))).*diff_log_eta(xi1),
 ↪  0,xiEnd,'ArrayValued',true); %fifth perturbed term
end
toc
end
T_0 = (unperturbed_1 + sum(unperturbed_2)); %transient
 ↪  temperature distribution for m=0
T = (unperturbed_1 + sum(unperturbed_2) + perturbed_1 +
 ↪  perturbed_2 + sum(perturbed_3) + sum(perturbed_4) +
 ↪  sum(perturbed_5));   %transient temperature
 ↪  distribution for m=1
T_inf = (unperturbed_1 + perturbed_1 + perturbed_2); %
 ↪  steady state temperaure distribution
% Note that the results of transient temperature
 ↪  distribution are tabulated as normalized by |T1|.
% End of the solution of transient temperature
 ↪  distribution
```

```
%% Solution of transient thermal distribution
% Solution of linear system of equations to calculate
 ↪  the coefficients
% A and B
first = trapz(x,E(x).*alpha(x)*(1+v).*T);
second = trapz(x,x.*E(x).*alpha(x)*(1+v).*T);
syms A B D F
first_var = trapz(x,E(x).*(A*x+B));
second_var = trapz(x,x.*E(x).*(A*x+B));
A = 1; B = 0;
a1 = eval(first_var)

A = 0; B = 1;
b1 = eval(first_var)

A = 1; B = 0;
a2 = eval(second_var)

A = 0; B = 1;
b2 = eval(second_var)
eqn1 = a1*D + b1*F == first;
eqn2 = a2*D + b2*F == second;
sol = solve([eqn1, eqn2], [D, F]);
A = sol.D;
B = sol.F;

sigma = E(x).*(A*x+B-alpha(x)*(1+v).*T)/(1-v^2);
 ↪  %Calculation of transient stress distribution
s_0 = E0*a0*abs(T1)/(1-v);
% Note that the results of transient stress
 ↪  distribution are tabulated
```

```
% as normalized by s_0.
TS_expo(:, timeCounter) = eval(sigma)'; %Transient
 ↪  thermal stress matrix TS(x,tn)
TD_expo(:, timeCounter) = T'; %Transient temperature
 ↪  distribution matrix TD(x,tn)
end
% End of the solution of transient stress distribution
```